

LDRD

2011 Annual Report

Laboratory Directed Research & Development Program Activities



BROOKHAVEN
NATIONAL LABORATORY

BNL-52351-2011

BROOKHAVEN NATIONAL LABORATORY
BROOKHAVEN SCIENCE ASSOCIATES
UPTON, NEW YORK 11973-5000
UNDER CONTRACT NO. DE-AC02-98CH10886
UNITED STATES DEPARTMENT OF ENERGY

March 2012

Acknowledgments

The Laboratory Directed Research and Development (LDRD) Program is managed by William Bookless, who serves as the ALD for Policy & Strategic Planning. Preparation of the FY 2011 report was coordinated and edited by William Bookless. He wishes to thank Kathi Barkigia, Sabrina Parrish and Liz Flynn for their assistance in organizing, typing, and proofing the document. A special thank you is also extended to the Production Services Group for their help in publishing. Of course, a very special acknowledgement is extended to all of the authors of the project annual reports and to their assistants.

Table of Contents

Introduction	1
Project Summaries	3
Strongly Correlated Systems: From Graphene to Quark-Gluon Plasma.....	4
Genomic DNA Methylation: The Epigenetic Response of <i>Arabidopsis Thaliana</i> Genome to Long-Term Elevated Atmospheric Temperature and CO ₂ in Global Warming.....	5
Nanoscale Electrode Materials for Lithium Batteries	7
Bioconversion of Lignocellulose to Ethanol and Butanol Facilitated by Ionic Liquid Preprocessing	9
Organic Photovoltaics: Nanostructure, Solvent Annealing and Performance	11
Surface Chemistry and Electrochemistry of Ethanol	13
Synergistic Interactions Between Poplar and Endophytic Bacteria to Improve Plant Establishment and Feedstock Production on Marginal Soils	15
<i>Petascale</i> Data Mining for BNL's Data Intensive Sciences	18
Solar Energy Source Evaluation for Smart Grid Development	20
High Throughput Quantitative Biochemical Phenotyping.....	22
Characterization of Materials in Extreme Environments for Advanced Energy Systems Using the National Synchrotron Light Source	24
Development of an Ultrafast Electron Diffraction Facility for Condensed Matter Physics Challenges.....	27
Design of Pt-free Electrocatalysts for Fuel Cell Oxygen Reduction Reactions.....	29
Charge Generation and Transport in Films of Conjugated Polymers for Organic Photovoltaics BNL Part of a Collaborative NREL, BNL, ANL LDRD	31
Photoelectrochemical Fuel Generation from Water and Carbon Dioxide	34

Table of Contents

Structural Basis of Light Perception by Phytochrome	36
New Model Organisms for Analysis of Plant Metabolism	38
Development of Microprobe, Multichannel Optical Multimodality for Biological Tissue Imaging	40
Development of Large Liquid Argon Time Projection Chambers (LArTPC) for Future Neutrino Experiments	40
Spin Waves in Artificial Magnonic Crystals: Fabrication, Imaging and Scattering	44
Atomic Structure and Bonding of Cellulose	46
EIC Polarized Electron Gun	48
Development of Laser System for Driving the Photocathode of the Polarized Electron Source for the EIC	51
Simulation, Design, and Prototyping of an FEL for Proof-of-Principle of Coherent Electron Cooling	53
Realization of an $e+A$ Physics Event Generator for the EIC	57
Exploring Signatures of Saturation and Universality in $e+A$ Collisions at eRHIC	59
Electroweak Physics with an Electron-Ion Collider	61
LSST – Astrophysics and Cosmology Initiative	63
Enzymatic Control of Plant Cell Wall Properties that Impact Conversion to Biofuels	65
Cloud and Precipitation 4D Radar Science	67
A Novel Approach to Parameterized Sub-Grid Processes in Climate Models	69
Deciphering the Molecular Mechanisms of Lignin Precursor Transportation	71
Touchless Micro-Crystallography	73
Multiscale Complexity of Energy and Material Use: Integrated Assessment of Technology and Policy Alternatives	75

Table of Contents

Indium Iodide (InI) - A Potential Next-Generation Room-Temperature Radiation Detector.....	77
Visualization Support Infrastructure for Global Climate Modeling with a Focus on the BNL FASTER Project	79
Single Crystal Growth of Novel Energy Materials by High Pressure Method	81
Complex Networks Approach to Power Grid Design and Stability	83
Protein Microcrystal Dynamics by Coherent X-Ray Scattering	85
High-Resolution Biological Imaging by X-Ray Diffraction Microscopy	88
Sub-10 nm Resolution Soft X-Ray Microscopy of Organic Nano-Materials by Novel Diffraction Methods.....	90
2D Membrane Solution Scattering for Probing the Structures of Membrane Proteins.....	92
Exploring the Role of Glue in Hadron Structure by an Electron Ion Collider.....	94
Study of FEL Options for eRHIC	94
Overcoming Electromagnetic Interference in Simultaneous PET and MRI for Biological and Clinical Imaging.....	100
Estrogen Biosynthesis as a Novel Imaging Target with Multiple Applications	102
Magnetic Nanoparticles as Tracers in Biological Systems	104
High Throughput Screening in Biological Systems Using Radiometric Approaches.....	106
Improving Safety with a Brain-Computer Interface.....	110
Astrophysics and Cosmology Initiative	112

Introduction

Each year, Brookhaven National Laboratory (BNL) is required to provide a program description and overview of its Laboratory Directed Research and Development Program (LDRD) to the Department of Energy in accordance with DOE Order 413.2B dated April 19, 2006. This report provides a detailed look at the scientific and technical activities for each of the LDRD projects funded by BNL in FY2011, as required. In FY2011, the BNL LDRD Program funded 37 projects, 16 of which were new starts, at a total cost of \$6,764,615. For FY2011, BNL solicited proposals in all areas of science and technology in support of the Lab's strategy and mission, i.e., 100% of the available new funding was awarded to openly competed LDRD projects.

The investments that BNL makes in its LDRD program largely support the Laboratory's strategic goals as outlined in the BNL Laboratory Plan. BNL has five Laboratory Initiatives: Photon Sciences, QCD Matter, Discovery to Deployment: A Path to 21st Century Energy Security, Physics of the Universe, and Biological-, Environmental- and Climate Sciences. These major initiatives support the growth and evolution of the major business lines (i.e. mission areas) of the Laboratory. In addition, there are four smaller initiatives that support growth and program development in targeted areas, i.e. Accelerator Science and Technology, Biological Imaging, Computation, and Homeland and National Security. All of the FY2011 BNL LDRD funds broadly supported one of the major or targeted initiatives, of which approximately 93% supported the five major initiatives. In total, these LDRD investments supported 77 postdoctoral researchers and graduate students in whole or in part. In FY2011, new LDRD investments of \$2,050,251 supported all five Laboratory initiatives and the Directorate initiative in Homeland and National Security. The allocation by initiative area is shown in Figure 1.

This Project Activities Report represents the future of BNL science; it is an impressive body of exploratory work that investigates many scientific and technical directions in support of the DOE and BNL Missions. We hope that you enjoy it.

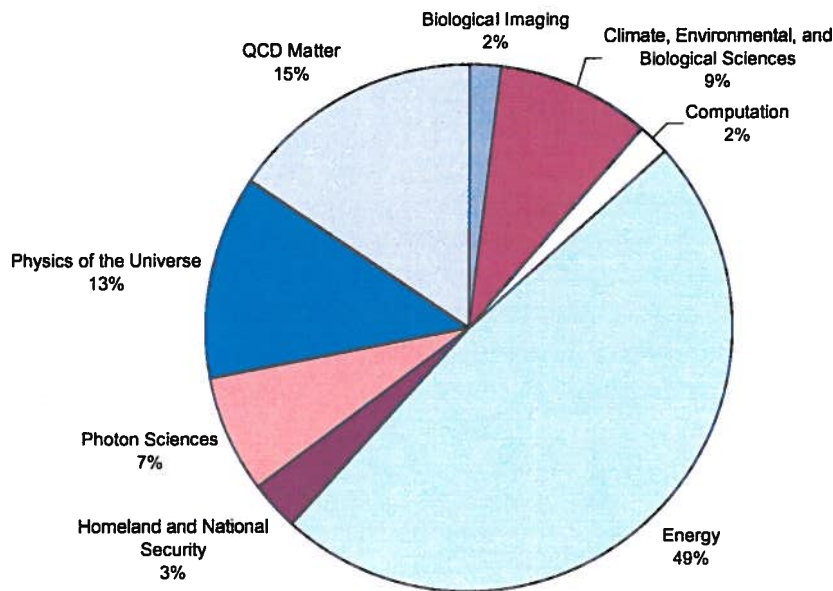


Figure 1. Allocation of FY2011 LDRD Funding by BNL Initiative Area

LABORATORY DIRECTED RESEARCH AND DEVELOPMENT
2011 PROJECT SUMMARIES

Strongly Correlated Systems: From Graphene to Quark-Gluon Plasma

LDRD Project 08-002

D. E. Kharzeev and A. M. Tsvetik

PURPOSE:

The fundamental goal of the project is to study the role played by the chirality describing the state of motion of the relativistic particles in a condensed matter setting, such as mono and multi layer graphene samples. The chirality manifests itself in a qualitatively different way depending on the number of graphene layers. The technical objective of our project is to study the effect of the chiral nature of the particle spectrum on the transport properties of mono and multi layer graphene.

APPROACH:

Graphene samples are unique in their high mobility, controllable properties and most notably the relativistic dispersion relation of carriers. Even though the fractional quantum Hall effect has been reported recently in suspended samples, the observation of effects of electron-electron interaction at low magnetic fields in exfoliated graphene remains a challenge. We have realized that working with multilayered graphene may provide a way to detect interaction effects. Indeed, in a n -layer graphene, the Berry phase associated with the chirality is $n\pi$. This corresponds to an n -th power of momentum in the dispersion of the quasi-particles. It follows that while the effective mass of carriers in mono-layer graphene vanishes at low energies, it is constant in a graphene bi-layer and is divergent in a graphene tri-layer. Experimentally this behavior has been reported in measurements made by our team of collaborators: Liyuan Zhang, Yan Zhang, Jorge Camacho, Igor Zaliznyak, Tonica Valla, and Myron Strongin at Brookhaven National Laboratory. Collaboration with the local group proved to be useful and essential for the project.

To provide our experimentalists with theory support, we developed a transport theory in graphene multi-layers including effects of screening due to the electron-electron interaction.

TECHNICAL PROGRESS AND RESULTS:

Quantum Hall effect in three-layer graphene was calculated which allowed us to explain the experimental data obtained by I. Zaliznyak and co-workers. The results are published in The experimental observation of quantum Hall effect of $l = 3$ chiral charge carriers in trilayer graphene, Liyuan Zhang, Yan Zhang, J. Camacho, M. Khodas, I. A. Zaliznyak, *Nature Physics* 7, 953-957 (2011).

Genomic DNA Methylation: The Epigenetic Response of *Arabidopsis Thaliana* Genome to Long-Term Elevated Atmospheric Temperature and CO₂ in Global Warming

LDRD Project 08-028

Qiong (Alison) Liu

PURPOSE:

The goal of this project is to determine the changes of DNA cytosine methylation in genome of *Arabidopsis* plants in response to elevated ambient temperature and CO₂ concentrations such as would occur during global warming. This epigenetic information will help us identify genomic and genetic loci that are regulated by elevated temperature and CO₂ that can impact on plant development, flowering time, grain and biomass production, and to understand how regulation of DNA methylation in plant genome can help plant's adaptation to environment.

APPROACH:

Exponential emission of CO₂ into the atmosphere resulted from human activities has led to an enhanced greenhouse effect or global warming. Prolonged increase of temperature has been shown to increase the growth rate and induces early flowering of plants in laboratory experiments (Balasubramanian, S. et al. PLoS Genetics, 2006 2(7): 980-9), and correlated to biomass and grain reduction in crops (Peng, S. et al. Proc Natl. Acad. Sci. USA, 2004 101(27): 9971-5). Paleobotanical evidence has linked a fourfold increase in atmospheric carbon dioxide and an associated 3° to 4°C greenhouse warming to a well-documented major faunal mass extinction during the period of Triassic-Jurassic boundary (McElwain, J. C. et al. Science, 1999 285: 1386-90). Some prior evidences suggest that plants may respond to altered temperature and CO₂ level via an epigenetic response. For example, microarray studies have identified many gene expression changes in *Arabidopsis* when the plant is grown at a few degrees higher temperature (Balasubramanian, S. et al. PLoS Genetics, 2006 2(7): 980-9). A few small RNAs are also generated or altered in *Arabidopsis* growing at a lowered temperature (Oh, M. et al. Journal of Plant Biology, 2007 50(5): 562-67).

We have taken several approaches to understand how elevated ambient temperature can function to affect epigenome. We have used HPLC and LUMA assays to analyze the overall genomic DNA methylation, and bisulfite sequencing method to identify altered methylation in cytosine in the single nucleotide resolution. We have also analyzed the deep sequencing results of small RNAs libraries to identify the miRNAs that are altered in their expression by elevated temperature and CO₂, and the altered siRNAs expression indicates regulation of genomic DNA methylation. We have completed analysis of 4 bisulfite sequencing libraries and 8 small RNA libraries in these plants.

For these progresses, Alison Liu has collaborated with (1) Dr. Michael Zhang at Cold Spring Harbor Laboratory for bioinformatics work, (2) Cold Spring Harbor Laboratory Genome Research Center for sequencing small RNA libraries, and (3) Dr. Ecker's lab at Salk Institute.

TECHNICAL PROGRESS AND RESULTS:

The summarized results are as follows:

(1) The phenotypic characterization and the paper: *Arabidopsis* plants were grown at 23°C and 26°C. We characterized newly identified phenotypes, and demonstrated that elevated ambient temperature reduces seed production significantly, and biomass production moderately, and promote root development in *Arabidopsis* plants. A paper reporting these results was submitted to a journal, but not published.

(2) The small RNA expression and genomic DNA methylation changes induced by elevated ambient temperature and CO₂. Duplicate small RNA libraries were generated using *Arabidopsis* plants grown at 22°C and 28°C, and 400ppm and 800ppm CO₂ following methods described in the Illumina small RNA preparation instruction manual. We found novel miRNAs and siRNAs with differentiated expression rates in *Arabidopsis* grown at different temperature and CO₂. We also sequenced bisulfite libraries to identify the genomic DNA methylation changes induced by elevated temperature and CO₂ concentration and analyzed the results using bioinformatics methods. These results also revealed the interaction between CO₂ and temperature.

Using deep sequencing in combination with bioinformatic analysis, we identified 17 known and 9 predicted miRNAs altered in expression by elevated CO₂, and 62 known and 35 predicted miRNAs by elevated temperature. Among them, the expression of 16 known and 6 predicted miRNA are regulated by both elevated CO₂ and temperature mostly in opposite direction. We have also found that both elevated CO₂ concentration and temperature can reduce significantly gross genomic DNA methylation, specifically in CHH context in CO₂ samples. Our results demonstrate that elevated ambient CO₂ concentration and temperature affect epigenome that may contribute to gene expression changes, and their counter-regulation of a common set of small RNAs suggest that they can “buffer” with each other to control the same biological processes through shared pathways. We anticipate that our results will lead to sophisticated studies in understanding how elevated CO₂ concentration and temperature interact in epigenetic levels to control plant phenotypes, and be a starting point to investigate other greenhouse gases such as water vapor, methane, nitrous oxide, and ozone for their roles in epigenetic controlled gene expression. A paper reporting these results was submitted to a journal, but not published.

The Principal Investigator completed this LDRD in March, 2011 and then accepted a new position as a Research Assistant Professor in the Department of Biochemistry and Cell Biology at Stony Brook University on September 30, 2011.

Nanoscale Electrode Materials for Lithium Batteries

LDRD Project 09-001

Jason Graetz, Yimei Zhu, Xiao-Qing Yang and Weiqiang Han

PURPOSE:

The objective is to develop a fundamental understanding of how electrode nanostructure and morphology affect electrochemical performance (e.g. capacity, cycle life, rate capability) and how morphology and nanostructure are affected by lithiation and repeated cycling.

APPROACH:

The development of high capacity, safe lithium battery materials requires a better understanding of how reaction conditions affect nucleation and crystallization, particle size, morphology and defects. Our approach is to develop bulk and nanoscale characterization tools to better understand the physical and chemical changes occurring during cycling. Insights gleaned from these studies are used to design new nanostructured electrodes with improved electrochemical properties (e.g., capacity, stability, rate capability, safety).

TECHNICAL PROGRESS AND RESULTS:

Anodes: In recent years, much research has focused on resolving the crucial problem of capacity fading in lithium ion batteries when carbon anodes are replaced by the high capacity group-IV elements (Si, Ge, Sn). Some progress was achieved by using different nanostructures and carbon coatings, which increased the electrode life to 100–200 cycles. However, further improvements in cycling stability are necessary to achieve $10^3 - 10^4$ cycles necessary for many applications. We recently demonstrated that an amorphous hierarchical porous GeO_x , whose primary particles are ~ 3.7 nm in diameter, has a very stable capacity of ~ 1250 mA h g^{-1} for 600 cycles (Figure 1). Furthermore, we show that a full cell, coupled with a $\text{Li}(\text{NiCoMn})_{1/3}\text{O}_2$ cathode, exhibits excellent cycling performance.

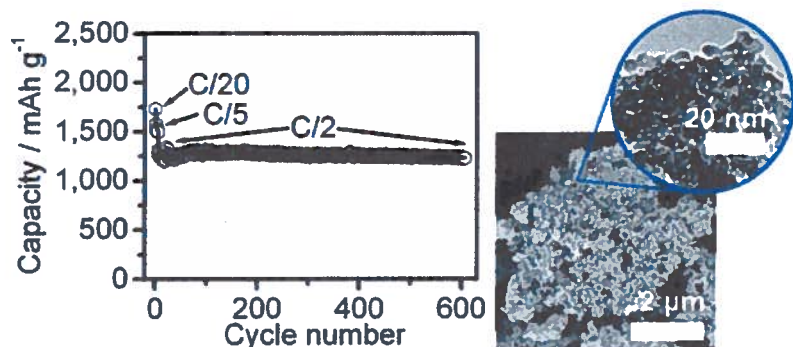


Fig. 1. Cycling capacity of a half cell using a GeO_x anode showing good stability over 600 cycles. Microscopy images (right) reveal the hierarchical porous structure.

Lithium titanate ($\text{Li}_{4+x}\text{Ti}_5\text{O}_{12}$) is another promising anode material for lithium batteries due to its excellent cycling stability within the range of $0 \leq x \leq 3$. However, lithium titanate exhibits a moderate capacity (175 mAh/g) and high-voltage redox potential (1.55V) within the typical cycling

range, leading to a low overall energy density in a full battery. It is of great interest to explore the possibility of inserting more Li^+ ions (i.e. $x > 3$) by cycling down to a lower voltage, which would increase the specific capacity of the electrode, increase the cell voltage and thereby raise the energy density of the full battery. Using a combination of electrochemistry, synchrotron-based *in-situ* X-ray diffraction measurements and first-principles calculations we investigated the electrochemical behavior and structural evolution in $\text{Li}_{4+x}\text{Ti}_5\text{O}_{12}$ when subjected to wide range of lithium cycling (2 V- 50 mV). Electrochemical measurements revealed a significant capacity increase, but also a reduced

‘cycling stability when the discharge was extended down to 50 mV. *In-situ* X-ray diffraction (Figure 2) revealed that the lithiation reaction occurs via a two-phase transition up to $\text{Li}_7\text{Ti}_5\text{O}_{12}$ with 16c sites fully occupied, then proceeds by a solid-solution reaction, forming $\text{Li}_{7+x}\text{Ti}_5\text{O}_{12}$ ($0 < x < 2$; with a gradual filling of 8a sites). Simultaneous occupancy of tetrahedral (8a) and octahedral (16c) sites can only be achieved when the voltage is low (below about 0.5 V); however, we found that only approximately half of the tetrahedral sites can be filled, corresponding to a composition of $\text{Li}_{8.5}\text{Ti}_5\text{O}_{12}$ with a maximum capacity of about 260 mAh/g. Further improvements may be possible by using dopants to open up the structure thereby facilitating lithium insertion/removal and improving the cycling stability.

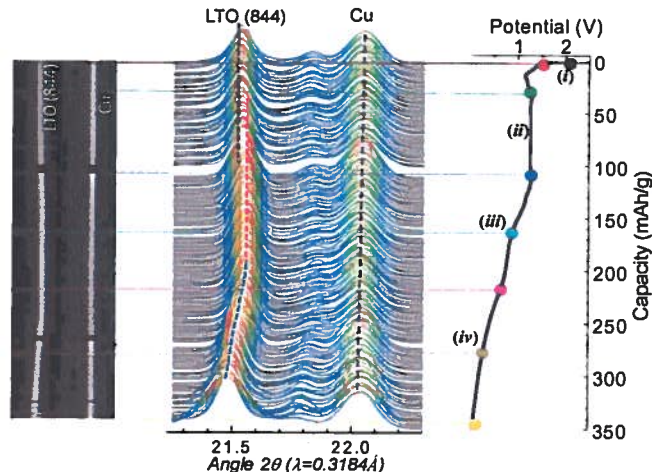


Fig. 2. Phase evolution of micron-sized LTO, as a function of discharge state between 2.0 V - 50 mV by *in-situ* synchrotron XRD. The position of the LTO (844) peak was used to resolve the subtle structural changes occurring during lithiation. The position of the copper peak (current collector) was used as an internal reference.

Cathodes: In 2011 we developed a new approach for studying the synthesis of Li battery electrode materials in real time using synchrotron techniques. A specially designed quartz capillary reactor (Figure 3a) was designed to track the hydrothermal synthesis of lithium iron phosphate (from precursors to product) using time-resolved *in-situ* synchrotron X-ray diffraction (Figure 3b). The reaction kinetics were determined by tracking the intensity of the Bragg reflections from the precursors and the products (Figure 3c). We provide the first evidence in support of a dissolution–reprecipitation process for the formation of LiFePO_4 , which occurs at temperatures as low as 105°C and appears to be a 3-D diffusion-controlled process. Lattice parameters and their evolution were monitored *in-situ*, as well as the formation of anti-site defects and their subsequent elimination under various synthesis conditions. The ability to characterize and tailor synthesis reactions *in situ* is essential for the rapid optimization of the synthesis procedures and ultimately, the development of new battery electrodes.

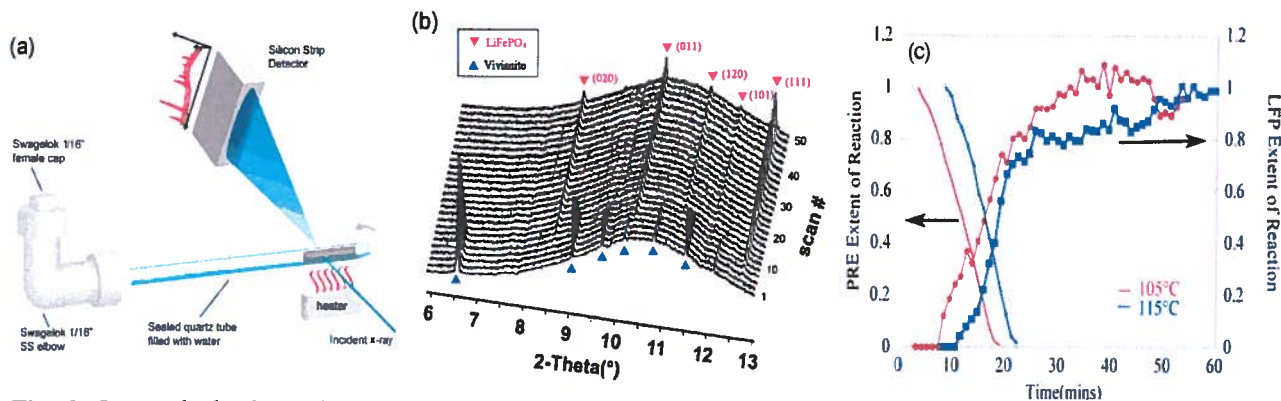


Fig. 3. *In-situ* hydrothermal synthesis of LiFePO_4 showing (a) *in situ* capillary reactor (b) time-resolved XRD patterns and (c) the reaction rates during the transformation of vivianite to LiFePO_4 at 105°C and 115°C.

Bioconversion of Lignocellulose to Ethanol and Butanol Facilitated by Ionic Liquid Preprocessing

LDRD Project 09-002

A.J. Francis, J. F. Wishart and J. Dunn

PURPOSE:

The overall goal is to develop a comprehensive process for bioconversion of lignocelluloses to ethanol and butanol using ionic liquids (ILs) as a pretreatment step followed by fermentation by *Clostridia*. The specific objectives of this project are to (i) develop a simple and low cost pretreatment process using physical-, chemical- and biochemical- based methods to convert lignocellulose to fermentable substrates by the anaerobic fermentative bacteria *Clostridia*. This project will advance the fundamental knowledge of potential application and development of environmentally benign new materials for biofuel production.

APPROACH:

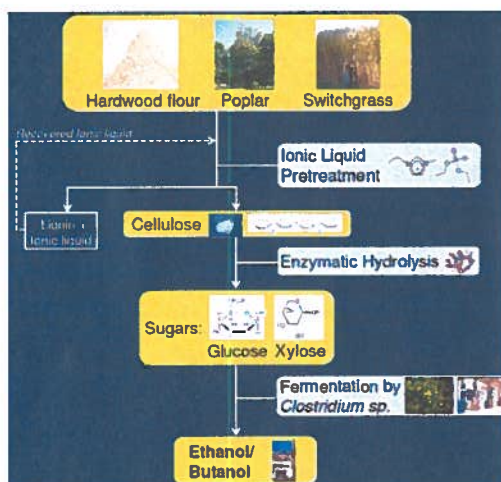


Fig. 1. Biomass conversion process flow chart.

- Ionic liquids (ILs), a new class of solvents, are known to solubilize cellulose and facilitate its separation from lignin.
- We are developing materials and methods to use ILs for the deconstruction of lignocellulose, yielding readily fermentable feedstocks for *Clostridium* to produce ethanol, butanol and hydrogen (Fig. 1).
- This is a greener approach compared to the toxic and acidic chemicals used currently for pretreatment.

This is a multidisciplinary collaborative project involving microbiologists, biochemist, molecular biologists, and chemists (physical, organic and analytical). Other members of the group included C. J. Dodge, M. Thomas, A. Gupta, and Y.V. Nancharaiah.

TECHNICAL PROGRESS AND RESULTS:

Ionic Liquid (IL) Pretreatment of Lignocellulosic Biomass. Dialkylphosphate ionic liquids 1,3-dimethylimidazolium dimethylphosphate [MMIM][DMP], 1-ethyl-3-methylimidazolium diethylphosphate [EMIM][DEP], and 1-butyl-3-methylimidazolium dibutylphosphate [BMIM][DBP] (Fig. 2) were investigated for pre-processing of biomass. These ILs are less viscous, cheaper and more stable than 1-ethyl-3-methylimidazolium acetate [EMIM][Ac], which

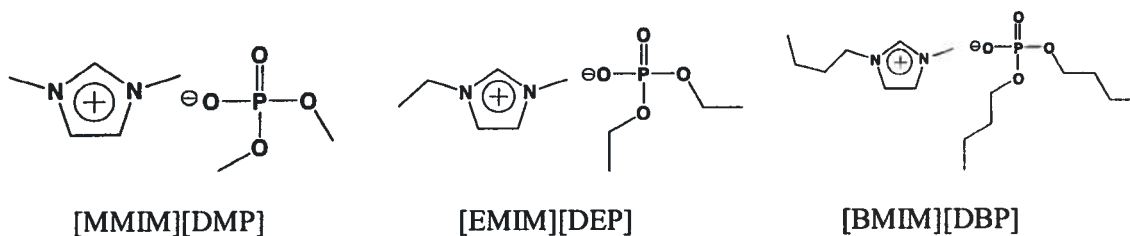


Fig. 2. Dialkylphosphate ILs for processing of lignocelluloses.

has been frequently used in cellulose dissolution studies. Of the imidazolium based ILs examined, [EMIM][DEP] showed the highest dissolution of hardwood flour. FTIR and SEM analysis of recovered cellulose showed reduction in lignin content and amorphous nature.

Effect of ILs on cellulase and β -glucosidase enzyme activities. We tested the effect of [EMIM][Ac], [EMIM][DEP], and [EMIM][Cl] on cellulase, β -glucosidase, and recombinant enzymes (BgLA, CelC, CelO) activities. The IL concentrations tested ranged from 1-40%. Higher concentrations of ILs affected all the enzymes tested significantly while the lower concentrations had little effect. Cellulase and β -glucosidase enzyme activities were not significantly affected in the presence of lower concentrations (<5%) of ILs.

We also investigated the activity of four metagenomic enzymes and an enzyme cloned from the straw mushroom, *Volvariella volvacea* in the following ILs, 1,3-dimethylimidazolium dimethyl phosphate, [MMIM][DMP], 1-ethyl-3-methylimidazolium dimethyl phosphate, [EMIM][DMP], [EMIM][DEP] and [EMIM][Ac]. Activity was determined by analyzing the hydrolysis of para-nitrobenzene carbohydrate derivatives. In general, the enzymes were most active in the dimethyl phosphate ionic liquids, followed by acetate. The activity decreased sharply for concentrations of [EMIM][DEP] above 10% v/v, while the other ionic liquids showed less impact on activity up to 20% v/v. These results show a substantial tolerance by the enzymes for the presence of ionic liquid residues, indicating that enzymatic saccharification (hydrolysis) of cellulosic materials can proceed under a wide range of process conditions. One of our goals is to recover and reuse of the attached enzyme from matrix after cellulose digestion in the presence of ILs.

Effect of ILs on growth of *Clostridium* sp and modulation of fermentation products by methyl viologen. We investigated the effect of ILs on growth of *Clostridium* sp and found that glucose fermentation was not affected in the presence of <2.5 g/L [EMIM][Ac], [EMIM][DEP] and [MMIM][DMP]. The addition of exogenous electron shuttle compound methyl viologen (MV) to the medium enhanced ethanol- and butanol-production by 28- and 12-fold, respectively with concomitant decrease in hydrogen, acetic- and butyric-acids compared to MS medium. The results show that MV addition affects hydrogenase activity with a significant reduction in hydrogen production and a shift in the direction of electron flow towards enhanced production of ethanol and butanol.

Fermentation of IL-pretreated hardwood flour, switch grass, and yellow poplar biomass by *Clostridium* sp. Saccharification of three IL pretreated lignocellulosic biomass yielded simple sugars (Table 1).

Table 1. Production of reducing sugar after enzyme hydrolysis and IL pretreatment of biomass

Substrate	Dry Weight (g)	Cellulase (mg)	Reducing Sugar (g/L)
Hardwood Flour	3.62	4.32	12.50
Yellow Poplar	4.50	6.84	8.44
Switchgrass	6.50	10.80	11.32

Clostridium sp fermented the IL pretreated hardwood, Poplar, and Switchgrass biomass cellulose hydrolysates to butyric and acetic acids as the major fermentation products. Modulation of the fermentation products by addition of electron shuttle compounds or genetic manipulation of the bacterium should result in the production of butanol and ethanol.

Organic Photovoltaics: Nanostructure, Solvent Annealing and Performance

LDRD Project 09-003

B. Ocko, C.T. Black and R. Grubbs

PURPOSE:

Organic photovoltaic devices (OPV) hold great promise as active elements in next-generation solar cells. Two significant factors both largely structural in origin limit the efficiency of organic photovoltaic devices, insufficient interfacial surface area between the donor and acceptor and low charge mobility and high recombination rate. Understanding these issues may lead to improved OPV devices with higher efficiency.

APPROACH:

Our approach to improving the performance of OPV devices involves (1) developing new materials, (2) providing increased control the nanoscale phase separation and (3) improving the internal microstructural characteristics of the material. The synthesis effort is led by Barney Grubbs (CFN/SUSB), the electronic device characterization is led by Chuck Black (CFN), and the x-ray scattering effort is led by Ben Ocko (CMPMS).

TECHNICAL PROGRESS AND RESULTS:

Nano-structured architectures:

We are investigating the use of nano-structured architectures to better understand and improve the performance of Bulk Heterojunction (BHJ) OPV devices. We are carrying out parallel approaches, as detailed below, to control the nanoscale architectures.

- (1) We are working to control the chain packing orientation of semiconducting P3HT by confining the material within large-area nanostructured surfaces patterned using electron-beam lithography. Through combined implementation of a space saving vertical channel device architecture and control of molecular orientation, we have demonstrated a polymer semiconductor Field Effect Transistor (FET) with high current drive (>30 mA/cm²) operating at one-volt power supply voltage. Performance of the vertical device with a sub-micron channel length shows good scaling behavior, comparing well with that of longer-channel planar FETs made from the same P3HT even though current flows in orthogonal directions in the two devices. Through analysis of Using Grazing Incident Angle X-ray Scattering (GIAXS) measurements, the polymer molecular chain packing reorients by 90 degrees from that of a planar film upon grating confinement. (Nature Nanotech, submitted).
- (2) We are investigating the use of nanoimprinting in fabricating BHJ devices. This process has advantages over conventional BHJ including larger Donor/Acceptor (D/A) interfacial areas, fewer shunt paths, and preferred orientation. We have now optimized the temperature and pressure for the imprinting process and successfully fabricated large area nano-grating structures of pure P3HT. We have obtained detail structural information including the periodicity, pattern height and side-wall slope angle of P3HT nano-gratings from GIAXS measurements. These show faithful pattern transfer from the master. Our results also revealed the reorientation of the P3HT crystalline domains from edge-on to face-on conformation. (ACS Nano, 2011)
- (3) We have also been imprinting P3HT/PCBM blends. We observed a consistent and substantial improved power conversion efficiency of the imprinted, inverted BHJ devices relative to similar devices made without nanoimprinting. Face-on oriented P3HT domains were induced by the imprinting process compared with the edge-on orientation that was found for the devices without

imprinting. The improved efficiency in imprinted devices appears to be correlated with both the larger interfacial area for charge collection and the P3HT reorientation. (paper in preparation)

- (4) We have nanostructured the electron-blocking layer (EBL), deposited directly on the ITO, through the use of water vapor assisted nano-imprint lithography and this has the potential to increase the interfacial area with the BH thereby reducing the shunt resistance. The excellent fidelity of the pattern transfer from the master template to EBL was confirmed by small angle GIAXS measurements. (submitted to Adv. Mat. Comm.). We have also filled the nano-imprinted EBL layers with blended materials and investigated their structure with wide-angle GIAXS.
- (5) We are using chemically nano-patterned substrates to control the phase-separation of OPV thin-films on a sub-100 nm lengthscale. These were fabricated by oxidation nanolithography of methyl-terminated self-assembled monolayers. These chemical patterns have been demonstrated to direct the phase-separation of polymer:fullerene blends due to the differential affinity of the blend components towards the methyl and carboxylic-terminated surface domains. Tapping-, contact-, and conductive-mode Atomic Force Microscopy studies on the effect of pattern feature size on the 3D morphology of the phase-separated blends have been conducted. These studies indicate that the chemical patterns are effective at directing the 3D morphology of P3HT:PCBM blends, but that the features in the blend films exhibit significant line edge roughness for films with features of > 200 nm. We are currently working to expand upon these results with new materials combinations and large-area patterned with e-beam lithography (paper in preparation).

Chemical Synthesis:

We have developed a method for the preparation of P3HT functionalized with a low percentage of azide functional groups that allow photo-cross-linking of the polythiophene domains of OPV devices. Our initial structural and device studies suggest that functionalizing 5 mol% of the polymer repeat units does not significantly affect polythiophene structure or device performance in BHJ devices. Photo-cross-linking enables us to stabilize the polymer layer so that we can introduce nanometer-scale features in the polymer layer that will persist. (Macromolecules, submitted)

We have also developed methods for the synthesis of new tellurophene/diketopyrrolopyrrole-based donor-acceptor molecules and polymers. We are currently investigating the optical, electronic, and energy conversion properties of these new materials and devices constructed from them. A manuscript comparing the properties and performance of thiophene, selenophene, and tellurophene analogues of these molecules is in preparation.

Push-Pull Polymers:

PCDTBT, a polycarbazole derivative, is one of the best performing semiconducting polymers exhibiting solar conversion efficiencies as high as 7.2% when used in bulk heterojunction devices. We have discovered the formation of bilayer ordering in PCDTBT and postulate that this structural motif is a direct consequence of the polymer's molecular design. This bilayer motif is composed of a pair of backbones arranged side-to-side where the alkyl tails are on the outer side. This is in stark contrast to the monolayer ordering found in other conjugated polymers. The crystalline bilayer phase forms at elevated temperatures and persists after cooling to room temperature. The existence of bilayer ordering may guide the synthesis of new materials with improved optoelectronic properties. (Nature Communications, submitted)

Surface Chemistry and Electrochemistry of Ethanol

LDRD Project 09-004

R. Adzic, J. Hanson, P. Liu, J. Muckerman, J. Rodriguez and M. White

PURPOSE:

The goals of this project are to understand the fundamental surface chemistry and catalysis of ethanol associated with its use as a source of renewable hydrogen (reforming), its direct synthesis as a liquid fuel from renewable sources of “syn gas” (CO/CO₂/H₂) and its use as a fuel for direct electrooxidation in fuel cells (DEFC). This effort is a response to the global need for an alternative fuel which can be generated from renewable sources and that can also serve as chemical source of stored energy for transportation or electrical power. This interdisciplinary program involves the close collaboration of scientists in surface science, catalysis electrochemistry and theory and is well-positioned to provide new approaches to alternative fuels that support BNL’s energy mission and respond to expected DOE-BES initiatives in catalysis for energy applications.

APPROACH:

Ethanol has been spotlighted as a source of clean, sustainable and readily used transportable fuel and it currently constitutes 99% of the biofuels produced in the United States. In addition to its use as a direct replacement for gasoline, ethanol holds significant potential for use in fuel cells for generating electrical power. Direct production of ethanol from fermentation of biomass, however, suffers from poor efficiency such that bio-ethanol could at best only supplement current needs for liquid fuels. Moreover, the direct electrooxidation of ethanol ($C_2H_5OH + 3H_2O \rightarrow 2CO_2 + 12H^+ + 12e^-$) suffers from slow kinetics even with the best available catalysts in current fuel cell designs. To address these issues, we propose to develop new catalysts for (1) the synthesis of ethanol from renewable sources of “syn gas” that are more readily scalable for industrial production; (2) the low temperature reforming of ethanol as an on-board source of hydrogen for powering fuel cells; (3) improving the performance of the DEFC. In addition to identifying new catalytic materials, we need to understand the surface reaction mechanisms which could tell us how to selectively make or break the C-C bond in ethanol in order to avoid intermediates or products that act as catalyst poisons, rate-limiting traps or unwanted products.

The work is being accomplished through the coordinated efforts of several groups with expertise in the surface science of model nanocatalysts (Hrbek, Rodriguez White), in situ catalyst characterization (Rodriguez, Hanson, Adzic, Zhou), electrochemical methods (Adzic, Zhou) and ab initio theory (Liu, Muckerman). Catalyst materials to be studied will generally consist of nanoparticles of a metal (e.g., Rh, Pd, Pt) or metal alloy (e.g., Pt/Rh, Pt₃Sn, PtMo) deposited on a metal oxide support (e.g., CeO₂) or onto a metal electrode (Pt, Rh). Our work will address the exact role of the metals and oxide in the catalytic processes and investigate the importance of nanoparticle size, and redox ability of the metal oxide components (CeO_x or SnO_x). This work builds on recent successes in the use of metal-ceria nanocatalysts for hydrogen production and the development of a novel ternary catalyst (Rh/Pt-SnO₂) for the electrooxidation of ethanol.

Characterization of the catalysts under reaction conditions make extensive use of unique *in situ* x-ray probes at the NSLS (AP-XPS, XRD, XAS) and atomic imaging probes at the CFN (e.g., HRTEM). In addition, a new instrument has been developed as part of this project that provides link well-defined model nanocatalyst prepared under controlled UHV conditions with their performance under realistic reaction conditions.

TECHNICAL PROGRESS AND RESULTS (FY11)

- Theoretical DFT calculations were carried out to gain a better understanding of the ethanol decomposition reaction on Rh metal, which is one of the best known catalysts for the electrooxidation and steam reforming of ethanol. Our results show that the most probable reaction pathway is through an oxametallacycle species, which is the precursor for breaking the C-C bond in ethanol. The complete reaction leads to the production of carbon monoxide (CO) and surface carbon (C) which can deactivate the Rh surface. Additional calculations show that alloying Rh with other metals (Pt and Pd) weakens the carbon-Rh bond which aids in the removal of surface carbon and facilitates ethanol combustion (Choi, Y.; Liu, P. "Understanding of ethanol decomposition on Rh(111) from density functional theory and kinetic Monte Carlo simulations," *Catalysis Today* **2011**, *165*, 64.)
- The newly constructed instrument funded by this program was used for studies aimed at establishing the role of the metal oxide (SnO_x) component in the ternary Rh/SnO_x/Pt electrocatalyst recently discovered by Adzic and co-workers. Surface science techniques were used to prepare and characterize model catalysts composed of SnO_x nano-islands deposited on a Pt surface. Their activity for ethanol oxidation was tested in an electrochemical reaction cell without exposure to air contamination. The catalytic activity of the Pt surface is significantly enhanced with addition of SnO_x nanoislands, with the highest activity occurring for the smallest nanoislands. The latter is attributed to unique surface sites on the SnO_x nanoislands, which activate water dissociation and the removal of CO which poisons the Pt surface (Zhou, W.-P.; Axnanda, S.; White, M. G.; Adzic, R. R.; Hrbek, J., "Enhancement in Ethanol Electrooxidation by SnO_x Nanoislands Grown on Pt(111): Effect of Metal Oxide-Metal Interface Sites," *The Journal of Physical Chemistry C* **2011**, *115*, 16467.)
- Density functional theory (DFT) calculations and Kinetic Monte Carlo (KMC) simulations were employed to investigate the methanol synthesis reaction from CO₂ hydrogenation (CO₂ + 3H₂ → CH₃OH + H₂O) on metal-doped Cu(111) surfaces. Our calculations showed that the overall methanol yield increased in the sequence: Au/Cu(111) < Cu(111) < Pd/Cu(111) < Rh/Cu(111) < Pt/Cu(111) < Ni/Cu(111). The calculations show that an ideal Cu-based catalyst for alcohol synthesis should be able to hydrogenate dioxomethylene easily and bond CO moderately, being strong enough to favor the desired CO hydrogenation rather than CO desorption, but weak enough to prevent CO poisoning. In this way, the methanol production via both the formate and the RWGS+CO-Hydro pathways can be facilitated. (Yang, Y.; White, M. G.; Liu, P., "Theoretical Study of Methanol Synthesis from CO₂ Hydrogenation on Metal-Doped Cu(111) Surfaces," *Journal of Physical Chemistry C*, in press).
- Recently, a Pd/Ga₂O₃ catalyst has been found to be effective for the hydrogenation of CO₂ to form methanol and the proposed mechanism suggests that it may be useful for the synthesis of higher C₂-C₄ oxygenates as well, including ethanol. In order to attain a better understanding of the electronic and structural properties of model Pd/Ga₂O₃ nanocatalysts, we explored the possibility of preparing highly ordered galia thin films by oxidation of a CoGa(110) single crystal. Previous STM studies suggested that oxidation of the CoGa(110) surface would result in a uniform galia film, however, XPS and ISS studies using the new surface science apparatus developed in this project showed that oxidation by O₂ or NO₂ leads to large galia islands with open areas exposing both Ga and Co metal atoms from the substrate. (O'Connor, D. C.; Axnanda, S.; Lofaro Jr., J. C.; Zhou, W; White, M. G.; "Synthesis and Characterization of Surface Oxide Films on CoGa(100)," submitted for publication).

Synergistic Interactions Between Poplar and Endophytic Bacteria to Improve Plant Establishment and Feedstock Production on Marginal Soils

LDRD Project 09-005

Daniel van der Lelie, Safiyh Taghavi, Lisa Miller, Richard Ferrieri, Alistair Rogers and Wei Zhu

PURPOSE:

To use a systems biology approach to understand, model and improve the growth of bioenergy feedstock plants on marginal soils without competition for agricultural resources. The project is characterized by the following elements:

- Understanding the plant growth promoting effects that endophytic bacteria have on their poplar host plant, with special emphasis on root formation and its effect on nutrient acquisition and growth on marginal soil.
- Explore plant-endophyte interactions to make biomass production (feedstock and food) on marginal soils economically feasible.

APPROACH:

We are following an integrated research plan to understand at the level of the genome, transcriptome and metabolome the interactions between poplar and two well-characterized endophytic bacteria, *Enterobacter sp.* 638 and *Pseudomonas putida* W619. These two endophytes were chosen, as preliminary genome analysis reveals the existence of distinct mechanisms by which these bacteria can affect the growth of their host plant: IAA production by *P. putida* W619 and production of acetoin and 2,3-butanediol by *Enterobacter sp.* 638. Our hypothesis is that both strains will affect the expression of different regulatory pathways in poplar, but that their altered expression will ultimately result in the same beneficial effects on plant growth and development, and nutrient acquisition. The involvement of different regulatory pathways also opens the possibilities for synergistic effects.

TECHNICAL PROGRESS AND RESULTS:

- **Metabolite analysis** (Years 1-2): *Our hypothesis is that the growth of Enterobacter sp. 638 and P. putida W619 in the presence or absence of poplar will result in changes in metabolite profiles, both for bacteria and plant, especially for compounds involved in plant-microbe signaling and plant growth promoting compounds.* The production of the plant growth promoting compounds acetoin and 2,3-butanediol by *Enterobacter sp.* 638 was specifically induced by the presence of sucrose in the medium. Similar results were observed for other related strains; however, 2,3-butanediol synthesis was not observed for all strains tested, showing that this is a unique property of strain 638.
- **Transcriptome analysis** (Years 1-3): *We expect changes in gene expression to be directly linked to changes in the plant's nutrient status, metabolite production, and altered plant growth and development.* As an alternative to microarray studies, that gave questionable results, comparative whole transcriptome sequencing was performed on cultures of *Enterobacter sp.* 638 grown on sucrose and lactate. Transcriptome analysis confirmed that growth in the presence of sucrose triggers a response in *Enterobacter sp.* 638 that seems to mimic its plant associated life style. This response seems to be controlled via quorum sensing and causes a change from planktonic growth to biofilm formation, essential for plant colonization. It also affects the expression of pathways involved in plant colonization and nutrient acquisition. This was quite surprising, as under the tested conditions nutrients were

not limited. This seems to indicate that strain 638 is anticipating nutrient limitation when colonizing and stimulating the growth of its host.

- **Plant growth promoting effects** of various endophytes were tested for other bioenergy feedstocks and food crops, including tomato, tobacco, peppers and sunflower. For all plant types, beneficial effects of plant growth and development were observed after inoculation with *Enterobacter* sp. 638, and included the induction of systemic drought resistance in peppers, earlier flowering of sunflowers, 10% increase in overall yield of tomato, and a doubling in biomass for tobacco.
- **Effects of endophytic colonization on the carbon and nitrogen status** of their poplar host. *Many of the signals for the plant's C and N status are well know regulators of gene expression (sugars, nitrate, amino acids). We expected to see changes in gene expression that are directly linked to changes in the plant's nutrient status, resulting from improved plant growth and development.* Using a high-throughput enzyme screening platform we found that *Enterobacter* sp. 638 is impacting central C and N metabolism and increasing the availability of amino acids for protein synthesis. These results were confirmed in year 2. Field experiments, performed in a hoop house, further confirmed the beneficial effects on strain 638 on the growth and development of poplar. After one year, inoculated plants had 25% more biomass than uninoculated control plants. It should be noted that the increase in biomass was observed for all plant parts tested.
- **Biomass Composition.** An unexpected observation was that the biomass of poplars inoculated with strain 638 was higher in cellulose at the expense of lignin. Since lignin is a main contributor to the recalcitrance of wood, it is expected that the biomass of the inoculated poplar trees will be more suitable for biomass production.
- **Data Integration and Modeling (Years 1-3).** Transcriptome data were analyzed via cluster analysis in order to identify common trends in expression profiles. This analysis will serve as the basis to develop comprehensive models.

Milestones from the start date of project:

Month 6: List of candidate genes for *Enterobacter* sp. 638 and *P. putida* W619 that are involved in endophytic colonization of poplar, including biosynthetic pathways for plant growth promoting compounds - completed.

Month 12: Used microarrays to study the transcriptome of *Enterobacter* sp. 638 and *P. putida* W619 - completed.

Month 18: Identify growth regulating compounds and other secondary metabolites that play a role in plant-microbe communication and plant growth regulation - completed.

Month 18: Identify genes and pathways that are potentially involved in the regulation of plant growth and endophytic colonization - completed.

Month 24: Description of the effects of endophytic colonization on the carbon and nitrogen status of their host plant – completed (Rogers et al., Global Change Biology Bioenergy, in press).

Month 30: Collection of endophytic strains mutated in genes involved in the synthesis of plant growth promoting compounds – targets for mutagenesis have been identified. This work was not completed at BNL due to our departure. However, we are trying to knock out some of these genes at RTI.

Month 30: Confirmed the involvement of previously identified genes and pathways (based on transcriptome and metabolome data) in the regulation of plant growth and endophytic colonization.

Month 30: A series of comprehensive models that describe the genetic networks necessary for the successful symbiotic interaction between endophytic bacteria and their poplar host plant. Preliminary data were obtained in collaboration with S. Maslov (BNL).

Petascale Data Mining for BNL's Data Intensive Sciences

LDRD Project 10-001

Dantong Yu

PURPOSE:

Our goal is to research and develop techniques of data management and data mining to support BNL's data-intensive science applications, such as climate modeling, computational biology, and extend the outcomes to other multidisciplinary data modeling and processing programs. Particularly, the focus of our work is to assure the availability of suitable data-mining techniques for identifying patterns and structures in massive datasets from these exemplary applications, along with high-performance tools for the particular application that will allow scientists to gather, organize, analyze, and model large heterogeneous datasets. The research outcome will strengthen Brookhaven National Laboratory's expertise over a broad spectrum, from domain knowledge in data-intensive sciences to the commensurate data modeling and analysis. The success of the project will help BNL to establish a scientific data-management program based on a strong partnership between science and computational research groups. These science groups include the Atmospheric Science Division and the Biology Department.

APPROACH:

Data-intensive applications, such as high energy and nuclear physics (HENP), astrophysics (LSST), computational biology, and climate science will generate exabytes of data in the next five years. This prospective explosive growth in storing and processing data poses new critical requirements for data mining technologies and automated tools. New capabilities sorely are needed to intelligently assist scientists in transforming such large volumes of data into useful knowledge, and to expedite scientific discoveries. Accordingly, we propose to develop a new generation of tools and techniques for mining data and acquiring knowledge using computational biology and climate modeling as example applications in a multidisciplinary, heterogeneous data-modeling and data-processing setting.

The fundamental challenge for data mining in today's data-intensive science environment is not in moving small subsets of homogeneous data into a computing cluster to run individual analyses and knowledge derivation routines. Rather, we face a system-level challenge to deal with complex mining processes simultaneously for thousands of scientists on their heterogeneous peta/exabyte datasets, and each of the data mining process has different requirements in time and accuracy. The following four items summarize the project's scope and milestones:

1. Devise real-time and offline scalable data-analysis methods enabling researchers to identify and select critical features from multiple features,
2. Improve existing methods, and devise new ones for statistical sampling and clustering that effectively extract known and unknown patterns, and support complex searches,
3. Enhance overall performance in data management, and parallelize the proposed data-mining processes to ensure better performance, and,
4. Transform the mined data-products into statistical models so to best represent knowledge in the presence of data uncertainties, inconsistencies, and incompleteness.

Our technical approach is to extend the successful Google MapReduce computing paradigm to solve complex mining problems. We will develop the proposed items in MapReduce's open-

source version, viz. Hadoop. The data mining and visualization techniques generated in this project will be deployed, evaluated, and vetted in close collaboration with scientists from two representative projects, viz., BNL's Climate Studies, and the DOE's system biology knowledge base project to manage large datasets, build data models, and to compare models with observations.

We hired a Postdoctoral Research Associate (Shinjae Yoo) to conduct his research in petascale data-modeling at the New York Center for Computational Science. We also are sponsoring and co-advising graduate students in data modeling and mining.

TECHNICAL PROGRESS AND RESULTS:

We collaborated with BNL's Atmospheric Science Division to investigate data-assimilation methods and modeling evaluation techniques. Formed a virtual climate visualization center integrating complementary areas of expertise, including remote sensing, climate modeling, computer science, and statistics. Collaborated closely with the FASTER team (Fast-physics System Testbed and Research) to establish, test, and assess techniques for comparing the climate models and observational data. Furthermore, we collaborated with research groups in BNL's Biology Department and the Cold Spring Harbor Laboratory for sequencing data analysis. The itemized contributions are listed as follows:

1. Doppler RADAR clustering: Successfully finished the first two iterations of preliminary data-analysis. Identified the preprocessing problems associated with our algorithms, and worked on those issues.
2. Climate Modeling with data clustering: Completed the pilot analysis of Doppler radar data. Based on the findings from this analysis, we continued to implement distributed clustering algorithm for the whole set of this data.
3. Knowledge base for system biology: Acquired funding from the DOE Office of Biological and Environmental Research. Developed software of gene network analysis.
4. Started to design and implement a solar power forecasting system to collect environmental data, to model the impact of weather on solar output via data mining techniques, to monitor and predict solar output, and to enable smart grid to schedule electricity in real-time in the power-grid system.

Solar Energy Source Evaluation for Smart Grid Development

LDRD Project 10-006

Meng Yue, Mike Villaran and Robert Bari

PURPOSE:

The purpose of the proposed study is to evaluate the stability, reliability, and power quality of the electrical grid when it is supplied by an increasingly significant contribution from intermittent solar energy generation. The study will also take advantage of a planned BNL solar facility. Systematic approaches featuring probabilistic stability assessment, coordinated control design, and dynamic inclusion of communication infrastructure will be developed. An existing integrated power system analysis tool, EPTOOL, previously developed at BNL, will be expanded and enhanced to facilitate the study of future Smart Grid development.

APPROACH:

The proposed approaches and tasks are discussed for the individual objectives of this study below. The novel features of the proposed approaches include (1) a stability assessment of the grid using of a probabilistic model of a PV system that accounts for its variability; (2) an advanced coordinated wide-area controller design; and (3) an incorporation of communication links into the power system dynamics. In addition, the integrated tool EPTOOL will be expanded and enhanced to facilitate the study of issues related to the Smart Grid development. The plan is to use the BNL solar energy system to provide parameters and data needed for developing and validating models for the PV system. However, hypothetical data can always be used to demonstrate the proposed approach.

TECHNICAL PROGRESS AND RESULTS:

This LDRD has been extended to a three-year program without additional cost. The only activity in the first half year of 2011 was to recruit a postdoc. The progress reported here was made during the second half year of 2011. In the up to date study of this project, an overall PV generation system was built in EPTOOL including the dynamic models of a generic solar generation model, a BESS model, a power conditional systems (PCS) for the PV and BESS and the associated control systems. The interfaces between the PV generation system and the power system were also developed to study the impacts of the intermittent PV generations on grid operations.

The major achievements of this study in 2011 include (1) development of a siting scheme of the PV plants in terms of losses reduction across the transmission lines; (2) the evaluation of impact of penetration level of the PV generations on the grid in terms of the frequency deviations; and (3) the frequency regulation capability of the PV generation with assistant of the incorporated BESS.

In order to select location for PV generation, load flow was performed and active and reactive power losses were calculated and ranked. To reduce the overall power losses, two PV plants are planned to be connected to receiving ends of the two transmission lines with the highest losses, respectively. In this study, the capacities of these two PV plants are identical with rating value of 430 MVA (under standard environment). With the load condition remaining unchanged, power flow is re-calculated and results validated a significant amount of reduction in power losses across the entire power system.

A transient (due to fluctuation of the solar irradiance) study was also performed to demonstrate the effectiveness of the controllers designed for the BESS and the grid-connected inverters of the solar PV generation systems after determining their locations. The frequency variations at Buses 130 and 119 (i.e., the receiving ends of the two transmission lines with the highest losses) are shown in Figure 1(a). The frequency deviations in this case study are very small because that the total capacity of the PV plants up to 8.6 p.u. (on a 100 MVA base) is insignificant compared with that of the overall system, 2428.3 p.u. A set of scenarios were studied with increasing penetration levels of the solar generation. The maximum frequency deviation, either from Bus 130 or 119, under each case is recorded and plot in Figure 1(b). The PV penetration level for this case study can be increased up to 25.4% while the frequency deviation is still less than 5%..

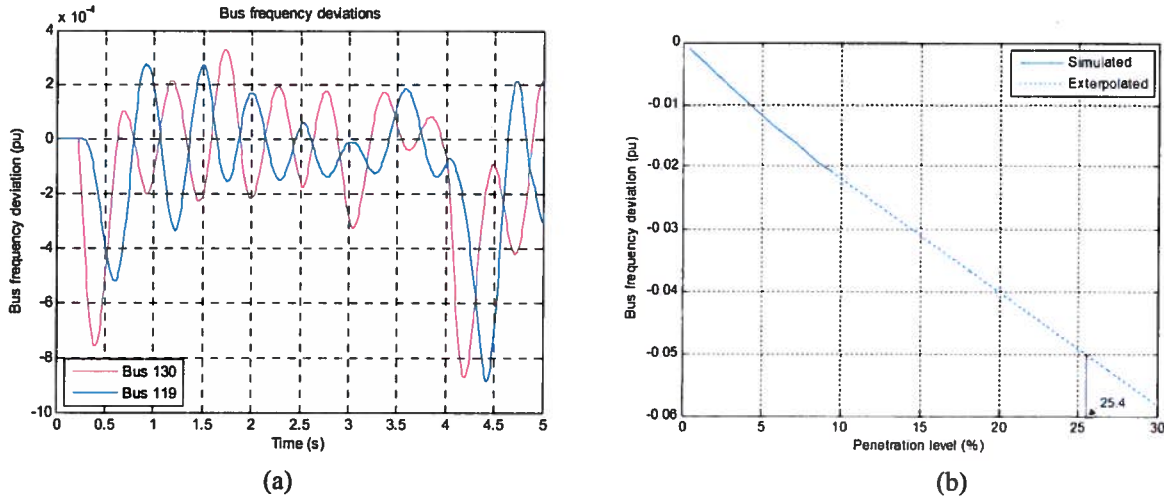


Fig. 1. (a) Frequency deviations at Buses 130 and 119 with a low PV penetration level 0.357% without BESS, and (b) the maximum frequency deviations vs. penetration levels.

The frequency regulation function designed for the BESS was investigated. Based on the PV generation incorporated 50-machine system, two identical BESSs are connected to the same buses where the PV plants are attached. The frequency profiles at Buses 130 and 119 are plot in Figure 2. Compared with the figure given in Figure 1(a), it can be found that the frequency deviations with assistance of the BESS are much less than that without regulations.

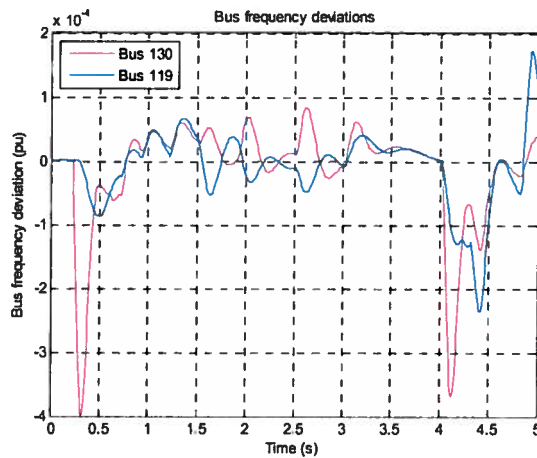


Fig. 2. Frequency deviations for a low PV penetration level 0.357% with BESS.

High Throughput Quantitative Biochemical Phenotyping

LDRD Project 10-007

Alistair Rogers

PURPOSE:

This LDRD will establish a platform for high throughput biochemical phenotyping. There are only three labs world-wide using robots to conduct automated biochemical and enzymatic assays, Dr. Rogers' lab is one of them. If successful this LDRD will establish Brookhaven as a major player in large scale phenotyping projects. Planned publications will demonstrate the capability of the platform to address critical questions in global change plant biology. The current focus of the research is central C and N metabolism in plants. Therefore, the platform is focused on measuring parameters associated with C and N metabolism. This complements existing analytical assets in plant systems biology at Brookhaven and can be readily adapted to address other challenges in plant biology at the intersection of climate, energy & environment.

APPROACH:

The project has three components (1) Set up a robot that is capable of conducting high throughput biochemical phenotyping, (2) identify and develop assays for diagnostic parameters of interest and adapt them to a 96-well format, and (3) use the platform to address science questions that will demonstrate the utility of the platform. In support of components (1) and (2) Dr. Rogers' is collaborating with Dr. Gibon (INRA-Bordeaux) who pioneered the use of robots to conduct biochemical assays in plant tissue. In support of component (3) Dr. Rogers is collaborating with Dr. Leakey and Dr. Ainsworth (SoyFACE-UIUC) on a projects where soybean have been grown at elevated [CO₂] with and without water stress and at high ozone concentration and Dr. Zhu (PICB, Shanghai, China) to understand metabolic controls on yield in rice. At Brookhaven Dr. Rogers is collaborating with Dr. Schwender (Biology). He is also leveraging sampling conducted as part of his own funded research into carbohydrate profiles in loblolly pines grown at the Duke Forest FACE experiment. He recently established collaboration with Dr. Osborne (University of Sheffield, UK) to understand biomass production in C3 and C4 grasses.

TECHNICAL PROGRESS AND RESULTS:

Component 1

During the first year Dr. Rogers hired a post-doc, defined the technical specifications of the robot and purchased it. He also began renovation of his laboratory to accommodate the new equipment. This included removal of two old plant growth chambers, repairs to the flooring, and upgrades to the electrical supply and purchase of a second -80°C freezer. In the first quarter of the second year the robot was installed and commissioned. Infrastructure upgrades continued in year 2 and are almost complete. These include installation of a water supply and drainage lines to the two robots, purchase and installation of cryogenic grinders, purchase and installation of a plate reader cluster. Although this took longer than anticipated, component 1 will be completed within a few weeks.

Component 2

At the onset of the LDRD project Dr. Rogers' lab had 96-well assays for c. 25 parameters of interest in central C & N metabolism. In the first fifteen months of the project his laboratory has

expanded this to include nine parameters associated with oxidative stress, five associated with the PEP branch point in central metabolism, four associated with the C4 pathway and three additional parameters associated with N metabolism. Additional parameters continue to be added and existing assays adapted for automation.

Component 3

The assays for oxidative stress were developed in collaboration with a graduate student at UIUC and were used to understand the impact of elevated [CO₂] and chronic ozone exposure to acute oxidative stress. This work has resulted in a paper (Gillespie et al. 2011). Analysis from Duke FACE, a third season of SoyFACE and the second rice project continue and will be completed in the Q2/Q3 of FY12. The final project to be undertaken is the collaboration with Dr. Osborne. Samples from this project will arrive at BNL in Q3.

PROJECT MILESTONES

Activity	FY11			FY12			
	March	June	Sept.	Dec.	March	June	Sept.
Complete Commissioning of Robot and remaining upgrades to the laboratory				X			
Hold an "open day" for BNL scientists and interested parties to see the robot							X
Complete analysis of <i>Brassica napus</i> tissue pilot study	X						
Complete analysis for the rice project pilot study	X						
Complete analysis of three seasons of samples from the SoyFACE CO ₂ x drought experiment		X					
Complete analysis of needle samples from the Duke Forest FACE experiment			X				
Present data at national meeting (TBD)		X				X	
Submit manuscript on data from SoyFACE experiment							X
Complete analysis of fine root samples from Duke Forest FACE experiment					X		
Complete analysis for the main <i>Brassica napus</i> experiment				X			
Complete analysis for follow up rice experiment					X		
Submit manuscripts on FY12 experiments					X	X	X
Present technical and experimental progress to BER					X		X
Conduct analysis for the Sheffield Project					X	X	X

Characterization of Materials in Extreme Environments for Advanced Energy Systems Using the National Synchrotron Light Source

LDRD Project 10-008
Lynne Ecker and Lars Ehm

PURPOSE:

The goal of this research is to develop new, cross-cutting materials characterization techniques that, combined with existing BNL facilities for material testing and modeling, will impact the design cycle of a wide range of materials for advanced nuclear energy systems. A long-term goal is to develop techniques for studying nuclear energy related materials at the National Synchrotron Light Source (NSLS) that will be transitioned to a new beamline at the NSLS II. It is high risk because many of the characterization techniques used here are not well developed for materials with nuclear energy applications.

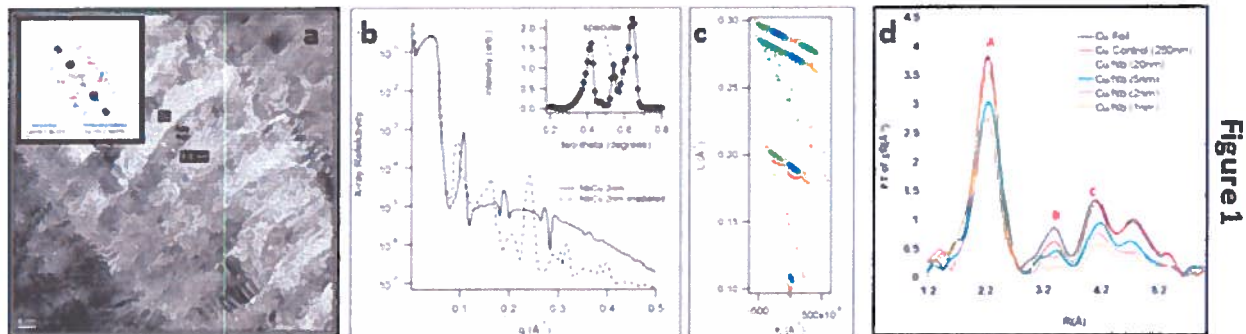
Nanocomposites

APPROACH:

Nanocomposites such as Oxide Dispersion Strengthened steels have metal-oxide nanoparticles dispersed in a ferritic matrix and utilize the metal-oxide interface as a sink for radiation-induced vacancies and interstitials. They are promising fuel cladding materials for future reactors but are difficult to study because of the low concentration and geometry of the interfaces. In order to understand the fundamental mechanisms of radiation-induced defect evolution and annihilation at interfaces, model nanocomposite systems with multilayer geometry were studied (obtained from collaboration with Dr. Amit Misra, LANL). The approach used was to utilize synchrotron-based X-ray studies including Extended X-Ray Absorption Fine Structure (EXAFS), X-Ray Reflectivity (XRR), X-Ray Diffraction (XRD) along with High Resolution Transmission Electron Microscopy (HRTEM) to study local atomic structure of nanocomposite Cu/Nb multilayer systems.

TECHNICAL PROGRESS AND RESULTS:

Cu/Nb multilayers of equal Cu and Nb layer thickness were synthesized by dc magnetron sputtering at room temperature on a Si (100) substrate. The layer thickness of Cu and Nb for Cu/Nb multilayer samples was varied from 1 nm to 20 nm, and total thickness of samples was kept constant at ~250 nm. For irradiated samples, Helium ion irradiation at 200 keV with 2×10^{17} ions/cm² at room temperature was used. HRTEM studies were performed at the Center of Functional Nanomaterials (CFN). XRD, XRR and EXAFS at the National Synchrotron Light Source (NSLS).



HRTEM (Fig. 1a) showed alternating Cu and Nb layers with atomic resolution in Cu/Nb multilayer samples. SAED analysis (inset in Fig. 1a) depicted preferential alignment of Cu (111)

and Nb (1-10) in the multilayer normal direction (dashed line) which allowed complete indexing of the diffraction pattern. XRR oscillations (Fig. 1b) showed that the irradiated film (dashed line) is significantly rougher than the as-prepared film (solid line). Local maxima at slight angles relative to the surface normal (Fig. 2B) are suggestive of buckling of the Cu/Nb multilayer samples. Diffracting planes with $d \sim 6$ and 9 nm, compatible with the observation of texture in the Cu and Nb Bragg peaks observed in SAED analysis, were also detected. Preliminary analysis of EXAFS data showed a decrease in signal intensity with decreasing layer thickness and a change in peaks' shape (Fig 1d), which can be attributed to the under-coordinated environment of Cu in thin layer samples and deviation from perfect FCC structure near Cu-Nb interfaces.

Pair Distribution Function (PDF) analysis of irradiated superalloys

Approach:

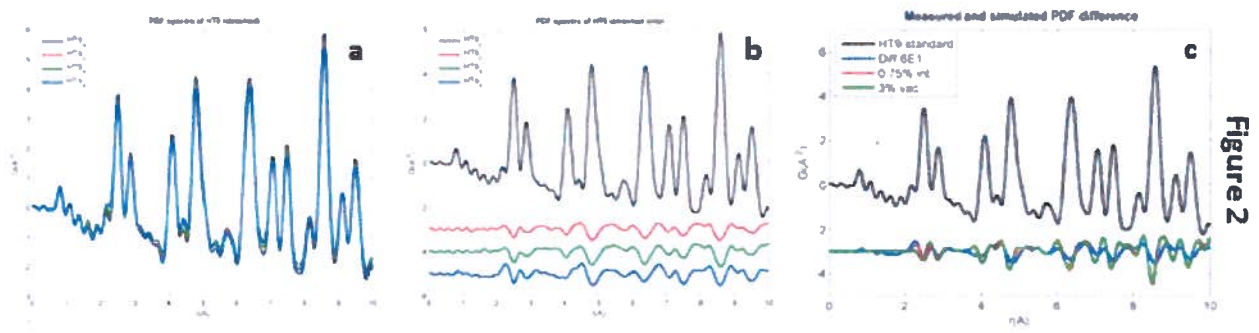
The goal for advanced nuclear energy systems is to develop materials that have a longer lifetime in high-temperature and high-radiation environments. Materials used for this research were obtained in collaboration with Dr. Stuart Malloy, LANL and are ferritic/Martensitic stainless HT-9 steel samples with neutron irradiation exposure up to a dose of 147 dpa at temperatures from 416 to 504°C. PDF analysis enables useful atomic structural information to be obtained from materials with broad and/or low-intensity Bragg peaks. Characterizing the defect structure with PDF analysis could provide a new tool to improve understanding of defect processes in materials and ultimately assist with developing better molecular dynamics (MD) simulation methods and design of radiation resistant alloys. Total scattering data for the samples was collected at the NSLS using X-ray energy of 80 KeV. MD simulations of point defects in BCC Fe were used to simulate their effect on the PDF spectrum, and were compared to the changes detected for the irradiated HT9 samples.

TECHNICAL PROGRESS AND RESULTS:

PDF spectra obtained for the HT9 samples was fitted to a BCC structure and the resulting lattice parameter (d), thermal parameter (U_{iso}) and the goodness of fit (R_w) are summarized in the Table. Larger R_w than that of the control is possibly due to the chemical short range disorder as a result of point and extended defects.

	Dose (dpa)	Temp (°C)	d (Å)	$U_{iso}(Å^2)$	R_w	R_{div}
HT9 control	0	25	2.881	0.0062	0.118	--
HT9-2E1	2.9	504	2.869	0.0050	0.149	0.110
HT9-5E1	147	441	2.870	0.0049	0.140	0.140
HT9-6E1	110	416	2.871	0.0054	0.188	0.127

The use of difference from the standard's structure gives the net changes in the samples regardless of the base structural changes. Thus, the deviation from the standard structure, R_{div} , was estimated similarly to R_w and showed a positive correlation between the deviation and the dose, which indicates larger changes in the short range atomic structure as a result of the irradiation. Preliminary MD simulation results (Fig. 2c) are in agreement with the measured data at low coupling range. For example, Fig. 2c depict better agreement of the irradiated sample (6E1, blue) with the simulated interstitials (red) than with the vacancies (green).



Development of an Ultrafast Electron Diffraction Facility for Condensed Matter Physics Challenges

LDRD Project 10-010

J.P. Hill, X. Wang, J. Murphy, C.-C. Kao, Y. Zhu and A. Cavalleri

PURPOSE:

The goal of this LDRD is to develop a unique Ultrafast Electron Diffraction (UED) instrument to study insulating ground states and fundamental photo-induced excitations in a class of materials called strongly correlated materials. The ground states in these materials are characterized by long range ordering of charges, orbitals, spins and lattice distortions. Using electron diffraction we will probe several of these ordered degrees of freedom in a single diffraction pattern, allowing us to understand how optical radiation couples to these materials and how energy is subsequently distributed. Our instrument is based on a radio frequency (RF) photocathode, providing 100 femtosecond pulses of electrons at 2-5MeV, an order of magnitude higher in energy than all existing UED instruments. At high energies, space charge effects are reduced and shorter pulses can be achieved at large pulse charge. Once operational, this instrument will form the backbone of an ultrafast program within condensed matter physics and material sciences. Based on this work, it is anticipated that a proposal for a new FWP will be submitted to DOE BES to carry out a new program in ultrafast science at BNL.

APPROACH:

The primary objective is to study the novel orderings of charge, orbital, spin and lattice distortions in strongly correlated materials and understand how optical radiation perturbs these ground states and lead to non-equilibrium phenomena. There are no instruments that can accomplish all of these tasks in a simple, compact configuration. Table-top, optical, pump-probe experiments can infer dynamics but can't singly probe a discrete degree of freedom. X-ray methods can probe single degrees of freedom but can do so only one at a time and several ordered degrees of freedom are inaccessible (they lie outside the Ewald sphere). Ultrafast electron diffraction fills this instrumentation void. Using UED, we probe several degrees of freedom independently in a single diffraction pattern, allowing us to understand how the excitation process affects different degrees of freedom on fundamental timescales.

There are several existing UED instruments capable of generating ultrafast pulses of electrons. However, in nearly every instance, these are pulsed sources based on DC acceleration of electrons with maximum achievable energies of 10s of keV to 100keV. While these instruments have contributed important science, there are several shortcomings associated with low kinetic energy electrons. Most importantly, at these energies, pulses of electrons suffer from Coulombic repulsion and hence, the pulse length is strongly dependent on the charge per pulse. Additionally, at low energies the electrons have reduced penetration depth requiring experiments to be performed at grazing incidence in reflection geometry. In recent years, questions have been raised about results obtained from these low energy systems. Specifically, it was proposed that in the grazing incidence geometry, deflection of Bragg peaks (that might imply a deformation of the lattice) could also be caused by a low density plasma near the surface of the material. These unbound electrons near the surface (photo emitted electrons) are exactly what occur when the sample is photo excited.

In collaboration with scientists from the Source Development Lab of the National Synchrotron Light Source, we have constructed a high-energy, short-pulse, electron source based on an RF photocathode. There are several advantages to using a high energy (2-5MeV) electron source. For one, electron pulse length can be finely tuned by varying the phase of the RF driving field relative to the time the electrons are emitted from the photocathode giving us fine control over the pulse length. Additionally, at high energies the increased electron penetration depth allows us to perform these experiments at normal incidence and in transmission, reducing spurious effects caused the optical excitation process.

TECHNICAL PROGRESS AND RESULTS:

During the first fiscal year of this project, we hired a post-doc, Ron Tobey and nearly completed construction of the instrument. We also carried out closely related experiments using optical-pump, Raman probe here at BNL, and optical pump, soft x-ray probe at the LCLS.

In the present fiscal year (FY11), we have completed construction of the UED apparatus. Specifically, we have achieved the following milestones:

- 1) Transported electrons down the beam path
- 2) Obtained the first powder electron diffraction pattern
- 3) Obtained the first single crystal electron diffraction pattern
- 4) Observed the first superlattice peaks from a charge density wave
- 5) Measured an upper limit of 300 fs on the electron bunch length
- 6) Delivered optical pump beam to the sample.

This represents really dramatic progress and a significant amount of effort was required to learn the operation of the system and put into careful optimization of the electron beam parameters. As part of this effort we hired a visiting post-doc, Pengfei Zhu who comes from the Institute of Physics, Chinese Academy of Sciences. He has experience in ultrafast electron diffraction and made an immediate impact in driving the commissioning of the instrument forward.

In the upcoming fiscal year (FY12), the first optical pump experiments will be carried out, likely on a CDW system. We anticipate writing two papers as a result, one focused on the instrumentation, the other on the science results that come out from this first commissioning experiment. Assuming success with these endeavors, we will be in a position to carry out the first real science experiments on strongly correlated electron systems, likely beginning with charge and orbitally ordered manganites. These experiments will complement equivalent optical pump, soft x-ray probe experiments carried out on the same materials at the LCLS. With the UED we will be able to study the charge degree of freedom, whereas the soft x-ray results probed the orbital and magnetic. Together we should have a complete picture of the energy flows in this system during the photoexcitation process.

Design of Pt-free Electrocatalysts for Fuel Cell Oxygen Reduction Reactions

LDRD Project 10-012

Peter Khalifah

PURPOSE:

The objective of this work is the synthesis and characterization of a number of novel conductive and acid-stable transition metal oxide systems to explore their potential for electrocatalysis. Although Pt-based hydrogen fuel cells have demonstrated impressive efficiencies (~60%), the current technology can never be implemented on a commercially relevant scale due to the extreme cost and the terrestrial scarcity of the platinum metal that is used to catalyze the recombination of protons with O₂ to form water in the oxygen reduction reaction (ORR). Furthermore, the ORR reaction is inefficient and requires a very large overpotential to proceed. A search for better catalysts is being pursued, integrating the materials synthesis and discovery experience of the Khalifah group with the fuel cell electrochemistry measurement expertise of the Adzic group. This search focuses on conductive transition metal oxide systems which offer the promise of activity, economy, and acid stability necessary to produce viable fuel cell systems. The search for effective new catalysts is a high-risk exploratory project, but one which can potentially offer large rewards. Success in this endeavor will provide the preliminary results necessary to compete for programmatic funding in this area, and will establish a strong collaboration between synthesis (Khalifah) and characterization (Adzic) groups in the BNL Chemistry Department.

APPROACH:

While a good deal is known about the general features of oxygen reduction reactions mediated by Pt and other noble metals, exploratory work is necessary to identify TMO materials with ORR activity, and to understand the structural and electronic features that promote this activity. What is the recipe for a good ORR electrocatalyst? Our target systems will allow the incorporation of a variety of transition metals with variable oxidation states to participate in reactions, have good electrical conductivity to avoid potential losses at the electrode, and have the ability to accommodate defects which may serve as active sites for ORR reaction steps.

The general approach has been to (1) start with acid-stable transition metal oxides, and see if ORR activity can be discovered / induced; or (2) start with systems likely to have ORR activity, and see if acid-stability is achieved. In pursuit of the first goal, oxides of Ti and Nb have been explored. Towards the second goal, complex materials related to Mo₂N and MoN have been studied. Both the synthesis and electrochemical characterization of these materials have been carried out by group members. The structural characterization of these compounds has been done via powder x-ray diffraction (in our lab), powder neutron diffraction (at NIST via user proposal), by transmission electron microscopy (collaboration with Eric Stach, at the CFN), and by XPS (collaboration with Gabriel Veith, ORNL), and XANES/EXAFS (at the NSLS).

TECHNICAL PROGRESS AND RESULTS:

In the first year of this project, conductive pyrochlores ($M = \text{Ti, Nb, and Ta}$) were explored but no promising results were found. Some hollandite compounds ($M = \text{Ti, Mn}$) were explored, with promising behavior observed for a Mn hollandite. Mixed (Ti/Nb)O₂ phases were prepared and tested, without promising activity being found. Powders and single crystals of the reduced

titanate $\text{La}_5\text{Ti}_5\text{O}_{17}$ were prepared; the growth of single crystals of $(\text{Ti}/\text{Nb})\text{O}_2$ was attempted unsuccessfully. In the second year of this project, we have made progress in the following areas:

Task 1: Study of acid-stable conductive transition metal oxides

The $\text{La}_2\text{Ti}_2\text{O}_7:\text{Nb}$ and $\text{LaNbO}_4:\text{Ti}$ systems were synthesized and characterized. The doping limits have been determined in both cases. Both systems exhibited ORR activity in acid. The activity of $\text{La}_2\text{Ti}_2\text{O}_7:\text{Nb}$ was found to be very low, while that of $\text{LaNbO}_4:\text{Ti}$ was somewhat better but was still not promising from an applications standpoint. A paper on these systems is currently in preparation. Powder synthesis routes for the reduced titanates $\text{La}_9\text{Ti}_7\text{O}_{27}$ and $\text{La}_5\text{Ti}_4\text{O}_{15}$ have been developed, and the electrochemical characterization of these phases has been undertaken.

Task 2: Complex relatives of phases with known ORR activity

The compounds Mo_2N and MoN were discovered by others to have ORR activity, but there is not yet a robust understanding of the structures of these compounds. A two sets of Co-Mo-O-N compounds have been synthesized, one with the Mo_2N structure and one with the MoN structure. Both compounds demonstrate reasonable activity for ORR in acid solution, and even better activity in basic solution. A paper on the Mo_2N -type compounds is currently in preparation. A variety of structural studies (STEM/EELS, XANES/EXAFS, neutron powder diffraction, etc.) are being carried out to better understand structure-property correlations.

In the final year of this project, we will work to wrap up our study of the MoN -type Co-Mo-O-N compounds as well as the La-Ti-O compounds, and test to see if other related chemical compositions can produce similarly good activities. An emphasis will be placed on producing publications that will support the application for external funds to support this research.

Charge Generation and Transport in Films of Conjugated Polymers for Organic Photovoltaics BNL Part of a Collaborative NREL, BNL, LDRD

LDRD Project 10-014

John Miller and Andrew Cook

PURPOSE:

This LDRD has three principal scientific goals that will be supported by two developments in instruments and technique. These and the APPROACH sections are similar to those described a year ago. In general, this project seeks to understand films of conjugated polymers in order to contribute to the development of high-efficiency organic photovoltaic (OPVs) devices. Specific scientific goals are:

1. Understand the nature of charge carriers (electrons and especially holes) in conjugated polymer films and determine their numbers (concentrations).
2. Measure and understand mobilities of charge carriers in polymers.
3. Measure and understand light-driven charge separation.

In addition to scientific and technical goals, an intent is to build a connection between BNL and NREL in the area of organic photovoltaics, based on complementary knowledge and capabilities at the two institutions. A BES program manager has indicated interest in adding funding for BNL/NREL collaboration, pending successful completion of this LDRD.

APPROACH:

To pursue these goals the two labs will develop new abilities based on the complimentary capabilities and apply the instruments to the scientific goals. These will include:

1. Two microwave conductivity instruments. One will be an upgrade of the laser excited instrument at NREL, where it will be sited. The second, at BNL, will measure charge carriers created by 9 MeV electron pulses at the BNL's Laser Electron Accelerator Facility (LEAF). This electron pulse excitation is expected to produce electron-hole pairs that have escaped the Coulomb attraction that binds them.
2. NREL expertise will develop methodologies to create thick (1 mm or more) films of conjugated polymers to enable spectroscopic interrogation of charge carriers created by ionizing electron pulses at LEAF. BNL expertise will develop methods to investigate the nature of the charge carriers in these thick films using, principally, optical spectroscopy, and possibly also infrared spectroscopy. Film data will be augmented by production of aggregates of polymers in solution. Comparisons will be made between films, aggregates and isolated polymer chains.

TECHNICAL PROGRESS AND RESULTS:

At the suggestion of NREL colleagues we explored attachment of holes in the solvent *o*-dichlorobenzene and also examined hole production in chloroform, while NREL colleagues dealt with delays in obtaining parts for the new microwave (μ Wave) conductivity system. A summary is given below.

1) Construction of the μ Wave system with attention to serious expect RF noise from the accelerator. To reduce noise the apparatus is constructed in a closed metal box without electrical connections to the outside. Power is from internal batteries and ethernet and triggers communicate without direct electrical connections. At this writing the apparatus will be tried next week.

2) Andy Cook proposed making thick films with a pellet press of the kind used for infrared spectroscopy and initial tests were successful. Rumbles (NREL) found that colleagues in the UK had tried this and could offer advice. In films of polythiophene made by this method 0.5 mm seemed an optimal thickness. Electron pulses at LEAF induced observable transient absorption signals with reasonably long (~ 80 ns) lifetimes. Observations are possible only at wavelengths longer than 850 nm due to intense absorptions in the films, probably arising from impurities, but in the accessible range the optical absorption signals resemble those of electrons or holes.

3) Aggregates of polythiophene have been produced in DCE solvent and holes have been attached both by pulsed ionization at LEAF and by chemical doping. These spectra, those in films and from single chains display considerable similarities.

4) Probing holes with dynamic infrared spectroscopy has potential to provide another method for measurement of charge mobilities, but a barrier is the inherent weakness of the infrared transitions. We have recently found that vibrational transitions in radical anions and cations of conjugated oligomers give rise to infrared bands with intensities that are ~ 100 times larger than typical IR transitions.

5) We examined the chemistry following pulsed ionization of liquid chloroform. Chloroform is an excellent solvent for conjugated polymers and is often utilized to inject holes into isolated chains. Its behavior may be a prototype for others, for example the DCE used for aggregates. Results depended on the ionization potential of the solute. Above ~ 7.8 eV, solutes were found not to be oxidized by the radicals, but likely only by $\text{CHCl}_3^{\bullet+}$. For IP $< \sim 7.8$ eV, like most of the conjugated polymers, oxidation by Cl^{\bullet} turns on as well, with the undesirable consequence that recombination of solute radical cations with Cl^- forms stable ion pairs, $[\text{S}^{\bullet+}, \text{Cl}^-]$. This observation makes the free ion yield (FIY) of solute radical cations a very important number, as it gives the number of polymer ions possible that are free of being ion pairs. The lifetime of $\text{CHCl}_3^{\bullet+}$ and its spectrum are difficult to assign; different bands in the visible have a short lifetime < 1 ns and appear to react differently with different IP solutes. The solvent radical cation likely also has a very short lifetime < 1 ns; calculations suggest that an important mode of loss is fragmentation in addition to recombination. While this makes the FIY of the neat solvent zero, solutes can capture ions that would have become homogeneous; measurements suggest this may be $\sim 10\%$ of the total number of ions formed. A key result for low IP polymers and aggregates is that cations will be formed as ion pairs; initially solvent-separated, but likely ultimately contact ion pairs, which likely will effect charge motion measurements.

Milestones for year 2012:

1. Test and surmount noise issues to get a working microwave conductivity instrument.
2. Apply that instrument to measure microwave conductivity in liquids and solids including both thick films made in the LDRD and packed powders from conventional thin films.
3. Measure optical transients in thick films of varied conjugated polymers. Confirm whether these are from electrons and holes instead of excited states. Determine absorption coefficients and in at least one demonstration case measure the numbers (concentrations) of carriers to enable determination of carrier mobilities from the combination of methods.
4. Compare optical spectra for holes in single-chains and aggregates in solution with those for films.

Photoelectrochemical Fuel Generation from Water and Carbon Dioxide

LDRD Project 10-015

James T. Muckerman, Carol Creutz, Etsuko Fujita and Kotaro Sasaki

PURPOSE:

Our research focuses on efficient electrochemical water splitting and CO₂ reduction which are necessary to convert the electrical energy to hydrogen and reduced C1 compounds for fuels. Hydrogen and carbon paths can be separate (water splitting to form energy-carrying H₂; or CO₂ reduction to form energy-carrying CO or formate). Together such independent paths can produce syngas, H₂ + CO, for use in liquid fuel generation. The hydrogen and carbon paths can also be combined in CO₂ reduction directly to methanol. We are exploring the electrocatalysis of reductive half-reactions relevant to artificial photosynthesis by heterogeneous and immobilized molecular catalysts containing earth-abundant, non-noble metals.

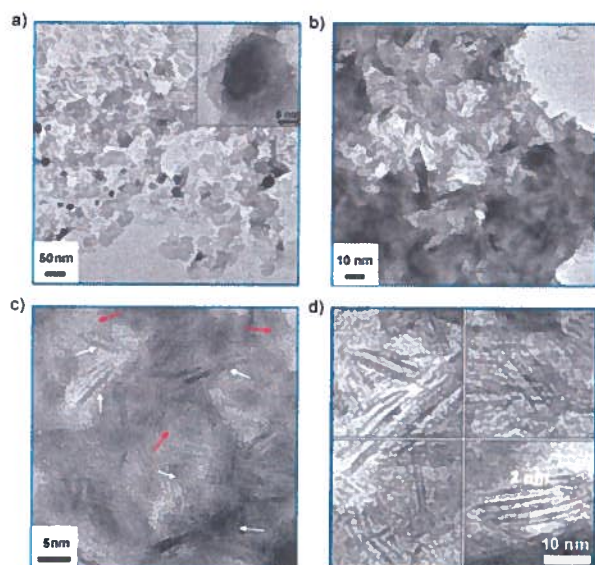
APPROACH:

We combine experimental and theoretical approaches in closely coordinated effort to understand and improve the catalysis of fuel formation half-reactions pertinent to artificial photosynthesis. The catalysts that are the subject of our studies are both molecular transition-metal (TM) complexes and heterogeneous catalysts in the form of nanostructures, particles, films and extended surfaces. Of particular interest is the immobilization of molecular catalysts on the surfaces of electrodes or semiconductors. As part of the work on exploring new non-noble metal containing heterogeneous electrocatalysts for the hydrogen evolution reaction (HER) in acidic media, we have developed a cheaper, stable and active molybdenum-nitride based electrocatalyst for the HER.

TECHNICAL PROGRESS AND RESULTS:

We are pursuing the elucidation of factors that determine selectivity of the products in CO₂ electro-reduction by a Re(tBu₂-bpy)(CO)₃ homogeneous catalyst. We are also continuing to make progress on CO₂ reduction catalyzed by a self-assembled monolayer of 4,4'-bipyridine on a nickel electrode, and related systems for electrochemical CO₂ reduction. In the area of heterogeneous systems, we have obtained remarkable results on electrocatalysis of the HER using subnanoparticles (approaching individual atoms) of Pt and Au electrodeposited on a carbon electrode, but our most significant and important result in this funding period has been the development of a nanostructured non-noble metal containing electrocatalist for the HER that outperforms any non-noble metal catalyst previous known (approaching the performance of a platinum electrode). Accordingly, the remainder of report on our technical progress will be devoted to this discovery, for which we are filing a Record of Invention, and are in discussions with the BNL IP Office regarding a patent application.

Guided by the 'volcano plot' in which the activity for hydrogen evolution as a function of the M-H bond strength exhibits an ascending branch followed by a descending branch, peaking at Pt, we [JTM, K. Sasaki and W.-F. Chen (RA)] designed a material on the molecular scale combining nickel, that binds H weakly, with molybdenum, that binds H strongly. Here we report the first synthesis of NiMo nitride nanosheets on a carbon support (NiMoN_x/C), and demonstrate the high HER electrocatalytic activity of the resulting NiMoN_x/C catalyst with low overpotential and small Tafel slope.



The NiMoN_x/C was synthesized by reduction of a carbon-supported ammonium molybdate ((NH₄)₅Mo₇O₂₄·4H₂O) and nickel nitrate (Ni(NO₃)₂·4H₂O) mixture in a tubular oven under H₂ at 400 °C, and subsequent reaction with NH₃ at 700°C. During this process, the (NH₄)₅Mo₇O₂₄ and Ni(NO₃)₂ precursors were reduced to NiMo metal particles by H₂, and then were mildly transformed to NiMoN_x nanosheets by reaction with ammonia. The transmission electron microscopy (TEM) images, as shown in panel a), display that the NiMo particles are mainly sphere-shaped. The high-resolution TEM image, as shown in the inset of Fig. 1a, corroborated the presence of an amorphous 3–5 nm Ni/Mo oxide layer, while NiMoN_x is

characterized by thin, flat and flaky stacks composed of nanosheets with high radial-axial ratios (panel b)). Panel c) shows that some of the nanosheets lay flat on the graphite carbon (as indicated by the red arrows), and some have folded edges that exhibit parallel lines corresponding to the different layers of NiMoN_x sheets (white arrows). The thickness of the sheets ranged from 4 to 15 nm. The average stacking number of sheets measured from panel b) is about six. It is noteworthy that a major part of the nanosheets was exfoliated and present in the form of single sheets. The HRTEM images in panel d) show the morphology of these single sheets. The gap between two single sheets was found to be up to 2 nm.

Catalyst	Onset potential (mV vs RHE)	Tafel slope (mV dec ⁻¹)	Exchange current density, j_0 (mA cm ⁻²)
MoN/C	-157	54.5	0.06
NiMoN _x /C	-78	35.9	0.37
Pt/C	0	30.1	1.44

The polarization curve recorded with the NiMoN_x/C catalyst an onset potential of -78 mV vs RHE for the HER. The Tafel curve recorded on NiMoN_x/C exhibited classical Tafel behavior, clearly indicating that the HER can be described using the Tafel equation. The curve in the low current density region showed a Tafel slope of 35.9 mV dec⁻¹. The onset potentials, Tafel slopes, and exchange current densities are listed in the table.

2012 Milestones

- Optimize the catalytic performance of the NiMoN_x/C catalyst with respect to composition (e.g., Ni/Mo ratio).
- Explore other non-noble metal containing catalysts based on the ‘volcano plot’ design paradigm
- Elucidate the products and mechanism of electroreduction CO₂ reduction catalyzed by self-assembled monolayers of 4,4'-bipyridine on a nickel electrode, and related systems.
- Optimize the performance of the Pt and Au subnanoparticle deposition on carbon catalysts for the HER.

Structural Basis of Light Perception by Phytochrome

LDRD Project 10-016

Huilin Li

PURPOSE:

The plant and certain bacteria use light for photosynthesis and for sensing their environment as well. The protein phytochrome is a well-conserved photoreceptor responsible for sensing light at the red light range. Despite its discovery nearly half a century ago, many fundamental questions remain unclear. A key to understanding the chemical basis of the process is the structure of phytochrome. The major challenge for the traditional structural approaches such as crystallography is that the protein is unusually large, containing over 1000 amino acids and multiple functionally distinct and dynamic domains. Cryo-electron microscopy (cryo-EM) is a powerful tool for elucidating the operational mechanism of the large biological protein complexes. Our group at BNL Biology Department is working on the phytochrome, a topic of great scientific significance and of direct relevance to BNL and to the DOE bioenergy programs.

APPROACH:

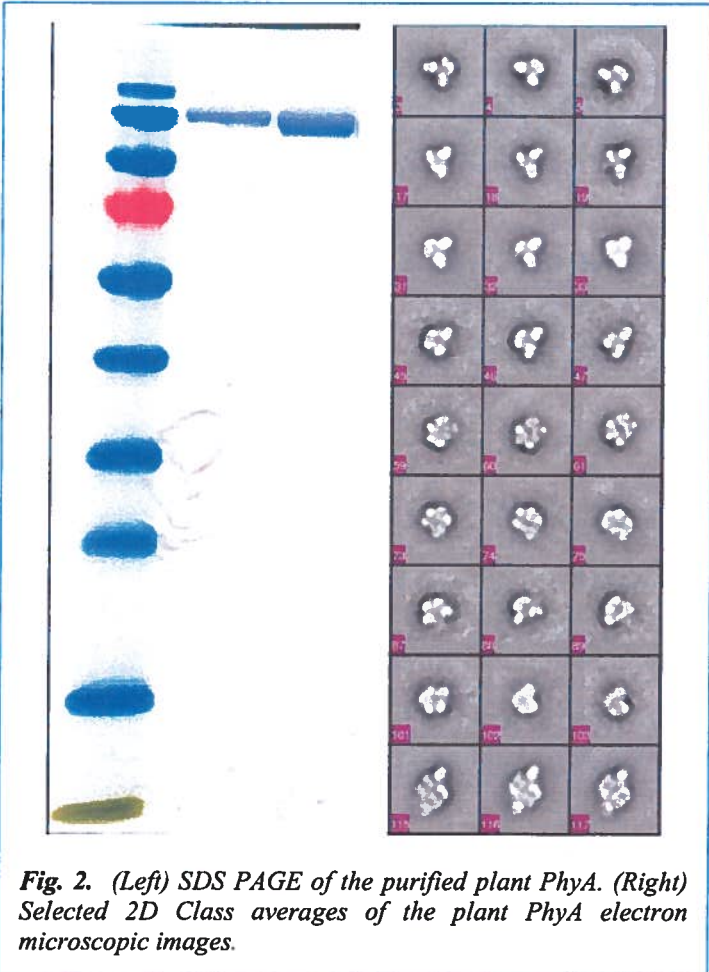
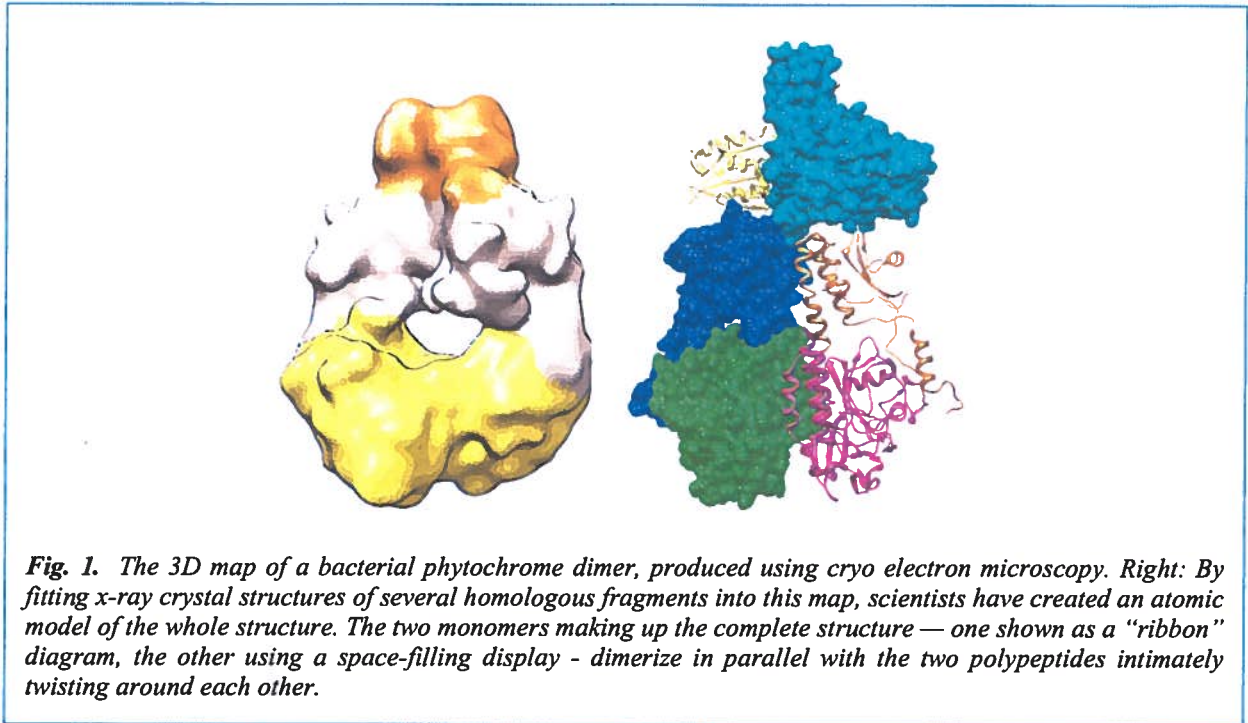
The light sensing process relies critically on dimerization of the full-length phytochrome. Existing structural studies involve breaking the large protein into smaller pieces, and solving the structure of the fragments by X-ray crystallography. This approach is insufficient to understanding how the multiple domains dimerize and cooperate to function as a whole. Our plan is to use cryo-EM and three-dimensional (3D) image reconstruction approaches to reveal the structure of the biologically functional phytochrome dimer.

Because phytochrome is well conserved from certain bacteria to plant, the structure of bacterial phytochrome will provide insight to the plant system. We therefore start our investigation with the bacterial phytochrome, which is much easier to produce in a sufficient quantity (100 micro gram (μg)) and in a highly purified form. The second step is to study the structure of purified plant phytochrome. In the longer term, we plan to reveal the conformational changes of the bacterial and plant phytochrome between red and far-red states. The latter is a highly challenging task. We collaborate with plant biologist R. Vierstra in the University of Wisconsin.

TECHNICAL PROGRESS AND RESULTS:

During the first funding year (2010), we worked on the bacterial system, specifically, the bacteriophytochrome from *Deinococcus radiodurans* (DrBphP). We obtained the cryo-EM structure to a resolution at which individual domains of the DrBphP dimer are resolved as different densities (Fig. 1). This level of detail in the structure enabled us to computationally “dock” into the 3D density map with several published crystal structures of the fragments of homologous bacteriophytochrome.

Our cryo-EM studies revealed that, contrary to the long-standing view that the two monomers are held together solely via their carboxyl terminal region, we found that the amino terminal bilin-binding region of BphP also provides a dimerization interface with the C-terminal kinase domain appearing as a more flexible appendage. The BphP monomers were found to dimerize in parallel



with the polypeptides intimately twisting around each other in a right-handed fashion. The DrBphP work was published in Proc. Natl. Acad. Sci. USA (2010).

Since the beginning of FY 2011, we have been focusing on the plant phytochrome A system. We have obtained the highly purified PhyA sample (Fig. 2). We also found good conditions to prepare the EM grids of the plant PhyA, which produced well-contrasted EM images (Fig. 2). We are in the process of producing 3D reconstruction and refinement. We expect that at the end of this fiscal year, a 3D density map will be obtained and we will compare this plant structure with the bacterial version, and will write a paper to report our research.

Our longer-term goal is to study the structural dynamics of PhyA at the different light absorption states. We are applying for a grant from DOE and NSF to sustain this line of research.

New Model Organisms for Analysis of Plant Metabolism

LDRD Project 10-017

Jorg Schwender and John Shanklin

PURPOSE:

The objective of this LDRD proposal is to establish expertise at BNL in new model plants which have relevance as energy crops that can undergo metabolic engineering and flux analysis approaches. Transgenic lines which are affected in the synthesis of storage products will be produced and their central metabolism studied by flux analysis of developing seeds.

A future target of funding will be the establishment of a Bioenergy Institute linking genetics/genomics expertise at Cold Spring Harbor Laboratory (led by R. Martienssen) with expertise in metabolic engineering and flux analysis of Shanklin/Schwender at BNL. Therefore support of this project will foster improved integration of BNL's Basic Energy Sciences-supported groups (Schwender, Shanklin) as encouraged by our DOE Program Managers.

APPROACH:

Criteria for selection of model plants are generation time, self pollination, suitability for genetic transformation, high sequence homology between genes of the new model plant and other well established model plants (*Arabidopsis*), and the complexity and size of the genome. For the purpose of studying seed metabolism by flux analysis, seeds must be of sufficient size. Developing embryos at an early stage of development will be dissected out of seeds under aseptic conditions and put into a synthetic liquid culture medium containing different organic substrates. The composition of storage compounds (oil, protein, starch) after culture should be similar between cultured embryos and seeds that matured in plants.

TECHNICAL PROGRESS AND RESULTS:

Identification of a model plant. As a good candidate for a new model plant we identified *Thlaspi arvense* (Field pennycress), a close relative to the widely used model plant *Arabidopsis thaliana*. *T. arvense* is a crucifer species that produces oil seeds. It's potential as a bio-energy crop has been reported in literature. While many crop plants are difficult to transform, different *Thlaspi* species have been reported to be easily genetically transformed by the flower dip method. Also the seed size appears to be adequate to allow for the intended cultures of developing embryos. The genomic organization of different *Thlaspi* species is reported to be diploid, which allows straightforward genetic manipulation.

We obtained a *T. arvense* strain from the Arabidopsis Biological Resource Center and determined the following growth characteristics: Growth from seedling to flowering 4.5 – 5.5 weeks; ca. 7.5 weeks until developing embryos can be dissected out of seeds for cultures. Weight per seed ca. 1.0 – 1.3 mg, 300 – 900 seeds produced per plant.

Genetic transformation: We grew successive generations of the initial transgenic material obtained by genetic transformation of *T. arvense* with the vector DsRed.

Genetic constructs: Work on two genetic constructs for overexpression in *T. arvense* was started. Full length transcripts for the transcription factor WRINKLED and for malic enzyme

were cloned from *A. thaliana*. Cloned gene sequences were verified by sequencing. Cloning into the plant expression vector was initially unsuccessful but will be done.

Embryo cultures: For the *T. arvense* wild type embryo culture experiments with ¹³C-labeled glucose were performed. Biomass fractions (Lipid, starch, protein, etc.) were quantified. Labeling signatures in amino acids, fatty acids, and other metabolites were measured by gas chromatography/mass spectrometry. Amino acid composition analysis of proteins and lipids were performed. Biomass composition of cultured embryos was compared to mature seed.

In addition, cultured embryos were harvested and the frozen tissue sent to collaborators at Cold Spring Harbor Laboratory for RNAseq. We still are waiting for the sequencing data.

Future goals (FY 2012):

- **Genetic constructs:** The genetic constructs (WRINKLED, malic enzyme) will be transformed into *T. arvense*. A full length transcript of malic enzyme in *Ricinus communis* will be cloned from *R. communis* plants and expressed as well. Seeds of transgenic plants will be analyzed to assess changes in lipids, protein, and carbohydrate content. Flux analysis will be performed with developing embryos. A comparison of wild type to transgenic will be made.
- **Genomic organization:** In collaboration with the group of R. Martienssen (Cold Spring Harbor Laboratory), we will determine genome size and genome organization (ploidy, chromosome number) in *T. arvense*. In collaboration with J. Dunn (BNL Biology) parts of genomic DNA will be sequenced to be compared to *Arabidopsis*.
- **Transcript profiling in developing seeds of *T. arvense*:** In collaboration with the group of R. Martienssen (Cold Spring Harbor Laboratory), deep sequencing of gene transcripts in developing seeds will be performed. By homology to the *A. thaliana* genome, this sequence information will allow to identify genes in central metabolism and the assessment of expression levels in developing seeds. This will allow us to validate a metabolic network of seed metabolism.
- **Flux analysis studies:** With the biochemical reaction network established based on the transcript profiling, flux analysis of the transgenics will be performed.

Development of Microprobe, Multichannel Optical Multimodality for Biological Tissue Imaging

LDRD Project 10-023

Congwu Du, Fritz Henn and Yingtain Pan

PURPOSE:

The objective of this project in FY10-11 has two focuses: 1) To examine the utility and potential applications of multimodality image platform (MIP) that enables simultaneous image of microflow, and morphology from biological tissue such as rodent brain or plant leaves *in vivo*; 2) To develop a high resolution needle-based multimodality image platform (NB-MIP). This micro-probe will permit to access the deep tissue area to image the cellular function, which is advanced technology to compare the conventional microscope. This instrumentation development directly supports BNL & DOE's missions while also providing technologies that are broadly transferable to other agencies.

APPROACH:

We have developed multimodal image platform (MIP) in FY 2009-2010. To examine the capability of MIP, we imaged a living corn plant, including both leaf and roots of the corn. The goal is to image the leaf's or root's pathology and physiology which are presented by angiography and intensity images of MIP, respectively. In addition, we integrated a needle-based micro-probe into the MIP to form needle-based multimodality image platform (NB-MIP) in order to image the cellular function in deep tissue area where the conventional microscope could not access (i.e., > 1 mm beyond the brain surface).

TECHNICAL PROGRESS AND RESULTS:

Validation of MIP technique: The MIP captures micrometer resolution, three-dimensional (3D) images from optical scattering media (e.g., biological tissue). The advantages of the technique include the high spatial and temporal resolution over a wide field of view. Fig. 1 illustrates the MIP images of corn leaf (left panel) and roots (right panel) of a living corn plant. The intensity in two/three-dimensions (i.e., 2D/3D intensity) presents the microflow of the plant, whereas angiography in 2D/3D reflects the morphology of the plant. We can see the 2D/3D sap microflow from the surface of the leaf (as shown in the top 1&2 panels in the left side on Fig. 1), indicating the physiology function of the leaf in the plant. Unlike in the leaf, the microflow in the roots seem more uniform (top panels of 1 & 2 in the right side of Fig. 1). Due to the high resolution of the MIP, the interior structure of the leaf and roots can be imaged by 2D or 3D angiographies as shown in the bottom panels in Fig. 1. These results validate MIP's

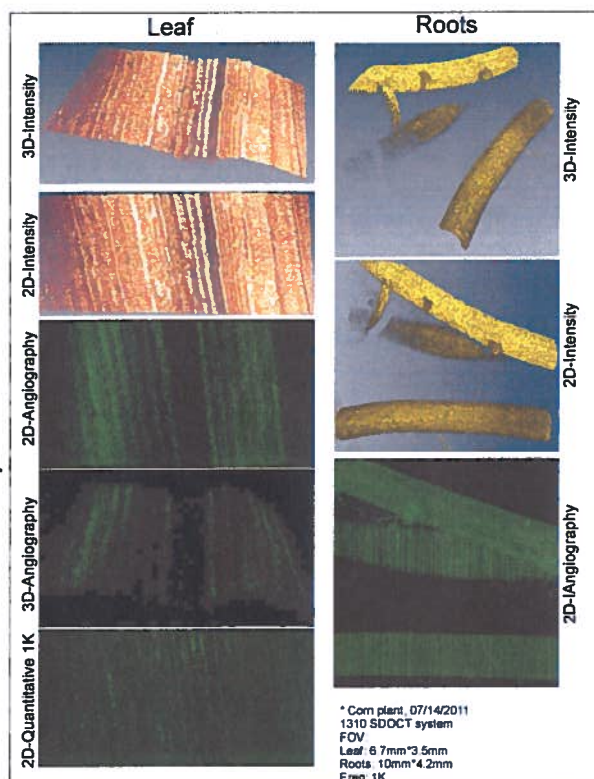


Fig. 1. MIP images of corn leaf (left panel) and roots (right panel) of a living corn plant. The intensity in two/three-dimensions (i.e., 2D/3D intensity) presents the microflow of the plant, whereas angiography in 2D/3D reflects the morphology of the plant.

feasibility to image the pathology and physiology of any part of plant in a living condition, which can be used as a new modality for functional studies of plant in the future.

Development of NB-MIP prototype: As being proposed in the Specific Aim 2, we developed needle-based multimodality image platform (NB-MIP). Fig. 2. illustrates the NB-MIP system that integrates the needle-based microprobe (Fig. 2c) to a modified upright fluorescence microscope (E800, Nikon) as shown in Fig. 2a. The needle-based microprobe is a custom GRIN

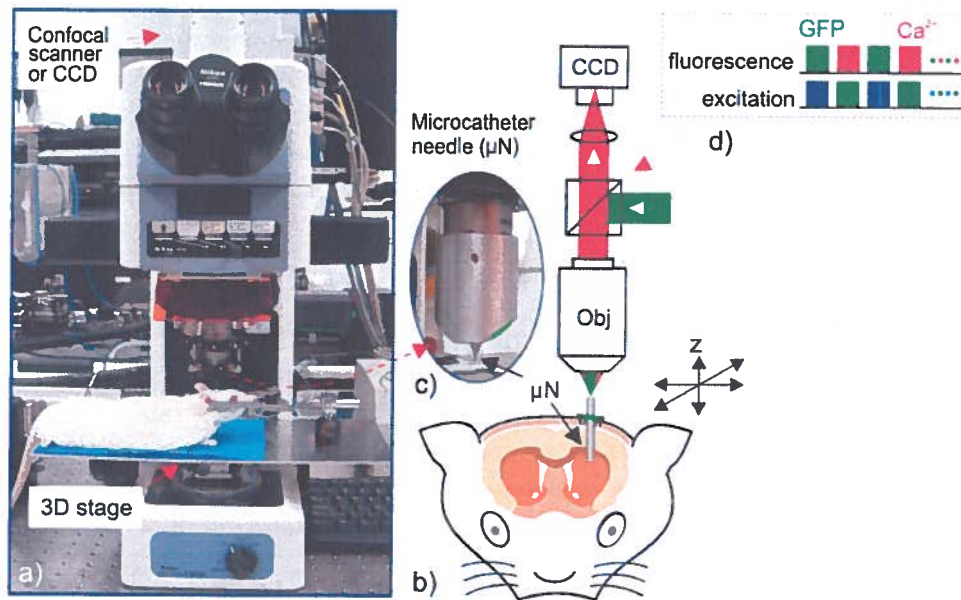


Fig. 2. A schematic illustrating the prototype of a needle-based multimodality imaging platform (NB-MIP) that permit to image the cellular function in deep tissue area, such as the sub-cortical region of a rodent brain.

lens ($\phi 1\text{mm} \times 20\text{mm}$) that relays the image from the biological tissue (e.g., mouse brain) at the distal end of the needle probe back to the focal plane of the microscope objective (e.g., PlanFluo 20 $\times/0.5$ numerical aperture (NA), Nikon). A custom motorized 3D micro-stage (Fig. 2a) facilitates accurate light coupling and focal tracking between the microprobe and the microscope objective as shown in Fig. 2b, which allowed the focus to be finely placed on the deep tissue region (e.g., striatum: $>2\text{mm}$ from the brain surface). This NB-MIP enables high-performance simultaneous image of the GFP and calcium fluorescence as shown in Fig. 2d.

In summary, we have been developing multimodal optical techniques for *in vivo* imaging of biological tissues, including living plant. The merits of the techniques include high spatiotemporal resolution over a large field of view. Specifically, MIP permits direct assessment of physiological and morphological imaging of living biological tissue. In addition, NB-MIP can image the deep region of the tissue at subcellular resolution, along with a real time record of its intracellular calcium changes as a function of time *in vivo*.

Development of Large Liquid Argon Time Projection Chambers (LArTPC) for Future Neutrino Experiments

LDRD Project 10-025

Francesco Lanni

PURPOSE:

Liquid argon (LAr) has been successfully used in many high energy particle calorimeters since it was first proposed at BNL in 1974. More recently, there has been a growing effort to develop giant LAr Time Projection Chambers (TPCs) as an alternative to Water Cerenkov Detectors for neutrino physics measurements. In order to develop and optimize LAr TPCs to exploit their high resolution 3D imaging and energy measuring capabilities, all of the physical processes that produce and transport charge and light signals in LAr must be quantitatively understood. Much engineering information is available (small LAr TPCs have been built) but scaling to future multi-kiloton detectors requires basic property determination with high precision data. This project will measure the fundamental properties of charge and light production and transport in LAr, investigate and optimize designs of devices and structures for charge and light collection, and develop the operation of electronics systems in LAr. The ultimate result of this project will be the knowledge to successfully construct a 100–kiloton scale LAr TPC for neutrino physics and proton decay experiments.

APPROACH:

We emphasize the fundamental physics and electronics that must be understood and applied to design the next generation of noble liquid TPCs. Basic properties of noble liquids are known only incompletely, and electronic systems optimized for operation in very large cryogenic detectors have not yet been developed. Aspects of the program include these:

Create the infrastructure for cryogenic measurements:

- Construction of cryostats to contain the noble fluids, recirculating purification systems to achieve and maintain high fluid purity, and the required instrumentation.

Measure basic noble liquid transport properties:

- Diffusion of electrons, electron attachment to impurities and electron-ion recombination will be measured to understand charge transport and production. Use of additives dissolved in the noble liquid to enhance charge or light production will be explored.
- Quantitative measurements of the partition of impurities between the liquid and gas phase of noble liquids and of the kinetics of impurity generation and transport will be measured.

Readout electronics development:

- For truly large detectors it will not be feasible to have one cable and cryogenic feed-through per readout channel. The entire signal processing chain through digitization and multiplexing must therefore operate in the noble liquid at cryogenic temperatures. This will be done by designing and fabricating analog and digital CMOS ASICs for cryogenic operation. The objective is to reduce the entire electronics system and the TPC structure to modules that are arrayed to scale to any detector volume or shape.
- Modeling and measurement of the entire signal formation process, for both charge and light, using measurements of the basic transport properties described above.

TECHNICAL PROGRESS AND RESULTS:

1. We have established a cryogenics lab for liquid noble fluid R&D. A postdoc (Yichen Li) has been hired to plan and execute the experiments. A 0.3 m³ cryostat has been instrumented to

evaluate electronics performance and reliability in LAr, and has been successfully evaluating the performance and lifetime of commercial voltage regulators for the past year. A small cryostat and purification system was designed, fabricated and is now being assembled and tested, for photocathode quantum efficiency and electron diffusion measurements in ultra-high purity LAr.



2. We have characterized the parameters of 0.18 micron CMOS devices at cryogenic temperature to establish device models for ASIC designs. of the noise at cryogenic temperatures of two CMOS ASICs: one is an existing device designed for room temperature (A) and the other is a new 0.18 μm ASIC designed for cryogenic operation (B). The new ASIC performs almost identically at room and cryogenic temperature (left panel, below), except the noise is lower at cryogenic temperature.
3. Measurements were made of the quantum efficiency of Au photocathodes in LAr to be used as

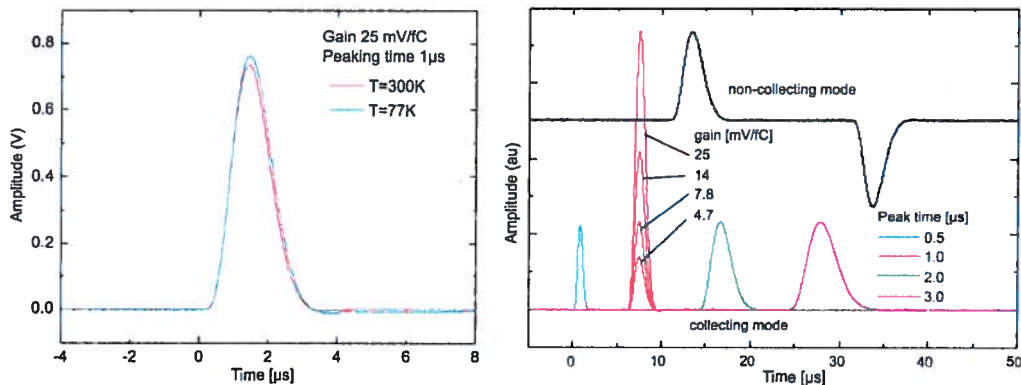


Fig. 1. The front end output pulse shape at room temperature and 77K (left), and the pulse shapes for some choices of peaking time, gain, and baseline offset.

a source of high brightness electrons for transport experiments. Results to date indicate that the quantum efficiency is limited by the absorption of impurities on the photocathode surface. This will be removed in measurements with the new high purity cryostat.

FUTURE MILESTONES:

1. Completion of cryogenic safety review of ultra-purity cryostat and first operation of system.
2. Measurement of gold photocathode quantum efficiency vs. electric field.
3. Measurement of longitudinal diffusion of electrons vs. electric field.
4. Measurement of transverse diffusion of electrons vs. electric field.

Spin Waves in Artificial Magnonic Crystals: Fabrication, Imaging and Scattering

LDRD Project 10-034

Dario Arena, Peter Warnicke, Aaron Stein and Yimei Zhu

PURPOSE:

Spintronics, where the electron's spin in addition to its charge is central to the operation of the device, is one possible replacement for CMOS electronics based on silicon. A subset of spintronics, spin wave (SW) electronics, hold great promise in moving into the post-CMOS era. SW electronics may also form a part in reducing energy consumption as their function derives from the propagation of spin, not charge, and hence there is little energy loss from Ohmic heating. The propagation and manipulation of SWs can be examined in lithographically-defined magnonic crystals (MCs), where now, instead of electromagnetic waves, the relevant excitations are spin waves, quantized as *magnons*, which are collective excitations of the spins of valence electrons in a ferromagnet (FM). In this LDRD, we have been utilizing the advanced lithography tools available at the CFN (in collaboration with Dr. Aaron Stein) to fabricate MCs. In addition, we have set up a laboratory to characterize their high-frequency (GHz range) properties. Also, we have been collaborating with Dr. Yimei Zhu at CMPMSD to eventually investigate the excitations in MCs using advanced TEM imaging. Lastly, we have been extending our ultrafast, x-ray-based spectroscopy to examine the excitations of the MCs, which we will investigate using x-ray microscopy. The techniques at these non-BNL facilities (x-ray microscopy, ultrafast time-resolved x-ray scattering) may be developed at NSLS-II.

APPROACH:

The program supported under this LDRD project consists of several tasks: (1) fabrication of MCs at the CFN; (2) characterization of the microwave excitation spectra of the MCs using ferromagnetic resonance utilizing a vector network analyzer (VNA); (3) examination of the SW standing wave patterns using Lorentz TEM microscopy; (4) measurement of x-ray scattering patterns of SWs in MCs; (5) imaging of SWs in MCs using x-ray microscopy. Task 1 will be conducted primarily at the CFN. Task 2 will be performed out at the NSLS using equipment purchased for this purpose under the LDRD program. Task 3 will be carried out at BNL in collaboration with Dr. Yimei Zhu. Task 4 will be executed at NSLS at beam line U4B, although access to more advanced facilities at 3rd generation storage rings may be required. Task 5 will be carried out at the XM-1 soft x-ray, full-field transmission microscope at the ALS at LBNL.

TECHNICAL PROGRESS AND RESULTS:

We are fabricating MCs using the physical vapor deposition and electron lithography tools at the CFN. To date, the MCs consist of periodic anti-dot arrays in a FM $\text{Ni}_{81}\text{Fe}_{19}$ film; the anti-dots represent a periodic modulation in the magnetic permeability (μ) of the $\text{Ni}_{81}\text{Fe}_{19}$. The $\text{Ni}_{81}\text{Fe}_{19}$ film has an in-plane magnetic anisotropy, and we are exploring using Co / Ni multilayers with out-of-plane anisotropy in future MCs. The Co / Ni multilayers would be grown by a collaborator (already identified). In addition to the MC fabrication efforts, we have set up a high-frequency magnetic characterization lab (RF Lab) to measure the microwave absorption characteristics of the MCs. The lab consists of three main components: (1) a 2 T electromagnet and power supply; (2) a high frequency (20 GHz) vector network analyzer; and (3) custom-designed co-planar waveguides (CPWs). The CPWs are necessary to deliver the microwave excitations to the sample and also fit within the poles of the electromagnet. The CPWs were designed by Dr. Peter Warnicke at the Instrumentation Division at BNL.

Figures 1 & 2 below show some of the capabilities of the newly commissioned RF Lab. Fig. 1 presents a waterfall chart of the microwave absorption spectra at different applied magnetic fields.

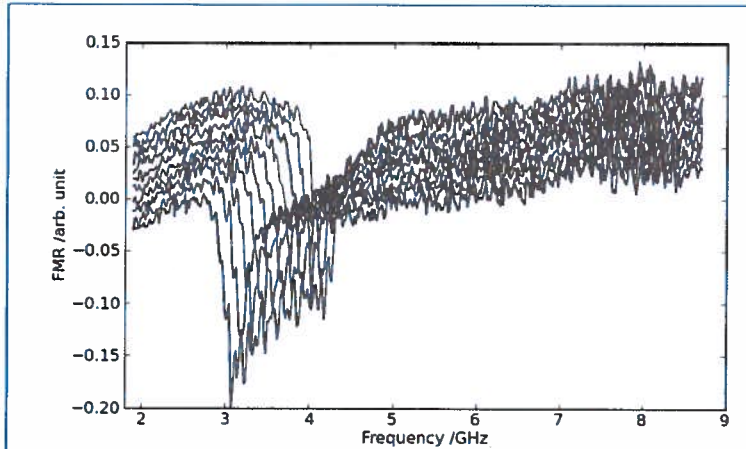


Fig. 1. Waterfall chart of microwave absorption (ferromagnetic resonance) for a 25 nm $Ni_{81}Fe_{19}$ film, with applied external magnetic fields from 100 Gauss to 200 Gauss.

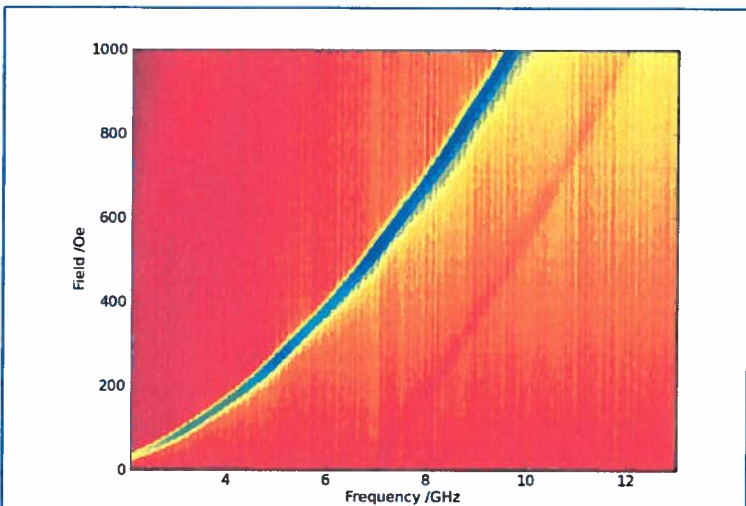


Fig. 2. False color field-frequency map of a magnetic tri-layer film ($Ni_{81}Fe_{19}$ [15 nm] / Cu [1 nm] / $Ni_{81}Fe_{19}$ [15 nm]). The main resonance is clearly visible, as well as a weaker 2nd

The sample was a single 25 nm layer of $Ni_{81}Fe_{19}$ on a Si substrate. The strong absorption feature clearly moves to higher frequency with increasing applied magnetic field. Fig. 2 shows an example of the capabilities of the system and presents a full frequency-field map of the microwave absorption from a magnetic tri-layer. A strong primary absorption is clearly identified, as well as a weaker feature starting at (7 GHz, 0 Oe) and dispersing up to (12 GHz, 1000 Oe).

In addition to these activities, we have been progressing on the other activities, including the x-ray microscopy efforts. A manuscript is currently under review at the *Journal of Magnetism and Magnetic Materials*. Also, we have been exploring the limits of x-ray detected ferromagnetic resonance (X-FMR), which is a key component in exciting spin-wave modes in MCs while simultaneously exploring their properties with x-rays. Towards that end, we have undertaken measurements at several synchrotrons (NSLS, APS, MAXLab) which seek to extend the frequency range accessible with X-FMR. Two manuscripts on those efforts are currently being written.

Finally, we have also been exploring use of Lorentz TEM for imaging of excited modes in magnetic nanostructures. For technical reasons, the initial experiments have concentrated on examining vortex gyrations in magnetic nanowires, which present a larger signal than can be expected in the MCs. These efforts are also supported by micromagnetic simulations of the vortex orbits under microwave excitation, which will be used to understand the modes imaged with Lorentz TEM. Shortly, we hope to be able to image SW modes in MCs with the advanced electron microscopy. The TEM efforts are undertaken in collaboration with Dr. Yimei Zhu of the CMPMSD.

Atomic Structure and Bonding of Cellulose

LDRD Project 10-038

Michael McGuigan and Yan Li

PURPOSE:

The purpose of this project is to study theoretically the atomic structure and bonding in crystalline cellulose and its interaction with water, therefore providing a new understanding of the possible structural rearrangements in cellulose. Furthermore, by employing the state-of-art, first-principles studies, we aim to provide realistic parameters for large-scale classical molecular dynamics studies of the interaction of cellulose with cellulose degrading enzymes.

APPROACH:

We have performed density functional theory total energy calculation with semi-empirical van der Waals dispersion corrections [1], implemented in the plane-wave package Quantum-Espresso [2]. In particular, we computed and analyzed structural, energetic, and vibrational properties and electronic structure (frontier orbitals, energy gap etc.) of crystalline cellulose and its surfaces [3]. We have utilized large scale quantum mechanical simulations on New York Blue, the 128 Teraflops Blue Gene/L, P computer complex at BNL and have actively collaborated with the Biomolecular Science Division at the National Renewable Energy Laboratory in Colorado to optimize the use of research data from both groups.

TECHNICAL PROGRESS AND RESULTS:

We have studied atomic structure and bonding in crystalline cellulose using dispersion-corrected density functional theory. We found that the crystal structures from experiments are well reproduced within 1-2% from theory. The computed energetic ordering of the two crystal phase ($I\alpha$, $I\beta$) agree well with hydrothermal healing results, and vdW dispersion interactions are proven to be equally important as hydrogen bonding for the crystallinity of cellulose. In addition, we found water adsorption cellulose surfaces are sensitive to the type of adsorption site whereas vdW contributions to adsorption energy are significant.

[1] S. Grimme, *J. Comput. Chem.* 27, 1787 (2006).

[2] P. Giannozzi, et al., *J. Phys. Cond. Matter* 21, 395502 (2009).

[3] Y. Li, M. Lin, and J. Davenport, *J. Phys. Chem. C* 115, 11533 (2011).

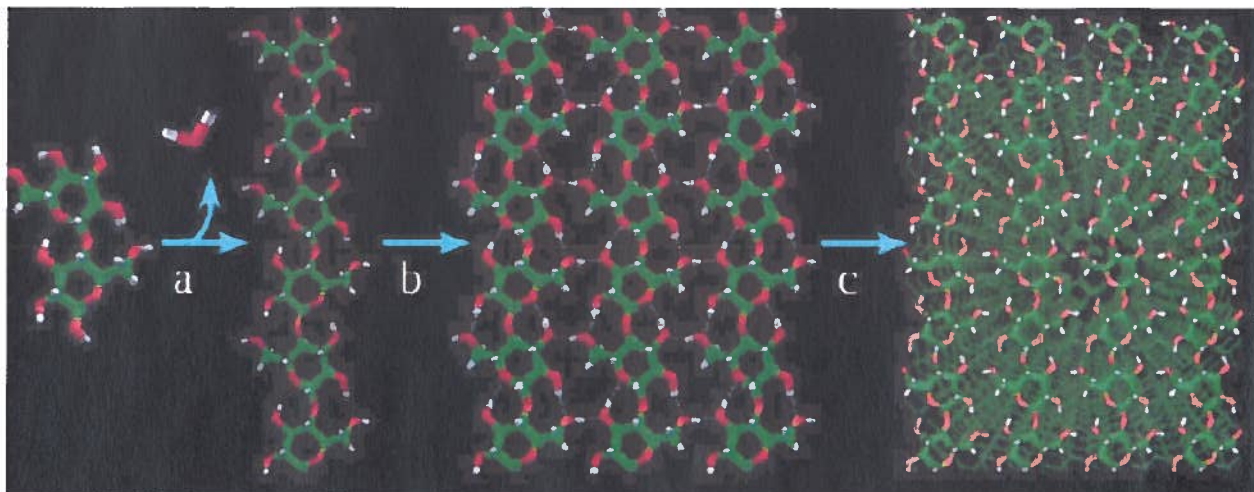


Fig. 1. Assembly of cellobiose units (a) into single chains, (b) single sheets and (c) the three-dimensional cellulose crystal.

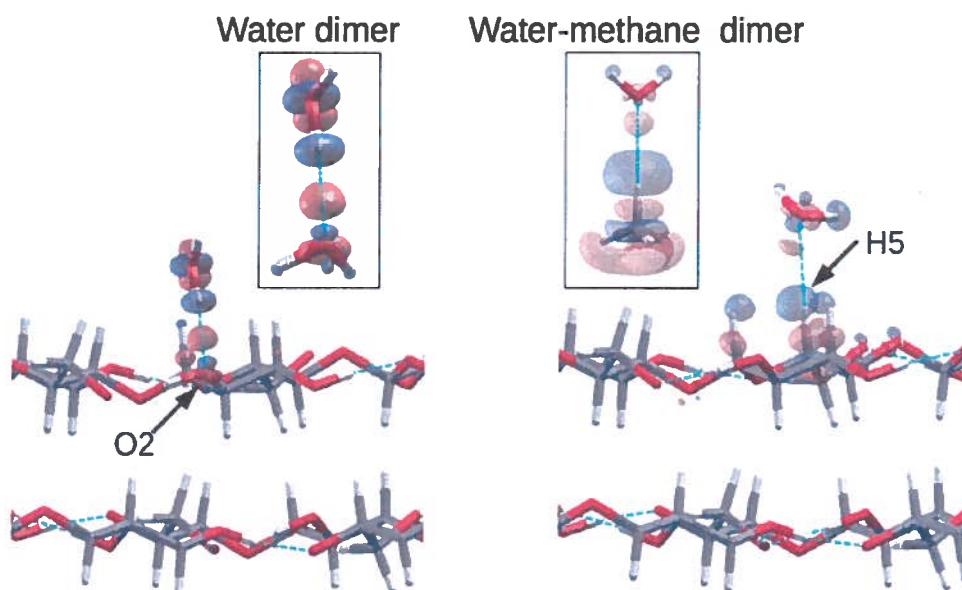


Fig. 2. Electron density difference maps of single water adsorption on two different types of sites (i.e. the "O" sites and the "H" sites) on the cellulose I β (100) surface clearly demonstrate hydrogen bond characteristics. Insets show electron density difference maps of the water dimer and the water-methane dimer for comparison.

EIC Polarized Electron Gun

LDRD Project 10-039

Ilan Ben-Zvi

PURPOSE:

Funneling is a technique used to increase the average current from particle sources by combining multiple sources. We are trying to prove that funneling works for polarized electron sources in a geometry and capabilities that are suitable for the future eRHIC (polarized electron collider addition to the RHIC heavy ion collider).

The eRHIC project requires a highly polarized electron source with high average current, which sounds ambitious based on state-of-art polarized electron source technology. Average current of about 4 mA of polarized electron beam has been obtained in Jefferson lab. But eRHIC requires 50 mA of average current. There are other requirements which make the source more challenging: final transverse emittance, one of the most important parameters describing beam's quality, needs be less than 20 mm.mrad; bunch charge should be about 3.5 nC; final bunch length should be less than 4 mm. A natural way of obtaining the 50 mA of average current is to employ multiple cathodes, for example 20 cathodes, and combine the beam bunches from each cathode together to form one bunched beam. It works like a "Gatling gun". With funneling, any improvement applied to single polarized sources will multiply the performance of the funneled source.

APPROACH:

The highest polarized electron current achieved to-date is 4 mA. We are constructing a funneling gun capable of supporting 20 cathodes, although only two will be used to prove the concept, but the geometry, which is important to the performance of the device, is compatible with a eRHIC device.

The key issues to be addressed are the design of the two main elements, the cathode preparation system and the gun chamber, that are compatible with XHV vacuum while providing for the frequent replacement of the cathode. Another issue is the design of the combiner that can merge individual beam-lets from 20 cathodes without degrading the quality of the electron beam.

Other investigators: Xiangyun Chang, Jörg Kewisch, Vladimir Litvinenko, Gary McIntyre, Alexander Pikin, Triveni Rao, Brian Sheehy, John Skaritka, Omer Rahman, Eric Riehn, Qiong Wu.

TECHNICAL PROGRESS AND RESULTS:

In the first fiscal year of 2011 we have finished the following:

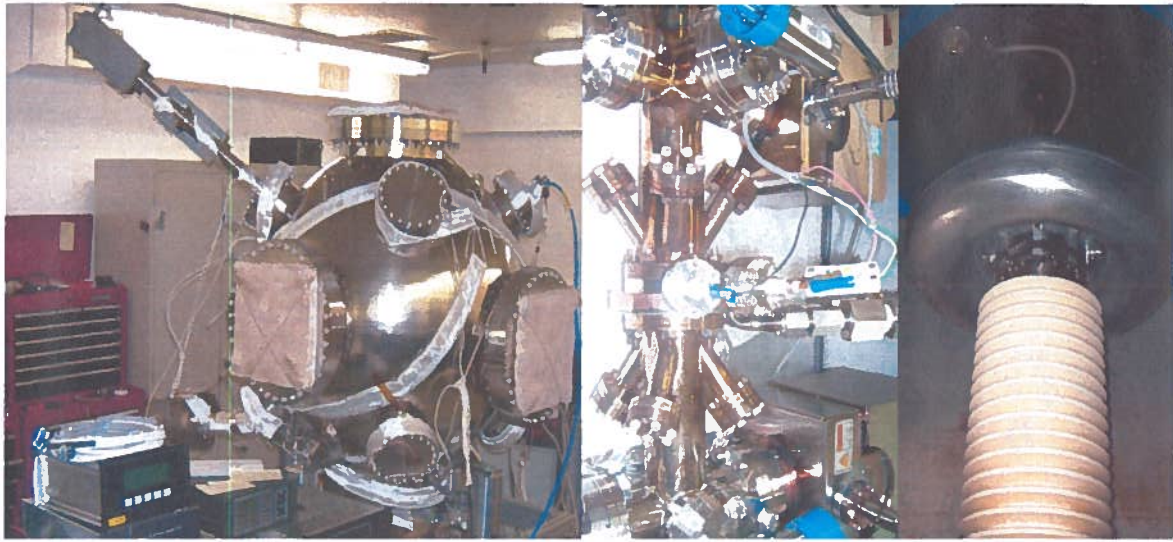
1. The electron beam transport in the Gatling gun was studied in details using 2D simulations.
2. Most of the mechanical design of the system was done.
3. We chose magnetic bends, carefully designed the combiner and did some proof of principle tests based on a simple prototype.
4. We determined the requirements for the building to house the experiment.

Present status of the project:

We have one post-doc (Eric Riehn) and one graduate student (Omer Rahman).
G-Gun Vessels- Detailed design complete, vessel manufacturing underway.
First Cathode Tree -Preparation system, components complete, under test at Atlas
G-Gun manipulators- Detailed Design complete, manufacturing underway.
Grand Central manipulators- Design complete, manufacturing underway.
Cathode service Flange Assy- Complete, testing underway
G-Gun End transition Assy- Detailed Design complete, manufacturing underway.
Cathode Shroud Assy- Detailed Design underway.
Cathode Cooling Ring- Detailed Design underway.
Anode Assembly- Detailed Design underway.
Grand Central Vessel- Complete, testing underway
Fused Silica Windows bakeable to 400C- vendor failure redesign underway.
Alumina Combiner Break- initial vendor failure, remanufacturing underway.
Testing of High Voltage Vacuum Feed through- Testing underway
Focusing Solenoids and Anode SubAssy- components being manufactured

MILESTONES FOR FY12 and beyond:

Single Cathode Prep system delivery and setup.....2/2012
Grand Central Vessel vacuum Spec achieved.....3/2012
Gatling Gun vacuum system components completed7/2012
Grand Central manipulators integrated and XHV tested.....10/2012
Cathode Shroud system and Anode Assembly completed.....12/2012
Gatling Gun vacuum system integrated and XHV tested.....2/2013
HV testing of completed Gatling Gun and XHV tested..... 3/2013
Gun Cathodes routinely produced in single prep system.....4/2013
Phase 1 Combiner tested and installed.....6/ 2013
One and Two Cathode operation9/2013



Figures from left to right: Cathode preparation chamber, cathode preparation assembly, 250 kV feed

Development of a Laser System for Driving the Photocathode of the Polarized Electron Source for the EIC

LDRD Project 10-040

T. Rao, T. Tsang and B. Sheehy

PURPOSE:

The objectives of the project are the development of the laser system that can drive a single cathode and improvement in the performance of the cathode of the “Gatling Gun”. The laser should be upgradable to deliver the 50 mA current required for the electron-ion collider (EIC) with appropriate timing and energy stability. In this project, three different laser systems will be investigated; appropriate system will be chosen and developed. The improvement in the sensitivity of the cathode is achieved by better understanding of the formation of the negative electron affinity surface. Different oxygen sources for creating the negative electron affinity surface as well as the changes in the surface morphology as a function of the cleaning temperature will be investigated. Polarized electron source (cathode and laser) capable of delivering up to 50 mA with life time significantly longer than its preparation time is crucial for the eRHIC project at BNL

APPROACH:

The quantum efficiency of the polarized electron source is in the range of a fraction of a percent at 780 nm. In order to meet the beam requirements of the Gatling gun, the laser should deliver ~ 4 W average power at 780 nm, at a repetition rate of 704 kHz with a pulse duration of ~ 1 ns at each of the gun cathodes. Formation of the negative electron affinity surface on the GaAs is crucial for the high QE, and the preservation of the polarization. Typically the electron affinity of a very clean GaAs surface is reduced by depositing Cs and an oxidizing agent to result in a fractional monolayer of Cs on the surface. The cleanliness of the GaAs surface, Cs and the oxidizing agent determine the ultimate QE of the cathode and its sensitivity.

The scope of the program is expanded to address both the development of the laser system and the understanding the negative electron affinity of the cathode in order to increase the life time of the cathode. In collaboration with Brian Sheehy of CAD, we investigated different laser architecture, decided on the most promising design, interfaced with the industry to complete the preliminary research and development and initiated the procurement process for the laser system.

Two alternate sources for the oxidizing agent are being investigated: a manganate compound in a silver capsule that releases pure oxygen upon heating and oxygen from a commercial high purity oxygen cylinder that is precooled to remove residual contaminants such as water vapor. Other characterizations include establishing the correlation between the QE and the surface properties of GaAs upon heating.

TECHNICAL PROGRESS AND RESULTS:

The fiber laser system operating at 1560 nm has been developed by Optilab, a commercial firm. Using pulses from a function generator with a repetition rate of 352 kHz and pulse duration of 2.4 ns, an average power of > 10 W and peak power of > 13 kW has been extracted from this device. Since the company did not have a function generator that can deliver 704 kHz and a pulse duration of ~ 1 ns, a delay generator with appropriate pulse shape and repetition rate has been

shipped to the company. As can be seen from Figure 1 the optical pulse follows the electrical pulse. Prior to shipping, the fiber was damaged during the attempt to increase the output power to 8W. However, this was attributed to improper setting of the system parameters. The device has been repaired and is scheduled for delivery shortly. The vendor has not yet been successful in converting the IR beam to 780 nm. In the conservative scenario, this will be accomplished by BNL personnel.

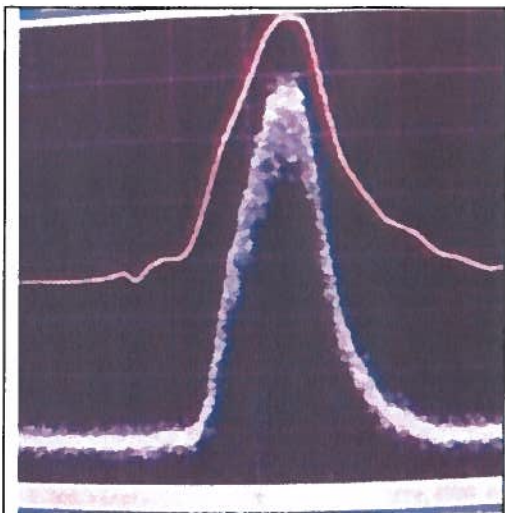


Fig. 1. Oscilloscope trace of electrical (upper) and optical (lower) pulses



Fig. 2. GaAs chamber modified for shorter turn-around time of the sample

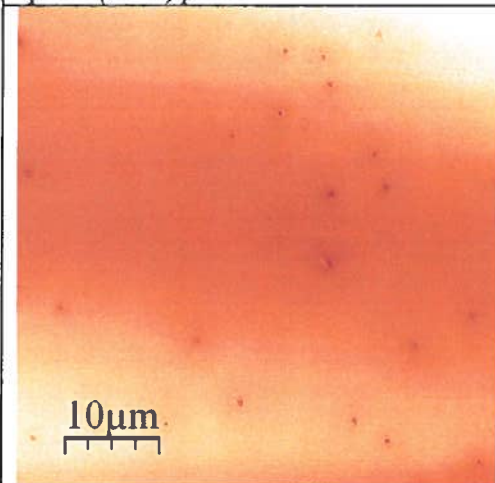


Fig. 3. Surface profile of GaAs after activation

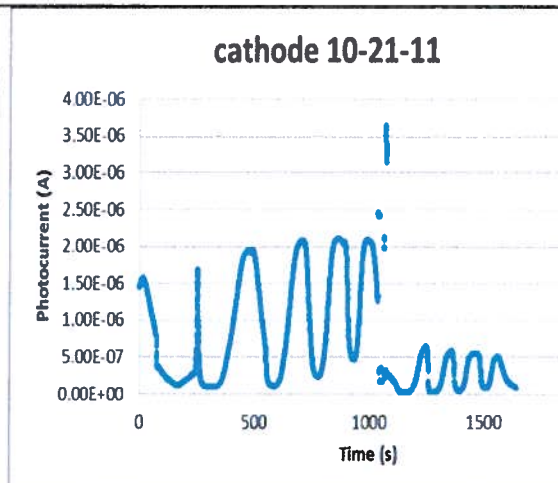


Fig. 4. QE of the cathode during activation

The QE with commercial high purity oxygen cylinder was comparable to that with Manganate source. Due to the ready availability of the commercial source, this will be used for further studies. As shown in Figure 2, the GaAs preparation chamber has been modified to reduce the turn-around time and measurements to correlate the surface roughness, temperature of heat cleaning and the QE have started. Figure 3 and 4 illustrate the surface morphology and QE respectively after heat cleaning and activation

2012 Milestone:

- Install and characterize the laser system
- Correlate QE of the cathode to its surface morphology

Simulation, Design, and Prototyping of an FEL for Proof-of- Principle of Coherent Electron Cooling

LDRD Project 10-041

Vladimir N Litvinenko

PURPOSE:

FEL-based Coherent Electron Cooling [1] (CeC) promises to become a revolutionary method that will significantly increase luminosity in proton-proton colliders, ranging from the RHIC to the LHC. We are addressing issues, theoretical and numerical, that the FEL community have put aside for at least two decades. We are modifying the well-benchmarked 3D FEL codes specifically for the CeC cooler. It is very unlikely that we can readily employ existing wiggler designs with their very small gaps suited for light sources and short wavelength FEL. Accordingly, we are designing and fabricating a prototype of such a wiggler to address possible shortcomings and limitations. This LDRD is the front-runner project for testing the CeC mechanism in a proof-of-principle (PoP) experiment. With the success of the CeC PoP, the CeC cooler certainly will greatly benefit future medium- and full-energy eRHICs. Importantly, it will ensure that we maintain our competitive edge against EIC projects, such as the ELIC.

APPROACH:

The theoretical part of our research focuses on the evolution of the e-beam phase-space distribution in the FEL with arbitrary initial conditions and under the influence of space charge. From our findings, we should be able to simulate and predict the cooling time for a realistic CeC PoP system. We address the following theoretical and design challenges:

1. Fitting the CeC system, including the FEL, into the space between the DX magnets; 2. Evaluating the space-charge and diffraction effects on the FEL's, and the CeC's performance at a relatively low energy of the electron beam (20 MeV), and a rather long wavelength of FEL (18 microns); and, 3. Establishing the tolerances on the FEL design and the wiggler fields.

The CeC PoP experiment requires a new helical wiggler, suitable for installing into RHIC's IP between two DX magnets. It should have an aperture adequate to avoid imposing any constraints on the RHIC's hadron beam. We are designing, and plan to build, and evaluate a short prototype of such a wiggler during our practical feasibility studies.

TECHNICAL PROGRESS AND RESULTS:

During this fiscal year we developed detailed lattice of CeC experiment-- see Fig. 1 [4,5].

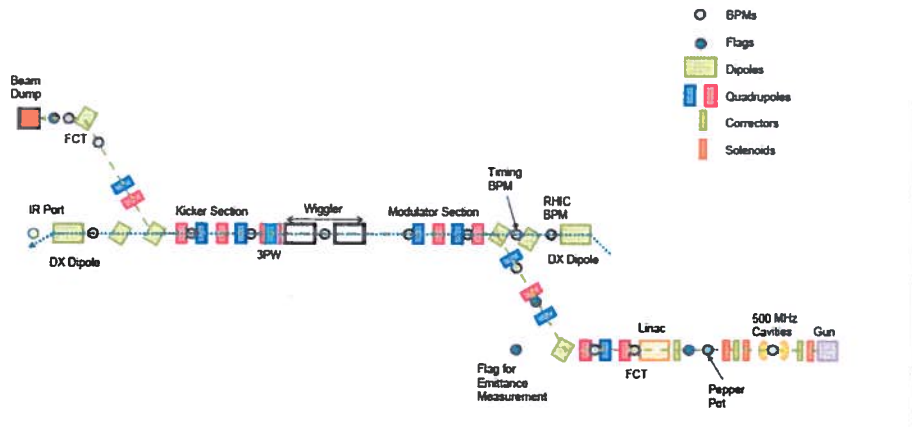


Fig. 1. Layout of the CeC PoP experiment.

We achieved significant progress both in the theory and computer simulations of the processes in coherent electron cooler [2,3, 6-12]. The main theoretical accomplishments are discovery of the beam-conditioning for CeC process [1] and rigorous prove that there is only a single growing mode in FEL [3,12]. In May 2011 Stephen Webb defended PhD “Theoretical Considerations of Coherent Electron Cooling” at Stony Brook University.

On the experimental side, there is significant progress in design and manufacturing of 50 cm prototype of helical wiggler, which is paid by this project’s funds. We placed the order for the designing, prototyping and measuring a 50 cm helical wiggler with 4 cm period with Budker Institute of Nuclear Physics (Novosibirsk, Russia). The prototyping proceeds close to the schedule and all components of the wiggler have been manufactured. Assembly of the prototype is in progress and the magnetic measurements should start in March 2012.

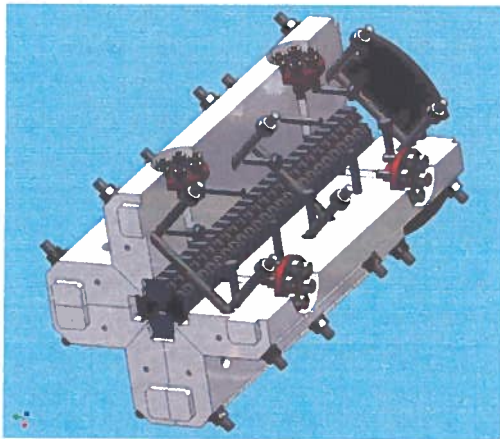


Fig. 2. Left (a) shows the wiggler 3D rendering (b) Four wiggler’s arrays after been manufactured at BINP workshop (Novosibirsk, Russia) in December, 2012.

We published two refereed and nine conference proceeding paper on the subject of coherent electron cooling during reporting period. We also were awarded FY11 \$1.46 funds from NP DOE competitive accelerator R&D program for experimental demonstration of coherent electron cooling. Our early start with LDRD funds in prototyping the wiggler for CeC was of critical importance for this success. We are preparing FY12/13 proposal for total of about \$2.6M to

continue this program. Results of the wiggler prototyping should be available by the time of submission, expected to be in April 2012.

Next year milestone – complete evaluation of the helical wiggler, up-date its design and place order (using DOE funds).

References

- [1] V.N Litvinenko, Y.S. Derbenev, PRL **102**, 114801 (2009)
- [2] Three-dimensional model of small signal free-electron lasers, Stephen Webb, Gang Wang and Vladimir Litvinenko, Physics Review Special Topics – Accelerators and Beams, **14**, 051003 (2011), 8 pages, <http://prst-ab.aps.org/abstract/PRSTAB/v14/i5/e051003>
- [3] On Free-Electron Laser Growing Modes and their Bandwidth, Stephen Webb, Gang Wang and Vladimir Litvinenko, Submitted to PR ST-AB
- [4] Vladimir N. Litvinenko, Sergei Belomestnykh, Ilan Ben-Zvi, Jean C. Brutus, Alexei Fedotov, Yue Hao, Dmitry Kayran, George Mahler, Aljosa Marusic, Wuzheng Meng, Gary McIntyre, Michiko Minty, Vadim Ptitsyn, Igor Pinayev, Triveni Rao, Thomas Roser, Brian Sheehy, Steven Tepikian, Yatming Than, Dejan Trbojevic, Joseph Tuozzolo, Gang Wang, Vitaly Yakimenko (BNL, Upton, Long Island, New York), Mathew Poelker, Andrew Hutton, Geoffrey Kraft, Robert Rimmer (JLAB, Newport News, Virginia), David L. Bruhwiler, Dan T. Abell, Chet Nieter, Vahid Ranjbar, Brian T. Schwartz (Tech-X, Boulder, Colorado), Pavel Vobly, Mikhail Kholopov, Oleg Shevchenko (Budker Institute of Nuclear Physics, Novosibirsk, 6300090, Russia), Peter McIntosh, Alan Wheelhouse, (STFC, Daresbury Lab, Daresbury, Warrington, Cheshire, UK, WA4 4AD), Coherent Electron Cooling Demonstration Experiment, Proc. of Second International Particle Accelerator Conference, San Sebastian, Spain, September 4-9, 2011, p. 3442, <http://accelconf.web.cern.ch/AccelConf/IPAC2011/papers/thps009.pdf>
- [5] Vladimir N. Litvinenko, Sergei Belomestnykh, Ilan Ben-Zvi, Jean C. Brutus, Alexei Fedotov, Yue Hao, Dmitry Kayran, George Mahler, Aljosa Marusic, Wuzheng Meng, Gary McIntyre, Michiko Minty, Vadim Ptitsyn, Igor Pinayev, Triveni Rao, Thomas Roser, Brian Sheehy, Steven Tepikian, Yatming Than, Dejan Trbojevic, Joseph Tuozzolo, Gang Wang, Vitaly Yakimenko (BNL, Upton, Long Island, New York), Mathew Poelker, Andrew Hutton, Geoffrey Kraft, Robert Rimmer (JLAB, Newport News, Virginia), David L. Bruhwiler, Dan T. Abell, Chet Nieter, Vahid Ranjbar, Brian T. Schwartz (Tech-X, Boulder, Colorado), Pavel Vobly, Mikhail Kholopov, Oleg Shevchenko (Budker Institute of Nuclear Physics, Novosibirsk, 6300090, Russia), Peter McIntosh, Alan Wheelhouse, (STFC, Daresbury Lab, Daresbury, Warrington, Cheshire, UK, WA4 4AD), PROOF-OF-PRINCIPLE EXPERIMENT FOR FEL-BASED COHERENT ELECTRON COOLING, Proc. of 2011 International Free Electron Laser Conference, Shanghai, China, August 22-26, 2011
- [6] G. Wang, V. Litvinenko, S.D. Webb, *Amplification of Current Density Modulation in a FEL with an Infinite Electron beam*, Proceedings of 2011 Particle Accelerator Conference, New York, NY, USA, March 25-April 1, 2011, pp. 2399-2401, <http://accelconf.web.cern.ch/AccelConf/PAC2011/papers/thp149.pdf>
- [7] Vladimir N. Litvinenko, Johan Bengtsson, Ilan Ben-Zvi, Alexei V. Fedotov, Yue Hao, Dmitry Kayran, George Mahler, Wuzheng Meng, Thomas Roser, Brian Sheehy, Roberto Than, Joseph Tuozzolo, Gang Wang, Stephen Davis Webb, Vitaly Yakimenko, Andrew Hutton, Geoffrey Arthur Krafft, Matt Poelker, Robert Rimmer, George I. Bell, David Leslie

- Bruhweiler, Brian T. Schwartz, *Proof-of-Principle Experiment for FEL-based Coherent Electron Cooling*, Proceedings of 2011 Particle Accelerator Conference, New York, NY, USA, March 25-April 1, 2011, pp. 2064-2066,
<http://accelconf.web.cern.ch/AccelConf/PAC2011/papers/thobn3.pdf>
- [8] B.T. Schwartz, D.L. Bruhwiler, I. Pogorelov, V.N. Litvinenko, G. Wang, Y. Hao, S. Reiche, *Simulations of a Single-Pass Through a Coherent Electron Cooler for 40 GeV/n Au⁺⁷⁹*, Proceedings of 2011 Particle BNL 703 MHz Superconducting RF Cavity Testing Accelerator Conference, New York, NY, USA, March 25-April 1, 2011, pp. 244-246,
<http://accelconf.web.cern.ch/AccelConf/PAC2011/papers/mop074.pdf>
- [9] G. Bell, D. Bruhwiler, B. Schwartz and I. Pogorelov, V.N. Litvinenko, G. Wang and Y. Hao, *Vlasov and PIC Simulations of a Modulator Section for Coherent Electron Cooling*, Proceedings of 2011 Particle Accelerator Conference, New York, NY, USA, March 25-April 1, 2011, pp. 235-237, <http://accelconf.web.cern.ch/AccelConf/PAC2011/papers/mop067.pdf>
- [10] S.D. Webb, V. Litvinenko, G. Wang, *Effects of e-beam Parameters on Coherent Electron Cooling*, Proceedings of 2011 Particle Accelerator Conference, New York, NY, USA, March 25-April 1, 2011, pp.232-234,
<http://accelconf.web.cern.ch/AccelConf/PAC2011/papers/mop066.pdf>
- [11] G. Wang, V. Litvinenko, S.D. Webb, *Amplification of Current Density Modulation in a FEL with an Infinite Electron beam*, Proceedings of 2011 Particle Accelerator Conference, New York, NY, USA, March 25-April 1, 2011, pp. 2399-2401,
<http://accelconf.web.cern.ch/AccelConf/PAC2011/papers/thp149.pdf>
- [12] G. Wang, V.N. Litvinenko, S. Webb, *Asymptotic behavior of 1D FEL dispersion integral at large |s|*, C-A/AP/428 note, July 2011,
http://www.cadops.bnl.gov/AP/ap_notes/ap_note_428.pdf

Realization of an $e+A$ Physics Event Generator for the EIC

LDRD Project 10-042

Thomas Ullrich and Raju Venugopalan

PURPOSE:

The prospects for a future Electron-Ion Collider (EIC) are closely tied to the strength of the physics case for an eA physics program at such a facility. Many of the key measurements that provide the motivation for this substantial investment are to come from the eA program. The capability of an EIC to collide electrons with heavy ions distinguishes the machine from any existing accelerators and makes it a unique facility. It is in these collisions where one expects new phenomena, such as saturation of the gluon densities, to be unambiguously discovered and studied. These studies will open a window into a regime where deviations from linear QCD, as probed at HERA and JLAB, become pronounced. To observe these new phenomena, it is important to verify that the proposed measurements can be conducted with both sufficient statistics and kinematic reach. An essential element of this program is a Monte-Carlo event generator that covers the broad range of physics to be investigated and goes one step further to generate events in a nuclear environment including all known and conjectured nuclear effects. Such a generator does not exist and it is the aim of this LDRD project to provide such an eA physics event generator. This is a crucial tool for determining requirements on the machine (energy, luminosity) and for the design of detectors at an EIC.

APPROACH:

To work on the realization of an eA event generator a postdoctoral fellow (Tobias Toll) was hired in summer 2010 after an extensive search. He works 100% on the LDRD project. We realized the complexity of eA collisions cannot be encapsulated in a single generator but that a suite of generators in a common framework will be necessary, *i.e.*, the overall generator will consist of various packages that provide a common input and output format. As a first step we have focused on one of the identified key measurements at an EIC in eA , the study of diffractive events. Diffractive events are expected to constitute up to 30-40% of all events in an EIC and allow the determination of the gluon momentum distribution and, as the only known probe, to measure the spatial distribution of glue in a nucleus. We first focus on exclusive vector meson production (J/ψ , ϕ , ρ) and DVCS based on an existing dipole model (b-Sat). Once established, the program will be extended to generate also inclusive events. Here we can re-use large portions of an existing event generator. In parallel we have to simulate the breakup of the nucleus, since the fragments need to be detected to distinguish between coherent and incoherent diffraction. Once completed we intend to move on to deep inelastic scattering (DIS) in eA . For DIS there is a rich set of ep event generators available and the most efficient path for us is to adapt an existing Monte Carlo programs and extend it to generate also eA events. We have already worked out a method to transform the existing Monte Carlo CASCADE into an eA generator for DIS, a task that will be pursued in close collaboration with H. Jung, principal author of CASCADE.

TECHNICAL PROGRESS AND RESULTS:

By now we have completed an event generator called *Sartre* for diffractive exclusive vector meson production for eA collisions. The generator contains two different physics models: one that assumes a "standard" scenario (linear QCD) and one that includes the new phenomena (gluon saturation, higher twist effects) we intend to explore with an EIC. We have developed and implemented a method of calculating the cross-section for nuclear breakup to an unprecedented accuracy. The generator consists of two parts. In the first step, all extremely

computing intensive tasks are performed and their results get stored in lookup tables. These massive computations could only be conducted through the intensive use of the Open Science Grid where we were able to obtain > 100k CPU hours to-date. These tables are then used as input for the event generator. The resulting event generation is very fast and allows the user to generate tens of millions of events in a matter of minutes. In ep mode the generator reproduces existing measurements at HERA very well. This task could only be completed with intensive help, especially from T. Lappi (Jyväskylä, Finland) and R. Charity (St. Louis). Tobias Toll spent several days in Finland to develop details of the generator with Dr. Lappi.

The goal in coherent diffraction in eA collisions is two-fold: to get a handle on gluonic spatial structure in nuclei, and its lumpiness. The key observable is the spectrum of the transverse momentum transferred from the initial nucleus to the final state, t , with only a vector meson in the final state, *i.e.*, events of the type $e+A \rightarrow e'+A'+V$. Here, and only here, can t be reconstructed from the kinematics of the final state particles. Events where the nucleus stays intact in the interaction are called coherent, when it breaks up they are called incoherent. It is the coherent cross-section as a function of t that ultimately will allow us to derive the spatial distribution of gluons in the nucleus, while the incoherent cross-section is a measure of the fluctuations/lumpiness of the gluons in the nucleus. These distributions are depicted in Fig. 1, which is generated by *Sartre 1.0* for $e+Au \rightarrow e'+Au'+\rho$.

One of the key signals the EIC is looking for is saturation phenomena in the large energy (low- x) regime. Figure 2 depicts the distribution of the center-of-mass energy of the photon-nucleus system, W , for ep , eCa and eAu collisions in $e+A \rightarrow e'+A'+\rho$ events generated with *Sartre*. One can see that the dramatic differences between saturation physics and the “conventional” physics scenario.

We are currently preparing two papers on the physics methods developed for *Sartre*. *Sartre* is now used in the preparation of the EIC White Paper.

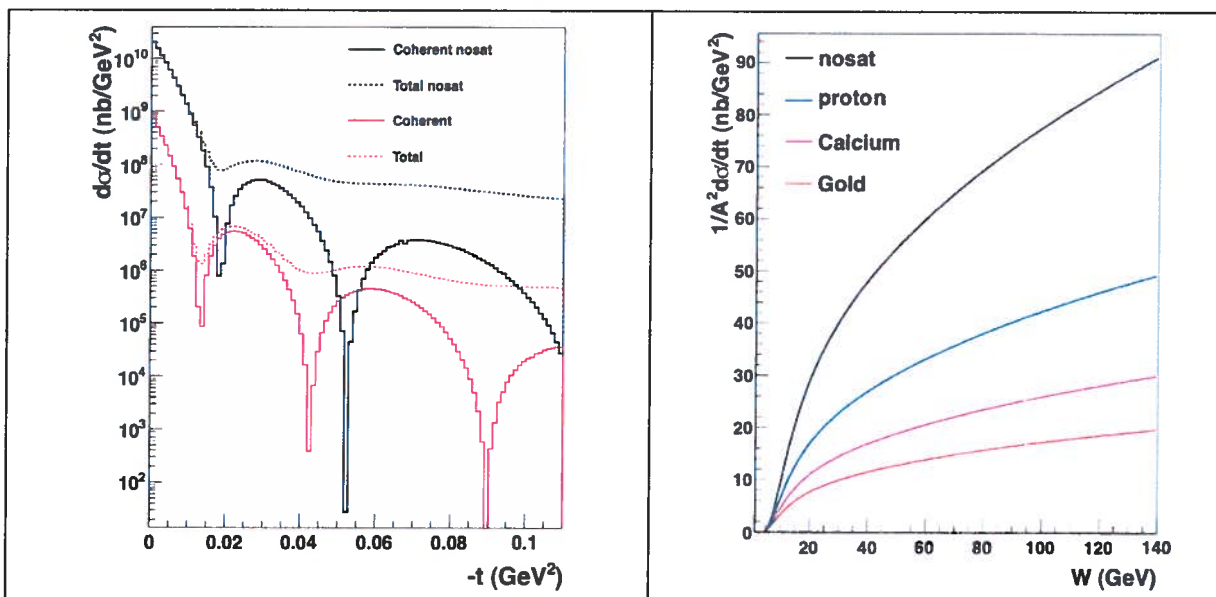


Fig. 1. The eAu cross-section for exclusive diffractive ρ production as a function of t , separated into its coherent and incoherent part for saturated and unsaturated low- x gluon matter. The coherent curve represents the Fourier transformation of the spatial source (gluon) distribution.

Fig. 2. The cross-section as a function of W and divided by A^2 . The saturated cross-section is quite different from the unsaturated one (nosat), which would be a clear signal for saturation when measured.

Exploring Signatures of Saturation and Universality in e+A Collisions at eRHIC

LDRD Project 10-043

Raju Venugopalan, A. Dumitru, J. Jalilian-Marian, A. Stasto, and T. Ullrich

PURPOSE:

A powerful motivation for an e+A collider is to study the properties of gluonic matter in nuclei at high parton density. Quantum Chromodynamics (QCD) predicts that the occupation number of gluons in nuclear wave functions saturate at a value inversely proportional to the QCD coupling. A dimensionful scale $Q_{SA}(x)$ separates maximally occupied “soft” from “hard” modes that are not. This scale grows with energy and with nuclear size—for large nuclei, gluon momenta up to GeV scales are saturated. An important consequence of saturation is universality. Though naively $Q_S^2 \propto A^{1/3}$, theoretical models predict that at very high energies, the saturation scales of all nuclei approach a common value independent of the properties of the nuclei in which the gluons are confined. What are the signatures of saturation in deep inelastic scattering (DIS) off nuclei and can we extract the saturation scale uniquely from these final states? Which signatures are most sensitive to saturation? Can we anticipate precocious onset of saturation in these final states? Can they be clearly distinguished from alternative descriptions? Can one reliably extract the nuclear dependence, the impact parameter dependence, and the energy dependence of the saturation scale? By varying x and A , can we observe hints of the onset of a universal fixed point—what energy range is optimal? Reliable quantitative answers to these relevant questions are of great importance in establishing the science case for an Electron Ion Collider (EIC).

In DIS at high energies, final states can be expressed in terms of universal multi-parton “Wilson line” correlation functions. The state-of-the-art description of the energy evolution of these correlation functions is the JIMWLK functional renormalization group (RG) equation, which correspond to an infinite hierarchy of integro-differential equations. Numerical solutions of these equations are challenging [4]. Solutions to these equations correspond to determining the primary many-body content of QCD in the high energy limit. In addition to computing the properties of final states in e+A collisions, the solutions to JIMWLK RG equations are inputs in factorized expressions for multi-gluon production in A+A collisions. They are therefore important for a first principles understanding of thermalization in the Quark-Gluon Plasma, the development of elliptic and radial flow, and jet propagation (parton energy loss) in heavy ion collisions.

APPROACH:

The technical advance required for quantitative studies was to solve the JIMWLK RG equations using functional Langevin techniques [1]. This goal was challenging albeit feasible as suggested by the one extant numerical computation [2]. Finally, theoretical approximations of the numerical data are essential to give insight into the underlying physics. A further challenge was to include running coupling effects properly in the JIMWLK computations. An outstanding post-doc candidate (Bjoern Schenke) was hired for this purpose and joined us in December 2010.

PROGRESS AND RESULTS:

The PI and collaborators have made significant progress on several fronts. Firstly, it was shown that the “ridge” correlations seen in AA and pp collisions are sensitive to the multi-parton correlators [3]. This was used to explain qualitatively [4] and quantitatively [5] the remarkable

“CMS ridge” seen at the LHC. The effect of multiple scattering contributions to the ridge was estimated in [6]. (This included contributions by Stanislav Srednyak, a Stony Brook student supported on the LDRD.) A global analysis (testing small x universality) of models explaining DIS data from HERA was applied to inclusive distributions in pp collisions at the LHC by the PI and a student Prithwish Tribedy [7]; this study further was extended to AA and pA collisions [8].

The importance of multi-parton correlators for a variety of processes was shown in refs. [9,10]. With Schenke joining our team, we were able to solve the JIMWLK equations and determine several multi-parton correlators for the first time; with our numerical solution, we were able to test and confirm the accuracy of a particular mean field approximation for computations of these multi-parton correlators [11]. We show below “snapshots” of strong gluon fields obtained from these numerical computations. Several follow up studies on i) unequal rapidity correlators (essential for detailed understanding of di-hadron correlations) ii) Glasma input for event-by-event initial conditions for relativistic viscous hydrodynamics, and iii) universality of higher multi-parton evolution, are underway and anticipated to be completed before the end of the LDRD this fall.

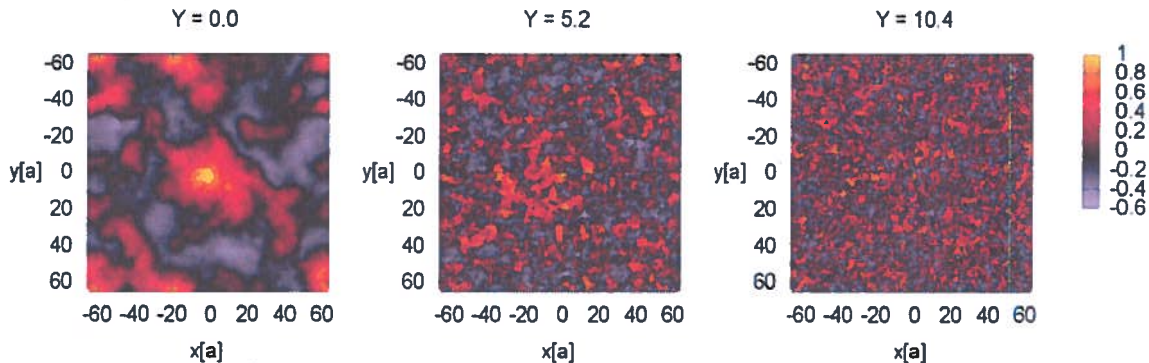


Fig. 1. Snapshots of spatial distribution of color fields in a nucleus as seen by a quark-antiquark probe

REFERENCES:

- [1] J. P. Blaizot, E. Iancu and H. Weigert, *Nucl. Phys. A* **713**, 441, (2003).
- [2] K. Rummukainen and H. Weigert, *Nucl. Phys. A* **739**, 183 (2004).
- [3] K. Dusling, F. Gelis, T. Lappi and R. Venugopalan, *Nucl. Phys. A* **836**, 159 (2010).
- [4] A. Dumitru, K. Dusling, F. Gelis, J. Jalilian-Marian, T. Lappi and R. Venugopalan, *Phys. Lett. B* **697** (2011) 21.
- [5] K. Dusling and R. Venugopalan, arXiv:1201.2658, submitted to *Phys. Rev. Lett.*
- [6] T. Lappi, S. Srednyak and R. Venugopalan, *JHEP* **01**, 066 (2010).
- [7] P. Tribedy and R. Venugopalan, *Nucl. Phys. A* **850**, 136 (2011); Erratum-*ibid.* **A859**, 185 (2011).
- [8] P. Tribedy and R. Venugopalan, arXiv:1112.2445, to appear in *Phys. Lett. B*.
- [9] F. Dominguez, C. Marquet, B. Xiao and F. Yuan, *Phys. Rev. D* **83** (2011) 105005.
- [10] A. Dumitru and J. Jalilian-Marian, *Phys. Rev. D* **82** (2010) 074023; *ibid.*, **81**, 094015 (2010).
- [11] A. Dumitru, J. Jalilian-Marian, T. Lappi, B. Schenke and R. Venugopalan, *Phys. Lett. B* **706** (2011) 219.

TECHNICAL PROGRESS AND RESULTS (CONTINUED):

A general analysis of parity violating structure functions unique to polarized ep scattering was undertaken by K. Kumar and W. Vogelsang.

Y. Li was in residence at the INT for the entire ten week program and coordinated the electroweak studies. An important outcome was the weak mixing angle sensitivity studies for DIS ep and eD scattering. As illustrated in figure 1 (attachment), the EIC can map out the running of $\sin^2\theta_w(Q)$ for large Q with a total statistical error rivaling the best measurements at Z pole colliders. Systematic errors are still being evaluated.

To better compare the EIC capabilities with ongoing and planned low energy experiments, Y. Li and W. Marciano computed the leading two loop electroweak corrections to QWEAK and polarized Moller Scattering.

For the case of lepton flavor violation, it was found that EIC can probe an interesting region of “New Physics,” but only if very high luminosity – $L \approx 10^{35} \text{cm}^{-2}/\text{sec}$ is available.

Results from those studies were included in a joint BNL/INT/JLAB report, “Gluons and the quark sea at high energies: distributions, polarization, tomography,” editors D. Boer, et al.

During FY 2011, we presented our results at the DIS conference, which was held in Newport News, VA, April 11-15, 2011. In addition, publication quality reports are being submitted to scientific journals.

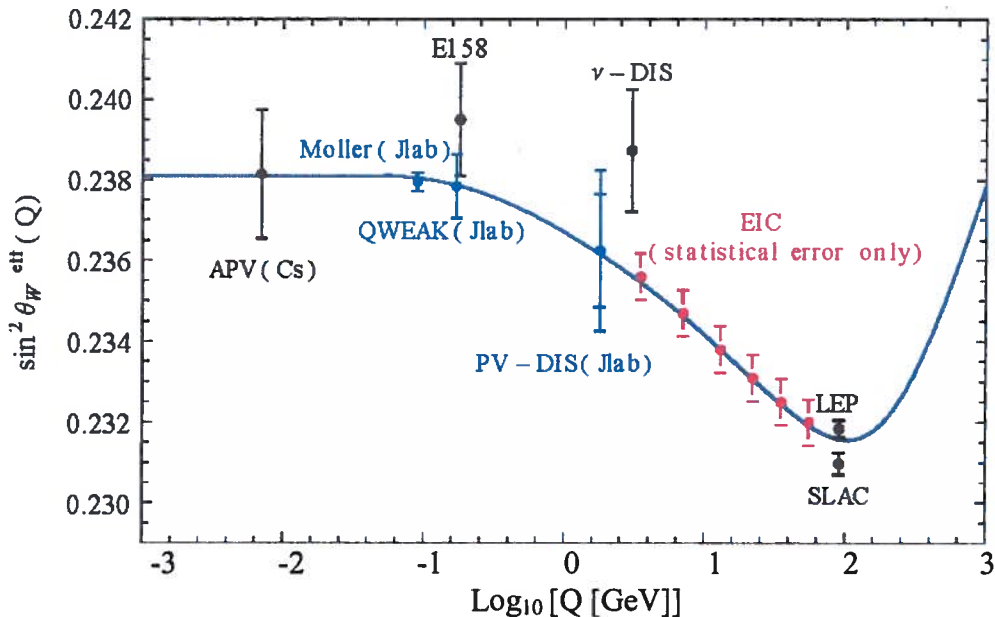


Fig. 1. Existing Measurements (black) of $\sin^2\theta_w(Q)$ as a function of Q . Also shown are anticipated goals of JLAB experiments (blue). EIC capabilities (red) are shown for DIS polarized ep scattering assuming an integrated luminosity of 200Fb^{-1} .

Electroweak Physics with an Electron-Ion Collider

LDRD Project 10-044

W. Marciano and A. Deshpande

PURPOSE:

We have been examining the potential electroweak physics capabilities of an Electron-Ion Collider (EIC). Topics of study include:

- 1) Parity violating deep-inelastic structure functions measured using high statistics polarized electron scattering on polarized proton and light nuclear beams.
- 2) Precision determination of the weak mixing angle over a broad Q^2 range and its implications for "New Physics."
- 3) Searches for lepton flavor violation.

The statistical and systematic errors required are being used to define the goals of an EIC electroweak physics program.

APPROACH:

The principal investigators along with Krishna Kumar (University of Massachusetts) and Werner Vogelsang (BNL, Tübingen University) have considerable experience in deep-inelastic, polarized electron scattering both at the theoretical and experimental levels. Their efforts are assisted by a post doc, Yingchuan Li, who has worked both in nuclear and high energy theory. The study of parity violating structure functions is being carried out by K. Kumar and W. Vogelsang. A related topic, the Bjorken Sum Rule and QCD coupling at intermediate Q^2 is being examined by W. Marciano. The precision weak mixing angle work is being pursued by Y. Li and W. Marciano. Lepton Flavor Violation is being studied by A. Deshpande with emphasis on $e+p \rightarrow \tau + x$.

TECHNICAL PROGRESS AND RESULTS:

Work during FY2011 and the beginning of FY 2012 progressed on several fronts and results were reported at various conferences and workshops including:

- European Centre for Theoretical Studies (ECT), Trento, Italy - Presentation title, "Precision Tests of the Standard Model: from Atomic Parity Violation to Parity-Violating Lepton Scattering," (November 2010).
- Gluons and Quark Sea at High Energies Physics Workshop - To facilitate the organization of the program, Dr. Marciano was a convenor in regards to the subtopic: Beyond the Standard Model - Test of the Bjorken Sum Rule and Electroweak tests, held at INT (September - November 2010).

A more complete list of conferences is included in the Data Collection Form.

LSST – Astrophysics and Cosmology Initiative

LDRD Project 10-045

Erin Sheldon

PURPOSE:

The primary focus of this LDRD is on measuring gravitational lensing effects to probe the expansion history and growth rate of massive structures in our universe. Dark energy accelerates the expansion of the universe, dramatically increasing the volume in comparison to a matter-only universe. Dark energy also inhibits the growth of massive structures under gravitational collapse. Thus the number density of massive objects such as galaxy clusters as a function of cosmic time is directly related to the properties of dark energy, in particular the equation of state parameter $w = \text{pressure}/\text{density}$. Critical to using the number density to constrain cosmology are the masses of the clusters, which we will measure using gravitational lensing effects in DES (Dark Energy Survey). Data from BOSS (Baryon Oscillation Spectroscopic Survey) will also be used to constrain dark energy. The analysis and infrastructure development for DES will lead naturally to work on the Large Scale Synoptic Telescope (LSST) which was accorded top rank among large ground-based initiatives by the Astro2010 Decadal Survey. Brookhaven has a key role in the LSST project and science.

APPROACH:

Erin Sheldon is a member of DES, and is co-leading the lensing effort in DES. This work will be in collaboration with Mike Jarvis and Bhuvnesh Jain from the University of Pennsylvania (not supported by this LDRD). Erin Sheldon and post doc Zhaoming Ma are supported at 100% by this LDRD.

DES will see first light in late spring 2012. The intervening time is spent developing data reduction pipelines and realistic simulations to test these pipelines. After first light, DES will take data for five years, during which the data will be processed as it arrives and analyses performed to extract dark energy parameters.

Lensing measurements are critical to the goals of DES. The primary dark energy probes used by DES are the power spectrum of mass density fluctuations in our universe measured from gravitational lensing (cosmic shear) and the number density of galaxy clusters as a function of their mass and cosmic time. The masses of these clusters are also measured using gravitational lensing. DES will use the combined probes to constrain the equation of state parameter.

This cluster lensing work is a natural continuation of earlier work by Erin Sheldon in the Sloan Digital Sky Survey (SDSS), which remains the most sensitive measurement of this type to date. The processing pipelines for DES are an extension of those used in the SDSS, as are the analysis tools used to extract cosmological parameters. The volume and depth of DES is sufficiently large to allow these measurements to be made in many bins of cosmic time, with which the cosmological analysis will be extended to constrain the properties of dark energy.

TECHNICAL PROGRESS AND RESULTS:

In FYs 2008-2011 software pipelines were developed to measure gravitational shear effects in astronomical images. A framework was created to process the large amounts of DES data in

parallel. The codes were tested on simulated DES data designed to accurately represent DES survey data.

The pipelines can now combine multi-epoch (multiple observations of the same object) data into a single best measurement for each detected astronomical object. The multi-epoch measurement code developed under this LDRD was a major milestone in DES lensing pipeline development. DES will visit each region of sky multiple times producing separate images at different epochs. This multi-epoch analysis is required to optimally process the data because each image is taken under different observing conditions, which results in a different point spread function (PSF). As this is the dominant source of systematic error in lensing measurements, it must be treated with care. The multi-epoch shear measurement code properly accounts for this effect when combining observations.

Using computers at BNL, all of the available simulated images were processed a large number of times during development; the quick turnaround of processing and code improvements has been important for efficient development. The processing includes the single-epoch exposures as well as the full multi-epoch simulated data.

Further DES simulations were created and tested which are a more realistic realization of DES observations and data, and have realistic gravitational lensing effects that can be used to extract the input cosmology. Significant progress was made in testing and stabilizing the code base. In 2010 Ma began developing an improved framework to determine and correct DES data for the PSF. Stellar images (point sources) are used to determine the PSF, which is then interpolated from the positions of the stars to that of the galaxies. Development for this project is completed and the code is ready to be used on the real data.

In 2011, Sheldon worked to further develop algorithms to measure photometric redshifts (photo-zs). These photo-zs are crucial to properly interpret gravitational lensing effects when spectroscopic data are not available, as will be the case in DES. This work is an extension to previous studies, and was applied successfully to SDSS data. In this process, the code was made “production ready” to be applied to the massive DES data set.

DES will see first light in spring 2012 and begin science operations in fall 2012. To prepare for the survey data, processing pipelines and analysis codes to measure gravitational lensing are being written and tested at BNL.

The primary challenge for 2012 is the processing of real DES data as it arrives, and much of the group activities in the ramp-up to operations will be preparing for the data flow. We must adapt the workflow of getting images, processing, and feedback into a streamlined operation. Because DES data management will only process the data a few times, development and testing of the lensing pipeline must occur externally. This testing must use all available data in order to probe low-level systematics, and is thus computationally intensive. BNL has taken on this responsibility, led by Sheldon. This careful attention to systematic effects will lead to accurate measurements of dark energy properties.

Enzymatic Control of Plant Cell Wall Properties that Impact Conversion to Biofuels

LDRD Project 10-052

Paul Freimuth

PURPOSE:

Plant cells secrete numerous different enzymes that are believed to function in the synthesis and assembly of cellulose, hemicellulose and lignin polymers in the cell wall, but the biochemistry and structure of these enzymes is largely unknown because of long-standing difficulties in producing secretory proteins, as a class, by recombinant expression technology. We focused on expressing secreted enzymes from *Arabidopsis thaliana* in the yeast *Pichia pastoris*, with the dual objectives of developing improved technology for recombinant expression of secretory proteins in general and of specifically characterizing the function of cellulases in cell wall synthesis and modification. Improved technology resulting from this research would enable the production and characterization of many secretory proteins that currently are inaccessible, and thus would lead to advances in understanding complex biological systems such as the plant cell wall. Secretory and membrane proteins account for about 30% of the protein coding capacity of eukaryotic cell genomes and will be ideal subjects for structural analysis using the advanced capabilities in protein crystallography planned for NSLS-II.

APPROACH:

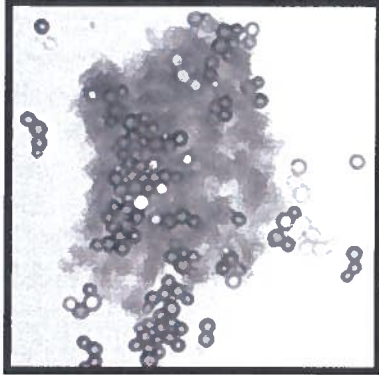
Cellulose is an abundant polymer of glucose found in plant cell walls, and thus is attractive as a renewable feedstock for fermentative production of ethanol and other liquid transportation fuels. However, the cellulose in plant cells walls is assembled with other polymers, including hemicellulose and lignin, which have no value as biofuel feedstocks and indeed must be removed from cellulose prior to biofuel fermentation. These processing steps are a major bottleneck in current methods to produce cellulosic biofuels. Arguably, a better understanding of the mechanisms whereby cellulose is assembled with these other polymers would provide useful insights for developing improved methods to process plant biomass for biofuel production. Assembly of these polymers occurs outside of the plant cell, and is orchestrated by enzymes that are secreted from plant cells into the cell wall. Characterizing the structure and function of these enzymes therefore will be of key importance to understanding mechanisms of polymer assembly in the plant cell wall.

The secretory and membrane proteins of eukaryotic cells are produced in the cell's secretory pathway, a membrane-bound compartment that contains many resident enzymes that carry out the specialized functions of protein folding and posttranslational modification. Many of these specialized functions are unique to eukaryotic cells, therefore as a general rule these proteins cannot be produced in functional form in bacterial host cells such as *Escherichia coli*. Alternative systems therefore must be developed for reliable expression of secretory proteins from eukaryotic sources. Yeast are attractive for this purpose, since they are nearly as simple to grow and genetically manipulate as *E. coli*, and they also contain the necessary specialized functions of the eukaryotic secretory pathway. Our collaborators J. Rose and D. Wilson at Cornell University had reported earlier that a tomato cellulase could be conditionally secreted in its active conformation from the yeast *P. pastoris*, but only in very small quantities. We started by replicating their approach, using two different cellulases from *Arabidopsis* (GH9-C1 and

GH9-C2) in place of the tomato enzyme, with the objective of troubleshooting the system to produce these enzymes in greater yield.

TECHNICAL PROGRESS AND RESULTS:

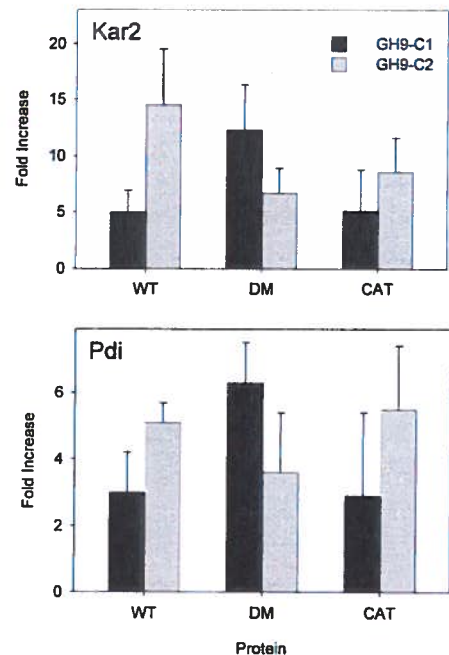
Expression clones were generated for production of each wild-type enzyme, as well as truncated enzymes lacking the substrate binding domain and catalytically disabled full-length mutant enzymes. In good agreement with the results of our collaborators, one of the truncated enzymes was conditionally secreted from *Pichia*. This enzyme was purified and characterized by mass spectrometry, but yields were too low for biochemistry and structural studies. None of the other enzymes was detectably secreted, however.



Expression of these proteins was highly cytotoxic, and caused large fractions of yeast cells in the cultures to lyse soon after induction of protein expression, as shown by vital dye staining (figure left: darkly stained cells are dead). Expression of the catalytically disabled mutants also caused a similar degree of cell lysis, indicating that lysis did not result from cellulase enzymatic activity.

Accumulation of unfolded and misfolded proteins in the secretory pathway is toxic for eukaryotic cells, and if unmitigated, can lead to cell death and disease. As a consequence, eukaryotic cells have evolved a regulatory circuit that adjusts secretory pathway protein folding capacity to match the load of unfolded protein present in the pathway at any given time. We found that this regulatory circuit, known as the unfolded protein response (UPR), was strongly activated in response to expression of the *Arabidopsis* cellulases, as shown by increased transcription of two UPR-responsive genes, Kar2 (BiP) and PDI, that encode enzymes required for protein folding in the secretory pathway (see figure at right). However, despite strong activation of the UPR, the cells still were unable to secrete these plant cellulases. While misfolding of these proteins potentially could account for their toxicity and poor secretion, we were unable to detect accumulation of these proteins in *Pichia* cell extracts.

Together our results support the conclusion that the toxicity and poor secretion of these proteins results from a defect at some point upstream of protein folding in the secretory pathway. Earlier experiments showed that folding of secretory proteins prior to their transport into the secretory pathway is cytotoxic in bacteria. This model can plausibly account for the toxicity and poor secretion efficiency of plant cellulases in yeast. Research in this LDRD has increased our understanding of problems that can arise during recombinant protein expression, and therefore could lead to development of improved technology for production of cellulases and other eukaryotic secretory proteins in yeast.



Cloud and Precipitation 4D Radar Science

LDRD Project 11-001

Scott Giangrande

PURPOSE:

Deep convective clouds (DCCs) play a critical role in Earth's climate system. Understanding the properties of these clouds and simulating their impact is a major challenge for current global climate models (GCMs) and cloud resolving models (CRMs). This LDRD capitalizes on a new cloud observing facility strategically positioned in an environment favorable for DCC development. This unique testbed provides an opportunity to overhaul traditional cloud observations and assess the environmental controls that influence the lifecycle and morphology of DCCs. Our objective is to innovate new multi-scale observations of cloud properties and atmospheric controlling factors towards significant improvements in CRM/GCM performance.

APPROACH:

A. Background and Scope: New Multi-scale Observing Facility Capability: The DOE Atmospheric Radiation Measurement (ARM) Climate Research Facility (ACRF) located in central Oklahoma underwent a major upgrade allowing unprecedented observations of DCCs. DCCs are particularly difficult to adequately observe/model since their dynamical, microphysical and radiative feedbacks act over a wide range of scales. Of immediate interest for characterizing DCC evolution is a suite of scanning cloud and weather radar, each tasked to operate over progressively larger and overlapping domains. These systems include first-ever scanning cloud radar (millimeter wavelength) to map initiating clouds, as well as large-umbrella weather radar (centimeter wavelength) for bulk quantification of deeper precipitating storms. Here, a unique opportunity exists to assume leadership in multi-sensor synergistic approaches to climate-cloud observations for GCM/CRM advancement. The traditional DOE ARM model relies on individual remote-sensing platforms, but this is insufficient since single radar systems only capture snapshots of DCC lifecycle. Further, DOE ARM lacks core expertise in observing deep precipitation processes. Exploiting multiple radar synergies for cloud and precipitation lifecycle study has never been attempted, yet has the potential to yield far more meaningful advances in our understanding of DCCs and for improving model parameterizations.

B. Methodology: Deep Convective Storm Tracking and Characterization: Scanning radar systems present an opportunity to map cloud evolution since they can observe clouds at spatial/temporal scales sufficient for continuous monitoring. An individual radar platform is only sensitive to specific stages of cloud development. We propose to observe DCC lifecycle as follows: (1) Capture 4D (space + time) cloud evolution by exploiting the synergy of complementary, overlapping radar platforms. This is our best opportunity for DCC monitoring, but for the observations of initiating clouds in particular, adaptive scanning of cloud systems is exploratory and therefore risky. The task requires (2) detailed tracking of initiating cloud elements using a variety of novel approaches to assess the best techniques to observe representative cloud properties. This task is performed in coordination with (3) identification of the specific cloud properties that best translate across the overlapping radar domains (e.g., radar reflectivity factor, cloud base/depths). Our efforts in (2) and (3) benefit from proposed subcontracted collaborations with McGill University and BNL cloud physics/modeling/radar strength. Individual case studies must then (4) package the 4D observations in a manner easily

accessible for GCM/CRM model improvement, including linking with the atmospheric conditions that forced these clouds.

TECHNICAL PROGRESS AND RESULTS:

Present Year Progress: Year 1 LDRD funding was critical towards conducting a successful field campaign (including new NASA collaborations) allowing application of first-ever climate monitoring systems to characterize DCC lifecycle. Accomplishments include PI coordination and directed scanning of networked radar facilities during an active 2011 Oklahoma storm season. LDRD motivations, results and collaborative goals were highlighted through 12 PI-supported conference efforts that included several novel demonstrations of scanning cloud radar tracking, modeler-driven core DCC intensity and DCC lifecycle metrics (rainfall, updraft strength). LDRD subcontracted partnership between PI and McGill graduate student provided initial proof-of-concept ‘golden’ event studies - successful in maintaining proposed LDRD FY11 milestones for radar-based capture of initiating clouds, tracking the evolution of these elements and beginning to upscale cloud radar fields into overlapping precipitation radar domains.

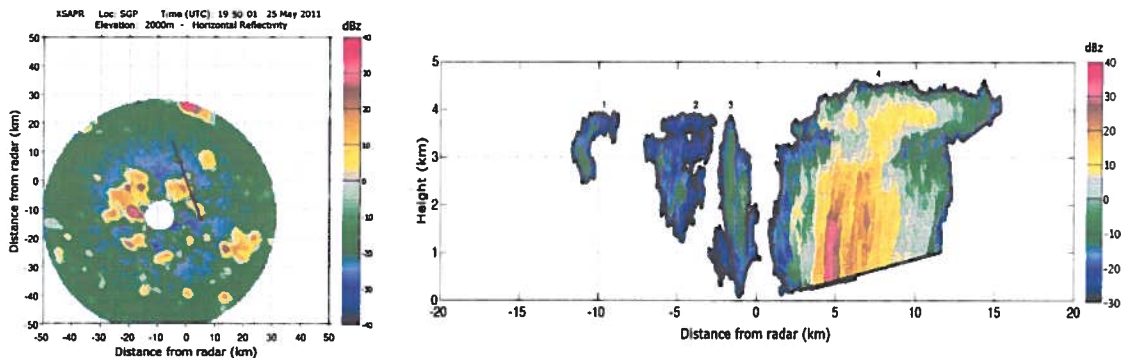


Fig. 1. Radar observations from surveillance weather (left) and detailed cloud radar (right, with tracking IDs) platforms during a shallow cumulus and light drizzle event on May 25th, 2011.

Year 2012/13 Milestones: Multi-scale radar-based DCC lifecycle LDRD motivations to be exploited/completed in FY12/13 through coupling novel FY11 campaign observations with cloud modeling collaborator insights. Initial McGill subcontract success in early-cloud lifecycle monitoring motivates continued FY12 tracking advances using additional atmospheric forcing and overlapping surveillance radar insights. This represents a realistic path toward the most complete depiction of cumulus cloud lifecycle to date. Emphasis in FY12/13 on capitalizing on BNL and McGill modeling expertise to assist in exposure of merged cloud/weather lifecycle observations and build towards measureable model improvement at various scales. This path includes a PI-driven mandate for FY12/13 peer-reviewed journal submission of novel radar-based efforts and climate model linkages.

A Novel Approach to Parameterized Sub-Grid Processes in Climate Models

LDRD Project 11-002

Dong Huang

PURPOSE:

The aim of this project is to develop a novel framework that allows for consistent treatment of sub-grid processes in Global Climate Models (GCMs). The framework will provide a model-observation bridge that can directly transfer knowledge learned from small-scale observations to climate models. This project will also facilitate collaborations between BNL atmospheric research group and wider climate modeling groups outside BNL.

APPROACH:

There are many processes acting at spatial and temporal scales that are too small to resolve by the numerical grids of GCMs and they are presented using parameterizations. A parameterization is a statistical description of the effects of the subgrid processes and interactions in terms of the resolved-scale state. Despite heroic efforts in the past decades, parameterizations of various subgrid processes (e.g., cloud feedback and aerosol-cloud interaction) are inconsistent with each other and remain the source of much of the uncertainty in predictions of climate change.

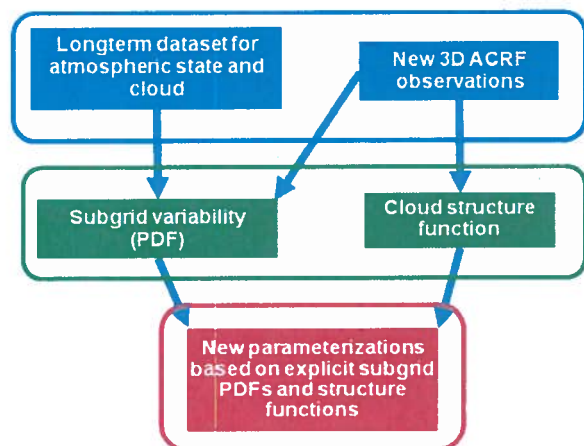


Fig. 1. Research approaches used in this project. Subgrid variability and structure functions are derived from long-term ARM observations. The observed subgrid variability is then parameterized as simple functions and serves as the basis for parameterizations of other relevant physical processes.

A fundamental limitation of conventional parameterizations is that they are formulated in terms of only grid-mean fields. Subgrid-scale variability is only indirectly accounted for using some sort of empirical "tuning knobs", which are usually optimized using observed global climatology. The approach used in this project is to formulate parameterizations based on explicit subgrid variability, i.e., subgrid Probability Distribution Functions (PDFs).

A chain of activities in different areas ranging from observation, to model simulation, and to statistical analysis have been or will be involved to implement this PDF parameterization approach. First, high-quality observations of small-scale processes are needed to characterize subgrid variability of important climate variables. The DOE Atmospheric Radiation Measurement (ARM) program has been

dramatically enhanced with unprecedented 3D observational capability through the American Recovery and Reinvestment Act of 2009. Second, new PDF-based schemes should be developed to enable climate models to predict PDFs of important atmospheric variables within a grid. Third, advanced statistics and probability techniques are needed to investigate the multivariate interactions and dependencies in the climate system. Close collaboration with other FASTER team member is required to integrate these activities.

TECHNICAL PROGRESS AND RESULTS:

I have been involved in several research projects related to this proposal. I was a member of the ARM science team where I developed several cloud remote sensing techniques. I am mainly supported by the BNL FASTER project and I worked on evaluation of physical parameterizations using the FASTER parameterization testbed.

This project officially started in October 2010. A decade-long cloud dataset based on three existing ARM cloud data products is compiled. I then examined the uncertainties in the cloud dataset by comparing the different cloud products across various time scales. It is found that different cloud products agrees well with each other in a statistical sense (Figure 2), though point-by-point comparisons showed a relatively large discrepancy.

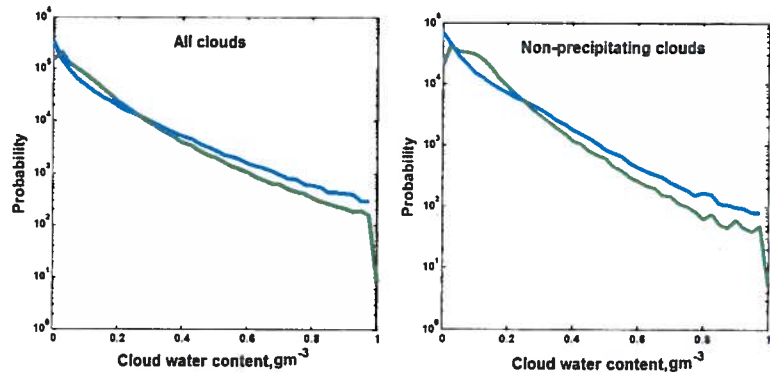


Fig. 2. Probability Distribution Functions of decade-long cloud water content derived from two different ARM cloud products (Blue: BNL MICROBASE product; Green: University of Utah product). It can be seen that subgrid PDF of cloud water content can be described by Gamma functions.

With the support of this project, Dr. Michael Galletti joined us as a research associate in August 2011. Dr. Michael Galletti was a NRC Postdoctoral Fellow at NOAA-NSSL before he joined us. His arrival greatly accelerated this project. We performed in depth analysis of the decade-long cloud dataset to answer an important question: Can subgrid-scale cloud variability (or PDF) and cloud structure be described and parameterized by simple functions across a wide range of spatial scales? Clouds were classified with regard to cloud phase (liquid/ice) and presence of precipitation. It is found that PDFs of cloud water content can be accurately described by Gamma functions at relative large scales (spatial scale > 100 km or temporal scale > 3 hours). For smaller scales, a combination of delta function (to describe the clear portion of the atmosphere) with Gamma function is needed for partially cloudy conditions. This result is robust for different cloud types (Figure 2). It was also revealed that subgrid cloud PDF is closely related to cloud liquid water path (i.e., total water content in a column). If the grid-mean water path is larger than 200 gm^{-2} , cloud variability can be reasonably described by Gamma functions. Otherwise, a combination of delta and Gamma functions are needed.

In summary, through the extensive data analysis performed in FY11, we found that subgrid scale cloud variability can be parameterized using Gamma functions at the resolution of current generation climate models and a combination of delta and Gamma functions is needed if the model grid size decreases below 50 km. This result indicates that subgrid cloud variability described by simple functions can be fed into parameterizations of other cloud-related physical processes. Therefore, the milestone for FY12 is to include explicit subgrid variability into the parameterizations of relevant physical processes such as radiation transfer and cloud microphysics.

Deciphering the Molecular Mechanisms of Lignin Precursor Transportation

LDRD Project 11-007

Chang-Jun Liu

PURPOSE:

Lignin is the second most abundant biopolymer after cellulose in plant secondary cell wall. While important for plant viability, its presence in cell walls contributes to the wall's recalcitrance and formidably impedes the conversion of cellulosic biomass to biofuels. The better understanding on cell wall lignification will facilitate the manipulation of lignin content and composition, thus to better tailor lignocellulosic biomass structural property and create new type of bioenergy crops for both the sustainable biomass production and effective cellulosic biomass conversion. Lignin is derived primarily from the condensation of three monomeric precursors. Previous studies noted that lignin is differentially deposited in particular tissues or cells, implying a tightly regulated and selective export and deposition of the precursors into cell wall by an active transport process, in which some membrane transporters may actively support both the intracellular sequestration, and the export of monolignols across plasma membrane for polymerization. However, the direct biochemical evidence is essentially lacking. Moreover, none of the particular membrane transporters have been identified responsible for lignin precursor transportation so far. The goal of this project is to biochemically evaluate the mechanisms underlying the intra- and inter-cellular translocation of lignin precursors in plants; and to genetically screen and preliminarily assess the particular membrane transporters potentially responsible for monolignol transport. Success in understanding lignin precursor transport process may lead to a rational solution for the temporal- and spatial-control of the differential deposition of lignin in the cell wall, therefore, producing desired lignocellulosic biomass for agricultural and bioenergy industrial applications.

APPROACH:

We are employing the reverse genetics approaches including gene knock-down/out, gene expression suppression and over-expression; and the comprehensive chemical analysis of cell-wall compositions to identify the particular membrane transporters functioning in depositing lignin precursors and in cell wall lignifications.

TECHNICAL PROGRESS AND RESULTS:

By gene expression correlation analysis, from large set of transporter proteins, we identified a small group of ABC transporters whose gene expressions are coordinated well with plant lignification. The expression patterns of those genes were further confirmed by quantitative reverse transcription-polymerase chain reaction.

Subsequently we screened and identified a set of Arabidopsis T-DNA insertion mutant lines deficient in the individual ABC transporter genes; the homozygosity of mutant lines was confirmed. In order to overcome the potential gene functional redundancy, we created a set of double and triple gene mutant lines by genetic cross; meanwhile for those ABC transporter genes lacking of mutant lines, we performed RNAi-mediated gene suppression. Furthermore, the chemical analysis on lignin content and composition and soluble phenolics were conducted for a number of selected mutant lines. Based on these analyses, a few particular ABC transporters were targeted for further biochemical and reverse genetic studies. For functional analysis of the

selected transporter proteins, we tested different heterologous expression systems on those membrane proteins, including in the *Escherichia coli* and different yeast strains; and we achieved an effective expression by using fission yeast system. Using that system we performed preliminary *in vivo* functional screening by feeding monolignols to the yeast culture based on the drug-resistance assays.

Meanwhile we have developed and established effective procedures in isolating and preparing organelle membrane vesicles from yeast and plant cells, which are the necessary tools for next step of *in vitro* functional assessment of transporter proteins.

Our genetics analyses suggest a number of ABC transporters most likely are involved in the plant cell wall lignification. Screening and creating the multiple gene mutant lines, and establishing the *in vitro* functional analysis procedure will facilitate the full identification of the particular transporter proteins.

Touchless Micro-Crystallography

LDRD Project 11-008

Alexei S. Soares, Allen M. Orville, Deborah Stoner-Ma and Marc Allaire

PURPOSE:

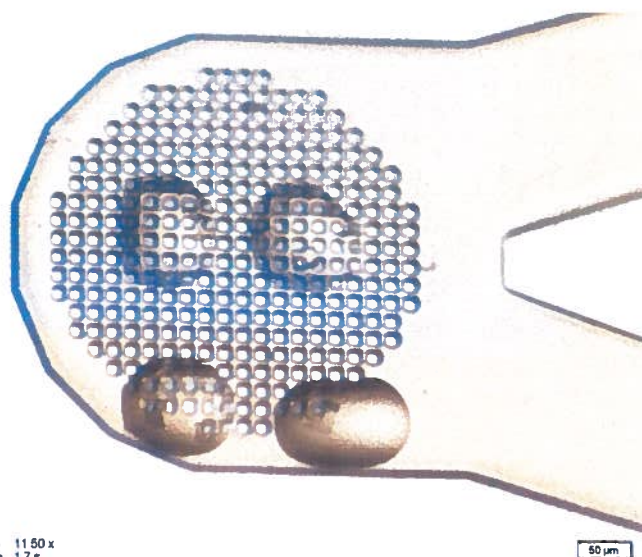
The purpose of the research is to demonstrate the suitability of acoustic droplet ejection (or possibly other advanced liquid handling techniques) to rapidly prepare crystallography specimens with low dead volume, zero lost volume, no tips or tubes to foul or replace, in a database compatible, automated and remote ready keyboard controlled environment. Specimen preparation will include growing protein crystals, improving the quality of protein crystals, combining protein crystals with chemical libraries, and positioning the crystals on data collection media.

APPROACH:

Microcrystals measuring only a few micrometers along an edge are easy to obtain but difficult to use because they are too small to yield a suitable diffraction pattern using conventional methods. Our strategy is to use advances in X-ray sources to generate useful data from micro crystals by reducing background noise using low-solvent acoustic crystal mounting, and by increasing specimen production efficiency using automated and remote specimen preparation.

Phase 1 is complete, as demonstrated in our published results. We have been able to generate structure-quality data from very small crystals that were prepared with low solvent using acoustic droplet ejection (ADE) methods.

Phase 2 has been demonstrated on a small scale. We have grown single protein crystals using as little as 2.5 nL of specimen. This allows miniaturization of protein crystallization trials, so that each crystallization condition consumes ~1 micro-gram of protein (three orders of magnitude less than any competing method). We have also combined crystals with chemicals, and reproducibly positioned the two-component system with ~20 micron x- and y-coordinate precision on data collection media (see Figure). Finally, we have demonstrated that very tiny crystals can be acoustically transferred into new crystal growth wells, containing fresh protein. This protein seeding procedure can increase the size of very small crystals. In the coming year, we will continue to work on expanding the simplicity and flexibility of these experiments.



We are also investigating the possible applications of ADE to other methods, working in collaboration with scientists in other disciplines. Initially, we will attempt to demonstrate that the ADE equipment can also prepare specimens for SAX and cryo-electron microscopy.

The project is carried out principally in collaboration with the commercial company LabCyte and the Almo laboratory at Albert Einstein College of Medicine.

TECHNICAL PROGRESS AND RESULTS:

Core goals: As described in our publication, we have demonstrated the viability of acoustic specimen preparation for test specimens (Lysozyme and Insulin). Unpublished results demonstrate the viability of acoustically prepared specimens using scientifically relevant proteins (nitro-alkane oxidase and an unknown gene product obtained in collaboration with the Radisky laboratory).

Stretch goals: We have demonstrated that multiple two-component systems can be reproducibly deposited on a single data collection substrate (Figure). We have also demonstrated that ADE can be used to screen crystallization conditions using 2.5 nL of specimen (~1 micro gram of protein) and that ADE can improve small crystals into larger ones using seeding.

Multiscale Complexity of Energy and Material Use: Integrated Assessment of Technology and Policy Alternatives

LDRD Project 11-012

J-K Choi

PURPOSE:

The specific research goals of the proposed work include theoretical and applied aspects as follows; 1) Develop a framework, which synthesizes environmental life cycle assessment with existing energy economic modeling tools for analyzing energy systems across multiple temporal and spatial scales, and provide valuable insights into their complex interrelationship with other systems, 2) Apply the framework to evaluate existing and proposed economic/energy policies for reductions in the environmental impacts of energy technologies, particularly for the transition to advanced renewable energy technologies and intermediate policies for a smooth transition between policy regimes. This research topic is intriguing not only because of its scientific and environmental relevance, but also due to the challenges it presents to engineers, economists and policymakers. This research will meet the LDRD Program goals and the DOE mission by employing the multi-disciplinary research approaches to develop technology and policy analysis tools to underpin the national climate change policy, as outlined in BNL's strategic plan for FY09 – FY18.

APPROACH:

Many different energy economy modeling tools are available but most methods for technology assessment and policy analysis tend to focus on the macroeconomic scale level. Methods for transferring information and effect of decisions across multiple scales are inadequate. Such methods are essential for evaluating the effect of changes or policies implemented at coarser scales on activities at finer industries scales or their value chains. Such techniques are also essential for determining the effect of engineering decisions and new technologies introduced at finer scales on coarser scales of the supply chain and economy. A combination of both Market Allocation (MARKAL) and Life Cycle Assessment (LCA) is promising to incorporate the strength of both methods. There are some studies to feed economic and environmental parameters into the MARKAL model that allows for the consideration of additional aspects such as restricted resource availability or learning curves. However, tools for analyzing the dynamic impact of certain policy to the life cycle environmental impact in a product system level are scarce. This research proposes a general framework for performing a multiscale futuristic LCA (MF-LCA) of a product system by combining these two tools. New energy standards such as ISO 50001 require industries to commit to the efficient energy use on their production process and supply chain management while meeting their emission abatement goal. In addition to these voluntary actions, different energy policies such as carbon taxes and cap-and-trade affect the supply and demand of energy commodities both directly and indirectly. Both policy makers and industrial managers need to understand the impact of energy policy to the environmental profile of industrial processes for preparing effective energy policies and strategic corporate management decisions respectively.

The proposed project will significantly enhance techniques for evaluating the life cycle economic, environmental, technological and social aspects of energy systems. The new framework will enable wide range of applications for integrated assessment of multiscale complex problems. The

framework will facilitate whole systems analysis for national/state level policy at by complementing well-established tools or providing alternative technology solutions. In addition, it will help various industries improve their strategic business decision making on production and service activities through the proposed integrated optimization process.

TECHNICAL PROGRESS AND RESULTS:

In FY 11, the research focus was on analyzing dynamic change of environmental life cycle impact of production system by anticipating policy developments. Therefore, dynamic LCI for a photovoltaic system was developed. After the static LCI for a system was formed, average electricity used for each product life cycle stage in the static LCI was disaggregated with respect to the percentage electricity generation mix information gathered from MARKAL for each time period and policy. And then the change in emission intensities for fossil fuel based electricity generation over the time period was considered to create a dynamic LCI database for a product life cycle. An impact assessment method, Tools for the Reduction and Assessment of Chemical and other Environmental Impact (TRACI), was used for analyzing the dynamic change of the various environmental impacts on the production processes. From MARKAL side, various carbon mitigation policies are considered in the U.S. Multi-region MARKAL (US MRM). The main source of technology assumptions for the US MRM is the Energy Information Administration (EIA). Much of the relevant information is published annually as part of the Annual Energy Outlook (AEO) and the associated National Energy Modeling System (NEMS) documentation.

As part of the milestone of this project in FY12, the proposed research will target on developing methodology for anticipating technology development since existing LCA recommendations do very little to advance the technology modeling. In addition, interfacing engineering decision with the broader implication of economic and environmental externality through the multi-scale modeling framework will be performed for FY12.

Indium Iodide (InI) – A Potential Next-Generation Room-Temperature Radiation Detector

LDRD Project 11-016

Anwar Hossain

PURPOSE:

There is widespread demand for high-performance, compact radiation detectors in many areas, including homeland security, medical imaging, and astrophysics. Cadmium Zinc Telluride (CZT) detectors are currently the leading candidate in these applications. However, their deployment has been limited by the dearth of high quality, large-volume single crystals due to material defects, primarily generated during crystal growth. A near-term remedy of such issues remains challenging, since the technical issues in growing crystals seemingly cannot be overcome easily. For better balance in our detector program, we opted to search for a suitable alternative detector material. While several materials are in the pipeline, all still are far from offering an alternative to CZT. Furthermore, current semiconductor detector materials contain toxic elements which might be deemed as health- and environmental- issues in the future. In view of the features, we proposed Indium Iodide (InI), a binary compound semiconductor, which may be a promising candidate for the next-generation, room-temperature radiation detectors.

APPROACH:

Indium Iodide possesses the required properties for an excellent radiation detector and offers several potential advantages over other materials for room-temperature radiation detection and imaging. It has a relatively low melting point (381°C) and does not exhibit a solid-solid phase transition between its melting point and room temperature. Therefore, we can grow flawless large single crystals readily via simple melt-based processes, like the Bridgman technique. We have well-established crystal growth and characterization facilities and supporting scientists at BNL to execute all the steps from crystal growth to device testing. Our goal is to complete comprehensive feasibility studies of InI as a next-generation room-temperature semiconductor detector.

TECHNICAL PROGRESS AND RESULTS:

We began the process of purchasing source materials immediately after this project began in October 2010. We received the source materials around February 2011. The initial purity of the InI source material was just 5N grade, and in order to improve the material purity we conducted zone refining with 50 passes at 405 °C and at 20 mm/hour speed in a quartz ampoule. Afterward, we used a floating zone method to grow the crystals. The growth temperature was 395 °C with a temperature gradient 25 °C/cm, and the growth rate was 2.0 mm/hour.

We anticipated problems during our first approach as one of the motors stopped functioning after 15 passes of the zone-refining process, which yielded a defective ingot. We optimized the system after replacing the motor and grew another ingot. We characterized its material properties, fabricated the detectors, and tested them as X- and gamma-ray radiation detectors. The purification system, crystal growth furnace and as-grown InI crystal are shown in Figure 1.

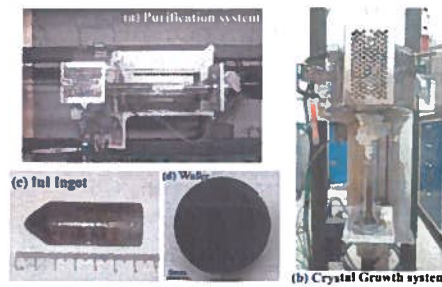


Fig. 1. (a,b) Material purification and crystal growth system; (c, d) As-grown ingot and a wafer of InI crystal.

The ingot was sliced and cut into the desired size, and processed them for characterization of its bulk properties. The band-gap was measured using Fourier Transform Infra-Red (FTIR) method, and a value of 1.96 eV was obtained. We investigated and captured infra-red (IR) transmission images of polished wafers, which displayed that the entire ingot was likely to be single crystal. There are some voids generated in the ingot during crystal growth; those are most likely due to improper cooling rate. We should be able to resolve this problem in our following growth process. We also analyzed the material uniformity using SEM integrated with an EDS system. The composition of elements was found to be fairly uniform along the radial direction of the wafer. We processed some selected crystals and attached metal contacts for electrical measurement and device testing. We measured the leakage current against bias voltage and calculated the resistivity of the crystal ($\sim 10^{11} \Omega\text{-cm}$). We tested them as radiation detectors using an Am-241 source and obtained reasonably good response. However, the detector showed a polarization effect, and the peak disappeared. More investigation is needed to understand and resolve the polarization.

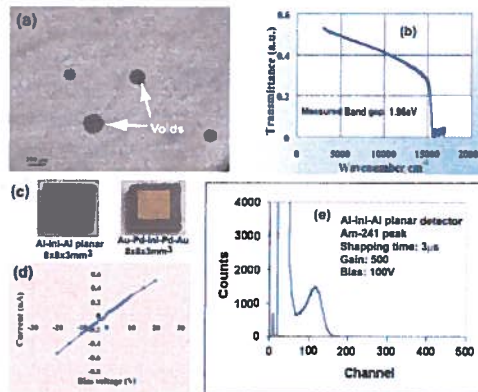


Fig. 2. (a) IR transmission image of InI wafer. Voids were found in the wafers; (b) Band gap was measured by FTIR method; (c) Images of InI planar detectors; (d) Current-voltage curve; (e) Am-241 gamma response of an InI planar detector.

High-resistivity, large-volume single crystals with fewer defects were successfully grown. Our research indicates that it is a promising candidate material for room-temperature and gamma-ray detectors in the field of homeland security, industrial/medical imaging and high energy research.

Milestones:

- Year 1: (1) Optimize material purification and crystal growth process; and
- (2) Material characterization, device fabrication, and testing.
- Year 2: (1) Crystal growth after modifying the parameters from acquired feedback; and
- (2) Material characterization, device fabrication and testing.
- (3) Apply for DOE/other funding based on these acquired data.

Visualization Support Infrastructure for Global Climate Modeling with a Focus on the BNL FASTER Project

LDRD Project 11-017

Michael McGuigan and Klaus Mueller

PURPOSE:

The objective of this project is to develop an interactive visual analytics system that can aid atmospheric scientists in the analytics and refinement of global climate models. Since climate data are both multivariate and have a geospatial reference, we have taken the unique approach of tightly integrating geospatial and multivariate information displays, each providing views on complementary but co-referenced aspects of the data. Further exploratory aspects of the project are how to deal with time-variant and uncertain behavior of the variables and how to integrate the system into the workflow of the participating scientists, developing modules that can be called from their existing workbench of tools. We have collaborated closely with the BNL Fast-physics System Testbed and Research (FASTER) team led by Yangang Liu to implement, test, and evaluate the developed system. The project is well in line with both the mission of BNL and DOE. The BNL laboratory plan 2008-2018 lists climate science as an activity with high impact and/or growth potential.

APPROACH:

The FASTER climate data has a wide range of time-variant variables, including but not limited to cloud macrophysics, such as cloud fraction, base and top height, liquid/ice water path, and precipitation, as well as aerosol properties and radiation fluxes. The data have significant variations in spatial scale. Many statistical data analysis and advanced data mining tools are available to efficiently distill information and patterns from the massive model and observation datasets, such as clustering, outlier detection, correlation analysis, etc. However, automated and unsupervised methods often fail once the number of variables grows beyond a dozen or even less. Recognizing this deficiency has given rise to the emerging field of *Visual Analytics* which puts the domain scientist into the loop of the data analytics, enabling them to interactively interrogate the data. Visual analytics requires suitable visualization support matching the complexity of the data. Devising such a visualization suite tailored to the data configuration of the FASTER project is the aim of this 2-year project. Our approach is to extend and adapt a suite of multivariate visualization tools we have already developed and link them with an interactive geo-spatial display based on Google Earth augmented to provide multivariate visualization capabilities.

TECHNICAL PROGRESS AND RESULTS:

Figure 1 illustrates the various components of our present system. The *parallel coordinate plot* shows the raw multivariate data – each vertical axis represents one attribute and each data point gives rise to a piecewise linear line going across the axes. The *dynamic scatterplot* is a projection of the multivariate data into an arbitrary vector basis controlled by the polygonal touchpad interface shown on the right – each vertex is due to one chosen data attribute, here 7. The *sight map* can be used to save interesting projections and arrange them in terms of their projection vector similarity. The *network display* arranges the data dimensions in terms of their correlation – nodes of closely correlated attributes are located nearby – and users can define a path across this

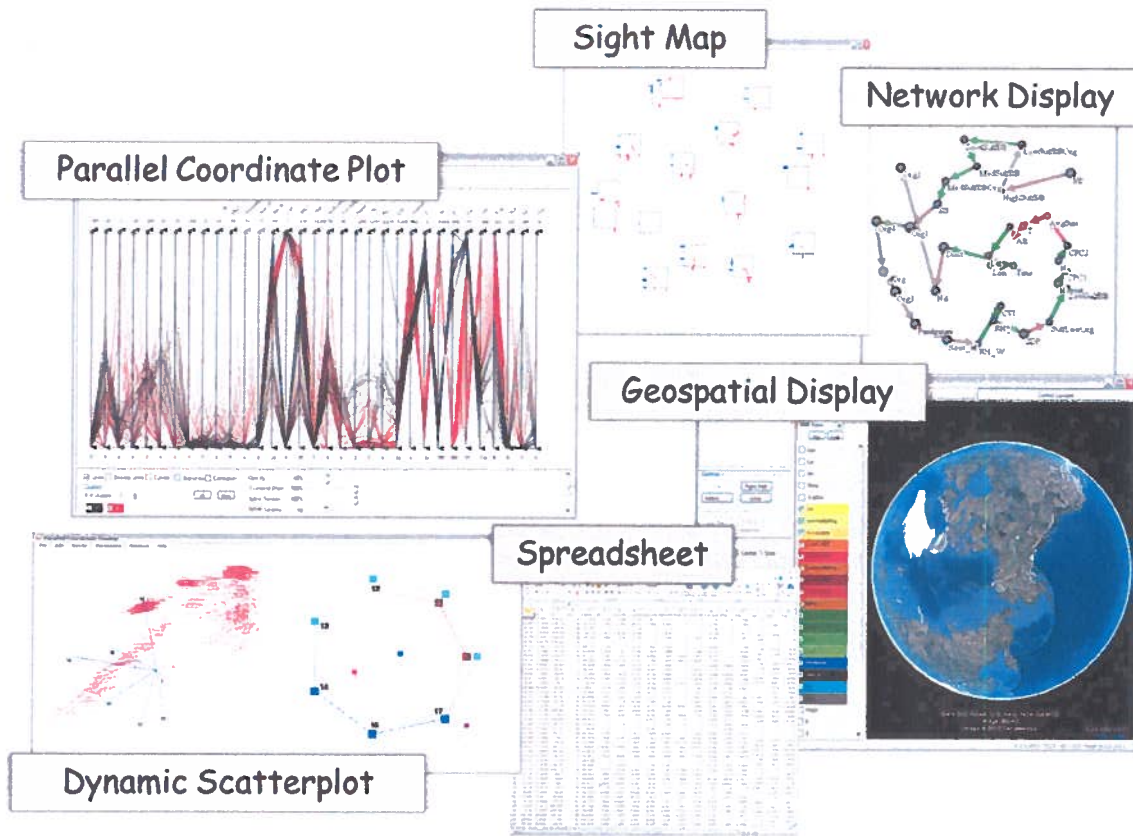


Fig. 1. Overall system architecture.

dimension landscape to specify and axis order in the parallel coordinate plot. The *geospatial display* allows users to visualize and select geo-referenced data within a Google Earth plug-in – the data marked there are then highlighted in different colors in the parallel coordinate and the dynamic scatterplot display where they can be further manipulated. Finally, the *spreadsheet* enables users to perform mathematical operations on the data and so create new attributes that can be visualized in the various linked display. In this LDRD year we have devised the geospatial display and the spreadsheet and their integration with the other modules of our suite. Figure 2 shows the current system in action, via Global Seawater Oxygen-18 dataset. The next LDRD year will focus on time-varying and uncertain data, as well as on the FASTER workflow integration.

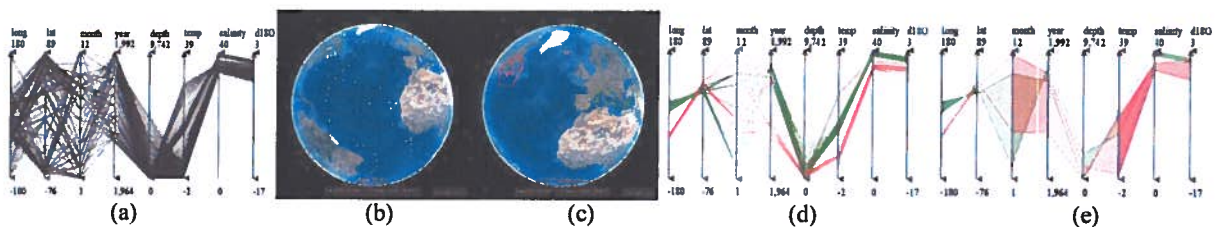


Fig. 2. Dual-domain analytics. (a) The analyst first uses the PCP (parallel coordinate plot) brushing handles to select the normal ocean data points (salinity from 32-40). (b) The GE (Google Earth) display responds by showing only these remaining data points. (c) Next the analyst uses mouse clicks to outline some interesting regions in GE (Mediterranean shown in green and Gulf of St Lawrence shown in red). (d) The points inside the selection polygon appear highlighted in the PCP. (e) Correlation-enhanced illustrative PCP display.

Single Crystal Growth of Novel Energy Materials by High Pressure Method

LDRD Project 11-020

Genda Gu

PURPOSE:

Our goal is to explore single crystal growth of advanced energy materials. In particular, we will address the problem of growing crystals with highly volatile components that cannot be grown at ambient pressure. Our approach is to develop a new technique to grow various single crystals involving our new and unique use of high pressure hot isostatic press furnace.

APPROACH:

By using a super-high pressure furnace, we will explore the growth of the single crystals of various new advanced energy materials, which cannot be grown at ambient pressure by traditional crystal growth methods. A new high pressure hot-isostatic press furnace, with capability of gas furnace, which will have a gas pressures (a gas mixture of 20% oxygen or nitrogen—80% Ar) up to 7000 bars and temperatures up to 1200°C initially (with the potential for 2000°C) and a working volume of 1.5 inch diameter by 6 inch high, will be installed in our group in Jan. 2011. The furnace is the first of its kind in the world, offering us new capabilities to explore various new single crystals, which cannot be grown in other groups in the world. We specifically address the newly discovered highly volatile energy materials that cannot be grown at ambient pressure, an area in which there is great potential for discoveries as well as for improvement in techniques and capabilities. For example, all rechargeable lithium electrode materials, such as LiMn_2O_4 (cathode materials), $\text{Li}_4\text{Ti}_5\text{O}_{12}$ (anode materials) can never be grown into mm-size single crystals due to the highly volatility of Li_2O high volatile nature at the melting point. In order to provide the major breakthroughs needed to address important fundamental science and technology questions, the large single crystals are indispensable for us to study the fundamental issues on the complex chemical and physical phenomena in the electrode materials. There are three types of energy materials we will try to explore: 1. Lithium battery electrode materials; 2. New nitride materials for solid state lighting; 3. New oxide and non-oxide superconducting materials. If the new single crystals of advanced energy materials are grown, it will put BNL to the forefront of the energy materials research which will bring future research funding from DOE and industries.

TECHNICAL PROGRESS AND RESULTS:

In FY 2011, we hired a new post-doc fellow Zhijun Xu to prepare the high pressure work. We had got the high pressure furnace from AIP (The HIP furnace is shown in Figure 1. The furnace was shipped to our laboratory last December.



Fig. 1. The picture of 1,000,000 psi hot isotatic pressure furnace

Our 1,000,000 psi hot isostatic pressure furnace is the best furnace in the world. This furnace is the key equipment for our project. We are installing and testing the furnace now.

For FY2011, we had all equipment for the project and had all personal for the project.

For FY 2012, we will grow the various new single crystal by using the new hot isostatic pressure furnace.

Complex Networks Approach to Power Grid Design and Stability

LDRD Project 11-023

Sergei Maslov and Meng Yue

PURPOSE:

We proposed to extend and modify the toolbox of algorithms developed in the complex network community and to subsequently apply it to improve the stability and optimize the design of the U.S. power grid and its regional components. In particular, the following applications of our study are anticipated: (1) to help the ongoing extension and upgrading plan of the U.S. transmission network by prioritizing criticalities, sizing, and optimizing the placement of the grid components under different fault and normal operating conditions; (2) to help determine optimal boundaries for splitting of interconnected power systems when islanded operation or load-shedding is required. Islanding strategies will be tested under various operating and fault conditions to minimize the extent of the blackout while still satisfying both the steady-state and dynamic constraints of the grid operation.

APPROACH:

The first measure of complex network architecture affecting its reliability of operation is the degree distribution. We and others convincingly demonstrated that in addition to degree distribution, the stability of complex networks is strongly influenced by their pattern of degree-degree correlations. More specifically, networks with peripheral architecture in which hubs prefer to connect to other hubs are more stable than the ones with centralized architecture. We proposed to investigate the profile of degree-degree correlations and quantify the effect it has on their stability with respect to breakup into disconnected components. This has been accomplished (see figure below).

TECHNICAL PROGRESS AND RESULTS:

- Reviewed the literature on complex networks approach to power grid.
- Processed the raw data for regional power grid provided by Meng Yue (1190 nodes, 1315 edges). Imported the resulting table to Matlab (Fig. 1).
- Constructed the correlation profile of the network (Fig. 2).
- Simulated diffusion process on the power grid network, analyzed the eigenvalues of the diffusion matrix and identified communities (Fig. 3).

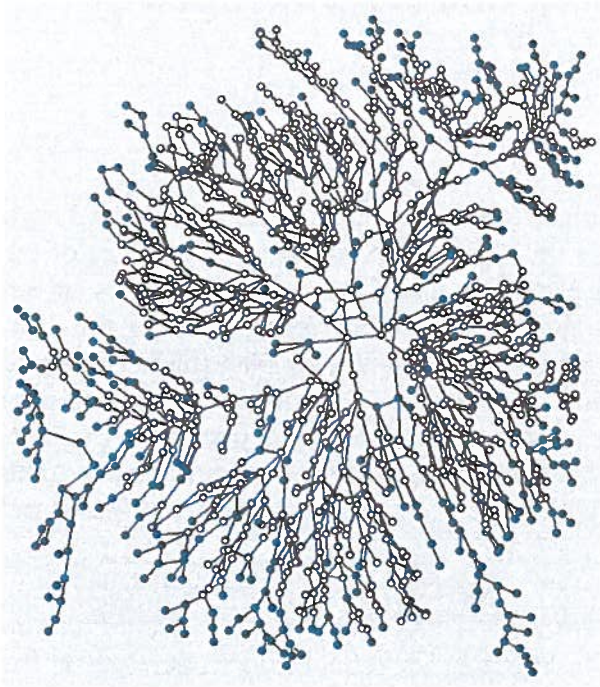


Fig. 1. Regional US power grid based on Meng Yue's data (1190 nodes 1315 edges).

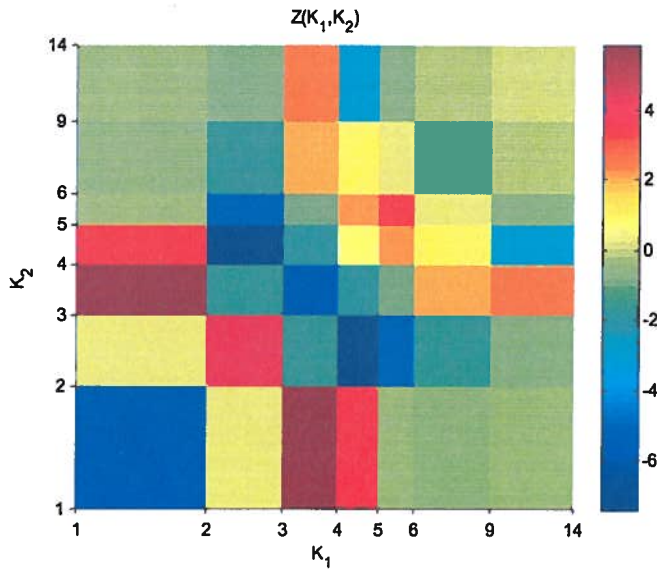


Fig. 2. Z-score of degree-degree correlations in the regional power grid network.

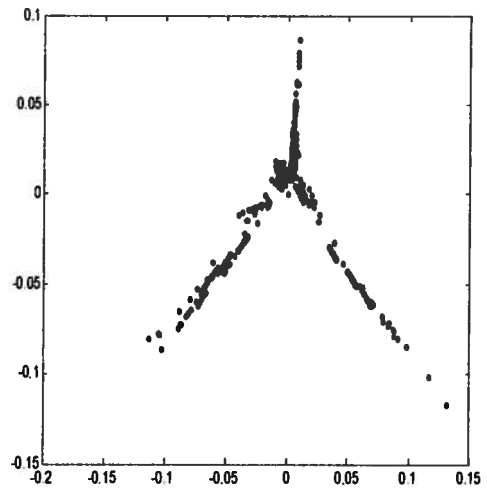


Fig. 3. 3rd vs. 2nd eigenvector of the diffusion matrix on the power grid. Rays correspond to communities.

Protein Microcrystal Dynamics by Coherent X-Ray Scattering

LDRD Project 11-025

Andrei Fluerasu

PURPOSE:

The project aims at measuring collective dynamics in protein crystals using intense coherent X-ray beams. The classic method giving access to such information is X-ray Photon Correlation Spectroscopy (XPCS), which essentially uses “movies” of coherent diffraction images (so called “speckle” patterns) to calculate correlations of fluctuations inside the sample. This method poses many problems related to beam damage induced by the intense X-rays to the samples and in particular to biological samples. In order to circumvent this problem, we propose to use an alternative method – speckle visibility spectroscopy – which uses only single speckle patterns, and measures the characteristic times of fluctuations inside the sample from the speckle contrast. The main purpose of this project is a feasibility study about the use of X-ray Speckle Visibility Spectroscopy as a tool for measuring motion of proteins (dynamics). If successful, these experiments could open many new possibilities in the field of structural biology by extending the structural information provided by classic protein crystallography and making connections between motion and biological function.

APPROACH:

This project poses several distinct experimental challenges and was naturally divided into different “sub-projects”. First of all the experimental technique – speckle visibility spectroscopy (XSVS) – was not yet demonstrated with X-rays but only with visible laser light. As a stand-alone task, we applied the XSVS technique to measure the dynamics of several “model systems” consisting of radiation-hard colloidal suspensions. This allowed a direct comparison between XSVS and XPCS experimental results and theoretical estimations for the expected relaxation times. This work was performed on experimental data collected at ESRF, is currently in progress and will be submitted for publication.

In order to measure protein dynamics, the coherent beams are incident on the protein crystal held at room temperature and a photon counting detector is used to monitor the scattered intensity around a main Bragg peak. The resolution needs to be high-enough to measure diffuse scattering and to resolve single speckles, and for this reason, the detector needs to be placed far-enough from the sample. The work on establishing the optimal conditions for XSVS on protein crystals benefited on several rounds of beamtime at the ID10 instrument of the European Synchrotron Radiation Facility (ESRF) and the 8-ID beamline at the Advanced Photon Source (APS).

Finally, a large part of the effort during the previous year was dedicated to establishing the growing conditions for protein crystals and finding the most suitable sample-handling methods (e.g. in terms of stability) for XSVS experiments. Several options for handling the crystals were tried and tested at NSLS (X6), ESRF and the APS.

Perhaps the highest challenge that we are facing during this project is managing the X-ray induced beam-damage. The experiments performed during the past year helped us in establishing the maximum allowable dose for some of the crystals that were studied and in designing the experimental strategy that circumvents beam-damage.

The LDRD project is a collaboration between an enthusiastic team consisting in Dr. Luxi Li, who was hired as a Research Associate (since March 2011) to lead this effort, Dr. Lutz Wiegart, CHX beamline scientist, Dr. Vivian Stojanoff, beamline scientist X13, NSLS, Mrs. Mary Carlucci-Dayton, CHX Lead Engineer, Dr. Jyotsana Lal, Scientist, Argonne National Laboratory, Prof. Simon Mochrie, Yale University, and AF.

TECHNICAL PROGRESS AND RESULTS:

Several options were tested for sample handling and sample preparation, including a room-temperature kit and a humidity stream developed at EMBL, Grenoble. The best results in terms of stability required for coherent scattering experiments were obtained with the samples held in quartz 0.3-0.5 mm capillaries. The crystals were grown directly inside the capillaries using a counter-diffusive method. The highest quality samples that were obtained thus far are tetragonal lysozyme crystals of 0.1-0.5 mm (Figure 1). The crystallization condition is 0.1M Sodium acetate, 80mg/mL sodium chloride, and 80mg/mL lysozyme, pH=4.7. These crystals showed rocking curves of about 8-10 arcsec which matches the quality of similar samples grown in low-gravity conditions in the outer space.

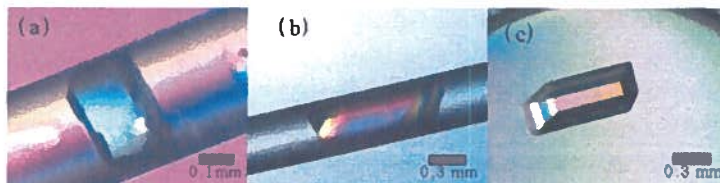


Fig. 1. Tetragonal lysozyme crystal grown in 0.3 mm quartz capillary using a counter-diffusive method, (b) tetragonal lysozyme crystal grown in 0.5 mm quartz capillary with the presence of agarose gel using counter diffusive method, (c) monoclinic lysozyme crystals (~0.6mm) grown using Batch method

The optimal experimental protocol was established during preliminary experimental runs at the ID10, ESRF and 8 ID, APS beamlines. The method consists in holding the capillary containing crystalline sample in a custom-made holder on a goniometer head and switching between a low angular resolution setup with an integrating CCD detector placed near the sample and used to orient the crystal and find particular Bragg reflections, and a high angular resolution photon counting detector used to resolve diffuse scattering and coherent diffraction patterns around particular Bragg spots. Usually the sample-detector distance for the high-resolution setup is about 3-3.5 m, depending on the exact experimental conditions, which makes finding particular Bragg spots quite challenging. In Figure 2 we show such a pattern obtained around the (100) reflection of a tetragonal lysozyme crystal. The data recorded at ESRF and APS is currently being analyzed and used in preparing the following experiment that we will hold at the 34ID beamline of the APS. Compared to the previous experiments, we will take advantage of a wider range of scattering angles available at this beamline to measure diffuse scattering around higher index Bragg peaks and a value of $q \sim 0.6 \text{ \AA}^{-1}$ (compared to $q \sim 0.1 \text{ \AA}^{-1}$ in Fig. 2). This will result in a significant increase in diffuse scattering (Meihold and Smith, *Phys. Rev. Lett.* **95**, 218103, 2005).

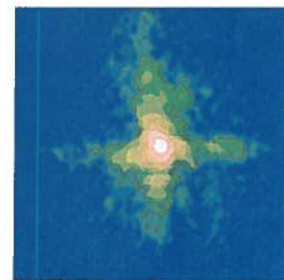


Fig. 2. Diffuse around a Bragg scattering scattering around the (100) peak of tetragonal lysozyme.

The main milestones that we have set for the second year of this project are summarized below:

- Crystallization of new protein samples with potential slow collective motions accessible by XSVS: monoclinic lysozyme (J. Doucet and J.P. Benoit, *Nature* **325**, 643, 1987),

hemoglobin (H. Frauenfelder *et al.*, *Science* **254**, 1598, 1991), motor proteins – myosin, kinesin (S. Mochrie, *private communication*)

- ID34, APS experiment (lysozyme and hemoglobin samples) with measurements at higher q values
- Paper describing XSVS results (on model systems)
- Paper describing the Coherent-diffuse scattering measurements from protein crystals establishing the optimal conditions (in terms of q-range) for XSVS analysis of collective dynamics on different protein crystals; performing XSVS data analysis
- Preparation (proposals and experiment preparation) of future – Fall 2012 - experiments at ESRF and/or APS

High-Resolution Biological Imaging by X-Ray Diffraction Microscopy

LDRD Project 11-027

Enju Lima

PURPOSE:

Among the advanced biological imaging methods, the task of imaging intact, a-few-microns-thick samples at 10 to 20 nanometer resolution, without the risk of structural artifacts remains out of reach primarily due to thickness limitations. The recently developed XDM has the potential to attain this goal by utilizing the high-penetration power of hard x-rays to image thick samples and by imposing no optics limitations to achieve nanometer resolution. This LDRD aims to demonstrate the high-resolution feasibility of cryogenic XDM for biological samples. This frozen-hydrated state provides the necessary cryo-protection for wet samples against ionizing radiation. The goal is to (1) demonstrate the achievable resolution by cryogenic XDM and (2) expand the scope of biological XDM. The high coherent flux of the future NSLS2 can greatly benefit cryogenic XDM in reaching the estimated achievable resolution of 10 nm. The work led by the current proposal will provide the framework for the future biological XDM at NSLS2.

APPROACH:

In biological imaging, preserving samples close to their native state is crucial yet challenging due to their delicate natures. Radiation damage is one of the fundamental challenges with biological samples. To overcome this difficulty, we will investigate frozen-hydrated sample preparation. *D. radiodurans* bacteria and extracted mitochondria are chosen for imaging. They are 1 to 4 microns in size. Our earlier work indicated that rapid plunge-freezing might not provide an adequate cooling rate for these thick samples to embed them in a uniform vitreous ice layer. In collaboration with C. Kim and S. Gruner at Cornell, we plan to explore the applicability of high-pressure freezing in XDM. The sample preparation at BNL is carried out in collaboration with S. Yang and H. Li of the Biology department. For the improvement of reconstruction methods, we are collaborating with A. Diaz and M. Guizar at Swiss Light Source to develop a scanning mode for cryogenic XDM, which is expected to expand its scope to extended samples of tens of microns in size.

TECHNICAL PROGRESS AND RESULTS:

The proposal was funded starting FY11 and the following summarizes the progress during FY11.

- 1. Mitochondria preparation.** Collaboration with K. Hartil and I. Kurland at Albert Einstein Medical School is to study mitochondria morphology changes due to functional changes, such as in diabetes. Extracted mitochondria were examined by cryo-electron microscopy (cryo-EM) to find a suitable extraction method. Figure 1 shows some of the

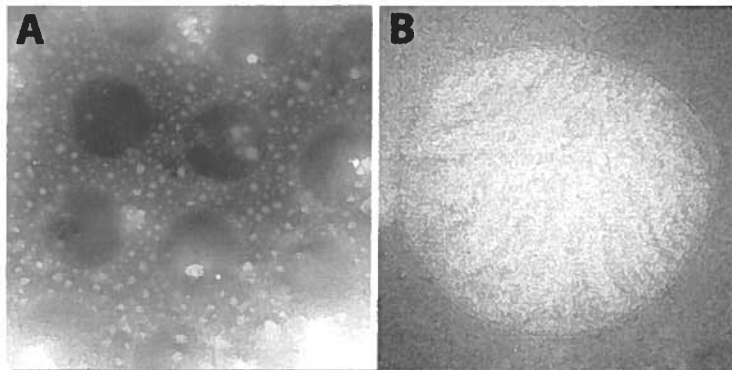


Fig. 1. (A) An overview of the sample grid prepared for cryo-EM with extracted mitochondria. (B) A zoomed-in mitochondria image.

mitochondria imaged by cryo-EM.

- High-pressure freezing samples for XDM application.** The challenge in applying the Cornell prototype high-pressure freezing to XDM is in maintaining around the sample a water layer of a-few-microns thickness for several minutes before high-pressure freezing is applied. With protein crystals, oil coating crystals is sufficient, but this technique cannot be applied to XDM when one needs to reach a-few-microns-thick uniform ice layer at the end. In collaboration with C. Kim, we tested different methods, such as a mini-humidity chamber created by capillaries as well as different freezing protocols by shortening the preparation time. One of these methods was tested at ESRF and yielded successful sample freezing into vitreous ice condition. Figure 1 (a) shows a frozen-sample loop imaged by optical microscopy and (b) the measured diffraction pattern from *D. radiodurans* bacteria sample using 8 keV x-rays. The data analysis is being carried out during FY12.

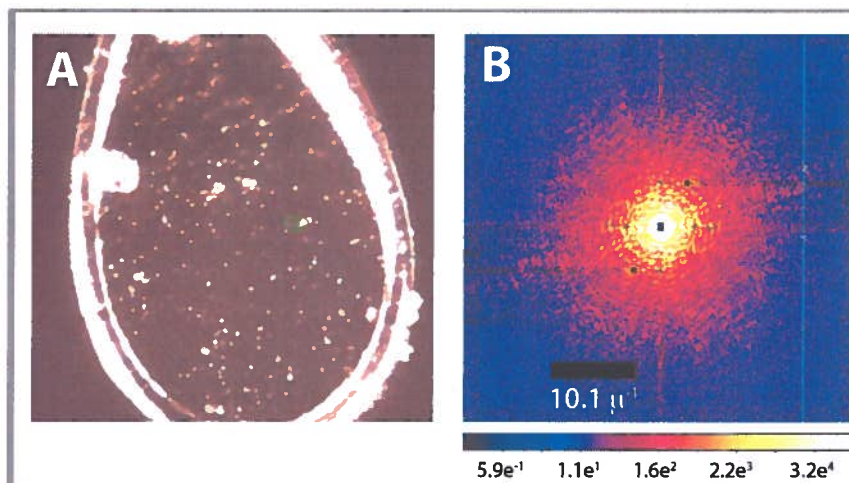


Fig. 2. High-pressure freezing *D. radiodurans*. (a) Frozen sample loop by high-pressure freezing, mounted on a diffractometer. The image was obtained by an on-axis optical microscope. (b) From the loop shown in (a), two samples of *D. radiodurans* were found and full 2D diffraction data were collected. One of the data sets is shown here.

- Post-doctoral fellow employment.** An interview process was carried out to select a post-doc candidate for the proposed work. The finalist, Li Li was offered the position in August 2011 and he started working on the project in September 2011.

Milestones for FY12 anticipated funding

- A 2-dimensional (2D) reconstruction of frozen-hydrated *D. radiodurans* at a resolution of 30 nm or below.
- A demonstration of 3D data collection and data assembly.
- 2D data collection from frozen-hydrated mitochondria.

Milestones for FY13 anticipated funding

- A 3D reconstruction of frozen-hydrated *D. radiodurans* and a demonstration of achievable resolution in 3D reconstruction.
- Reconstruction of mitochondria in 2D by scanning XDM.

Sub-10 nm Resolution Soft X-Ray Microscopy of Organic Nano-Materials by Novel Diffraction Methods

LDRD Project 11-030

David Shapiro and Konstantine Kaznatcheev

PURPOSE:

The goal of this LDRD project is to develop novel coherent diffraction methods for ultra-high resolution imaging of organic nanomaterials. The technique, soft x-ray ptychography, will extend the capabilities of currently existing x-ray microscopes by providing additional information about the sample (the x-ray diffraction pattern) which can be used to enhance the image resolution. The diffraction enhancement of our data will allow for imaging at a resolution that is superior to that provided by the standard x-ray imaging optic (a zone plate lens) which is currently around 25 nanometers (nm) during standard operation. If a resolution of a few nm can be achieved it will be extremely valuable for structural studies of self-assembled nanomaterials which are typically formed from building blocks with sizes of 10-20 nm. Such materials are commonly assembled from nanoparticles functionalized with DNA molecules and are of particular interest to the Center for Functional Nanomaterials at Brookhaven National Lab. Soft x-ray ptychography is a “photon hungry” technique and will benefit greatly from the very high brightness of NSLS-II. It will be an advanced tool for the materials sciences at the Coherent Soft X-ray (CSX) beamline.

APPROACH:

A ptychographic x-ray microscope works very much like a scanning transmission x-ray microscope (STXM). In a STXM, a coherent x-ray beam is focused by a zone plate lens onto a small (~25 nm) spot on the sample and the transmitted intensity is measured by a point detector. If the sample is scanned, a two-dimensional map of the optical density can be measured. In a ptychographic microscope, the point detector is replaced with a Charge-Coupled Detector (CCD) which typically has more than 1 million pixels. Thus, at each sample position a complete diffraction pattern is recorded. The large increase in the amount of information available allows for numerical reconstruction algorithms to recover not only the electron density of the sample at very high resolution but also the structure of the x-ray illumination, or probe. Therefore, this technique is also very powerful for optical metrology. The reconstruction algorithms require a few conditions to hold in order to be successful. First, the sample must be scanned such that neighboring positions of the probe overlap by at least 50%, second the sample positions must be known to high precision, and finally, the probe must be stable during the measurement.

Ptychography has a long history; having been demonstrated with electrons and hard x-rays, but it has never been used to enhance an already high-resolution x-ray optical system. Since the technique does not rely on the probe size to determine its resolution (the extent of the diffraction pattern does that) we should be able to achieve fine detail whether or not the optical system is in focus. Our approach is to utilize a de-focused probe (large spot with low intensity) for projection type imaging with a large field of view and a focused probe (small spot with high intensity) for high resolution of regions of interest. This combination provides a great deal of flexibility in the imaging system and provides a more radiation-dose optimized scheme for imaging organic matter. These imaging experiments proceed in collaboration with the SM beamline of the Canadian Light Source and our post-doctoral scholar, Dr. Shengyu Wang.

TECHNICAL PROGRESS AND RESULTS:

In fiscal year 2011 we have made our first complete demonstration of soft x-ray ptychography using a STXM and we have recorded diffraction data from nanoparticle samples to a resolution of 2.5 nm. Figure 1(a) shows a typical diffraction pattern recorded by the microscope and Figure 1(b)-(c) show the reconstruction of the object and probe, respectively, which were derived from the complete set of 25 diffraction patterns. In this particular case the lens was defocused to such an extent that a near projection of the object can be seen in the diffraction pattern. Though the x-ray probe was 2.5 micrometers in diameter, the reconstructed image has a pixel size of 18 nm, 140 times smaller. The resolution of the image is limited by the weak scattering due to the low intensity of the de-focused beam. Figure 1(d) shows a diffraction pattern, extending to 2.5 nm resolution, from a sample made of Fe_2O_3 nanoparticles functionalized with DNA molecules using a focused probe. The very high intensity in the focus of the lens provides much higher resolution in the diffraction data. Successful reconstructions of such data and application of the technique to a structural study of these materials under different physical conditions will proceed in FY2012.

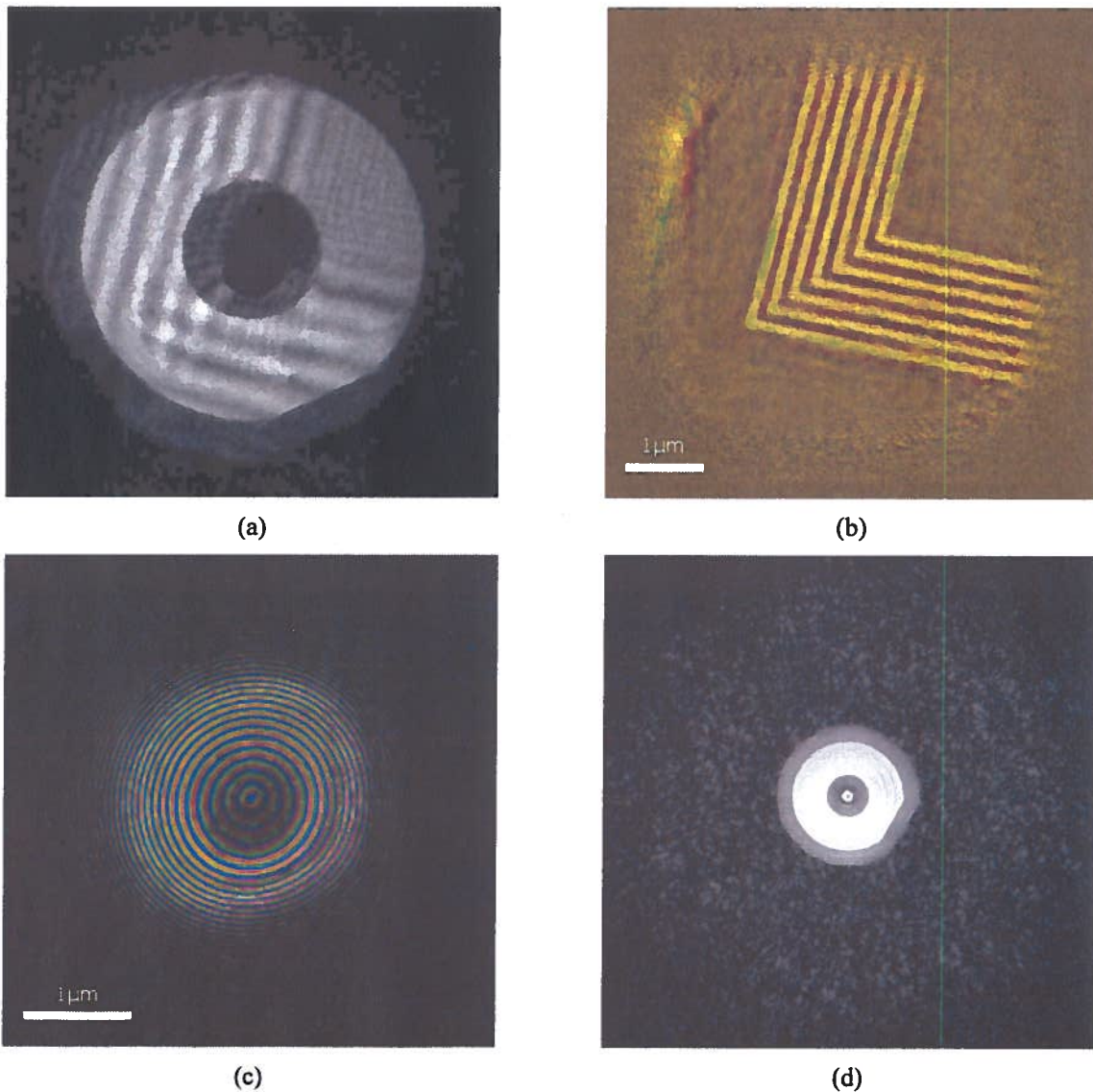


Fig. 1

2D Membrane Solution Scattering for Probing the Structures of Membrane Proteins

LDRD Project 11-032

Lin Yang

PURPOSE:

This LDRD project aims to develop the experimental methods needed to utilize X-ray scattering to study the structure of membrane proteins embedded in single-layered lipid membranes that resemble the native environment of these proteins. While this technique has never been demonstrated, similar results on plant viruses (much larger than membrane proteins and therefore easier to measure) already exist. The difficulty is to collect high quality data free of background scattering and without introducing radiation damage to the proteins, which we will overcome by flash freezing the membrane sample and performing the measurements at liquid nitrogen temperature.

APPROACH:

Structural determination of membrane proteins is a grand challenge in structural biology. A key limitation in these studies is that the membrane proteins must be extracted from membranes using detergents, so that the resulted soluble protein-detergent complex can be studied using methods available for soluble proteins. Unfortunately, the presence of detergents creates some unwanted side effects: progress in protein crystallography has been slow since these complexes are notoriously difficult to crystallize and data interpretation in solution scattering is nearly impossible due to the unknown contribution of detergents.

Measuring the membrane proteins in substrate-supported, single-layered lipid membrane that mimic the proteins' native environment is a promising alternative. The membrane sample can be created under well-defined chemical conditions that are required for the proteins to function. We have showed that plant viruses adsorbed these membranes produce X-ray scattering data that can be analyzed following methods widely used in conventional solution scattering. However, membrane proteins are much smaller than plant viruses and therefore produce weaker scattering signals. In order to apply this method to membrane proteins, the scattering from the bulk water under which the membrane is submerged therefore must be reduced. On the other hand, the data collection time must be increased, implying higher probability of radiation damage to the sample.

Under this project, we will develop methods to flash freeze the membrane samples and measure them at liquid nitrogen temperature. It is known that radiation damage due to the diffusion of free radicals can be dramatically reduced at low temperatures. Once the membrane sample is frozen, it will also be possible to remove the substrate on which the membrane structure is created. Doing so will expose the membrane structure directly to the X-rays, thus virtually eliminating the background scattering from bulk water.

This effort is in collaboration with Masa Fukuto of CMPMSD and Dax Fu of Biology Department.

TECHNICAL PROGRESS AND RESULTS:

FY11 is the first funding year of this project. After a long search process to fill the research associate position, we are fortunate to have Dr. Yimin Mao from Prof. Ben Hsiao's group in Stonybrook University joining this project. In the past few months, we have performed preliminary measurements to assess the severity of radiation damage to membrane samples at room temperature. We are current in the process of constructing the apparatus for freezing and measuring the membrane samples at liquid nitrogen temperature. As of the writing of this document, the experimental apparatus has been assembled and will be tested first in the lab before X-ray scattering measurements at the X9 beamline of NSLS.

For the remainder of FY12, we will continue to development of the experimental apparatus and aim to obtain high quality data from streptavidin, a model membrane protein, by the end of FY12. In FY13, we will shift our focus to analyzing the scattering data and measurements of actual membrane protein supplied by Dax Fu's group, with the goal of publishing the streptavidin data before the end of the appointment of the research associate.

Exploring the Role of Glue in Hadron Structure by an Electron Ion Collider

LDRD Project 11-033

Jianwei Qiu

PURPOSE:

After almost 40 years' successes of Quantum Chromodynamics (QCD) in interpreting the data from high energy collisions, we only know very little on how the quarks and gluons make up nucleons and nuclei. Since the current quark mass for the light quark sector of QCD is so much smaller than the mass of nucleons, it is the glue that binds matter into strongly interacting hadronic particles. The proposed eRHIC by BNL with both e+p and e+A capability could be a powerful femtoscope (or even an attoscope) to explore the quark-gluon structure of hadrons and nuclei. The goal of this LDRD project is to identify a set of semi-inclusive observables in e+p and e+A collisions that could provide the direct access to the glue content of a hadron or a nucleus and to explore the role of glue in forming stable hadrons or nucleus. Our investigations focus on two types of observables: jets and heavy flavor production in the DIS regime of both e+p and e+A collisions. The knowledge gained from this project could help articulate the physics case as well as machine parameters of a future eRHIC.

APPROACH:

Data from HERA – an electron proton collider at DESY, Germany, demonstrated a very strong growth of the number of soft gluons inside a proton. Since the growth is so strong that it could lead to a violation of the Froissart's unitarity bound on hadronic cross sections, soft gluons in a hadron must interact with each other strongly and coherently. The interaction and the coherent strong color field dynamics in QCD could lead to a novel form of saturated gluonic matter, referred as the "Color Glass Condensate" (CGC). Since gluon does not carry electromagnetic charge and cannot interact with the electron beam at eRHIC directly, it is very important and crucial to identify observables that are sensitive to the role of gluons inside the colliding hadron.

With a large momentum transfer, gluons can only interact with the colliding electron at the *short distances* via a highly virtual quark or antiquark, which leads to a characteristic event structure with two nearly back-to-back jets in the Breit frame. At a relatively small x_B , the two-jet final-state should be an excellent observable to directly probe the gluon content of the colliding hadron because of the dominance of photon-gluon subprocess. Our goal is to calculate the jet cross section in the deep inelastic scattering (DIS) regime as well as semi-inclusive DIS regime at eRHIC. The result for e+p collision provides a unique tool for measuring the gluon content of a proton, while the jet modification in e+A collision provides a more direct way to explore the properties of the glue and color structure inside a heavy nucleus.

Since nucleon does not have valence heavy quarks, heavy flavor production at eRHIC is another direct probe of gluon content of colliding hadron or nucleus. In particular, the transverse single spin asymmetry (SSAs) of open-flavor (anti)D (or B) meson production at eRHIC provides a unique opportunity to measure two types of color quantum interference between a single gluon and a two-gluon composite state (or two types of tri-gluon quantum correlation functions) due to the difference in color structure. The co-existence of these two types of tri-gluon correlation functions is a unique feature of non-Abelian color interaction. Our goal is to identify the requirements for the machine parameters of EIC in order to explore these two unique tri-gluon correlation functions and the role of their non-Abelian color structure.

In addition to the open flavor heavy meson production, heavy quarkonium production in the DIS regime of $e+p$ and $e+A$ collisions provides not only a good probe of the gluon content of the colliding hadron but also a better laboratory to test the neutralization of color and the production mechanism of a QCD bound state where the major contribution to its mass is from the quark not from the energy of gluons. Our goal is to develop the correct formalism for calculating the cross section of heavy quarkonium production in high energy collisions and to explore the role of color in the formation of a color singlet and bound heavy quarkonium.

TECHNICAL PROGRESS AND RESULTS:

Fiscal year 2011 was the first year of funding for this project. Dr. Yang-Qing Ma was hired as a postdoc for this project. He arrived in August, 2011 and has been working on the heavy quarkonium production. Since January 1, 2011, a graduate student of Stony Brook University, Mr. Hong Zhang, has been supported by this LDRD grant working on quarkonium production as a part of his Ph.D. thesis. The PI has been working with both the postdoc and the student on heavy quarkonium production, and working with visitors and other collaborators on the jet as well as quarkonium physics. We briefly summarize below results of completed works.

By measuring the scattered lepton at eRHIC and an identified large momentum transfer, DIS and SIDIS are ideal processes to probe the short-distance dynamics of partons inside a hadron or a nucleus. With Kang, Metz, Zhou, we found that observables with an observed large momentum transfer, but without identifying the scattered lepton at eRHIC, can be very interesting and complementary probes of hadron's partonic structure. We demonstrated that QCD factorization for such observables are as rigorous as that for hard probes in hadron-hadron collisions, and derived results for a complete set of polarization observables for jet production in lepton-proton collisions. Our work was published in Phys. Rev. D84, 034046 (2011).

With Zhong-Bo Kang of RBRC and George Sterman of Stony Brook University, we developed a new QCD factorization formalism for heavy quarkonium production in high energy hadronic collisions valid to both leading and next-to-leading power contributions in an expansion of the quarkonium's transverse momentum. We extended the proof of all order QCD factorization for the leading power contribution (Nayak, Qiu, and Sterman, 2005) to the next-to-leading power terms, which is necessary and critical for producing a pair of heavy quarks perturbatively in QCD. Our work provides new physics insights on how a physical quarkonium is produced in a high energy collision. A part of our work has been accepted for publication in Physical Review Letters (arXiv: 1109.1520).

Correlation of a linear polarized gluon inside a unpolarized hadron could carry important information on gluon's spin-orbit correlation, and generate a very unique $\cos(2\phi)$ -type azimuthal correlation of two final-state hadrons or jets. With Dominguez, Xiao, and Yuan, we demonstrated that the linear polarized gluon distributions appear naturally in the color dipole model for calculating the full cross sections of the DIS dijet production and the Drell-Yan γ^* -jet correlation. We also derived the small- x evolution of these linear polarized gluon distributions and found that they rise as x gets small at high energy. The results of our work was submitted for publication in Physical Review D for publication (arXiv:1109.6293).

We expect more results will be obtained in jet and heavy flavor production in the remaining time of the project, which will help support the physics case of building eRHIC.

Study of FEL Options for eRHIC

LDRD Project 11-040

Vladimir N Litvinenko

PURPOSE:

Potential performance of X-ray FELs driven by eRHIC's high-energy electron ERL was studied since 2004 [1] and recently returned to the focus as potential future direction for BNL's light sources [2]. This project will be focused on detailed studies of various X-ray FEL options for eRHIC including single pass SASE FEL, seeded and HGHG FELs, and X-ray FEL oscillators [3,4,5]. Advanced FEL and beam dynamics codes will be used to evaluate various FEL options, compare them and connect them to potential applications.

APPROACH:

During this fiscal year eRHIC design went through a successful external accelerator physics review eRHIC team is in process of costing this design to be reviewed later in 2012.

The goal of this LDRD project is to explore the potential of eRHIC as a driver for a farm of X-ray FELs as well as a driver for a X-ray FEL oscillator.

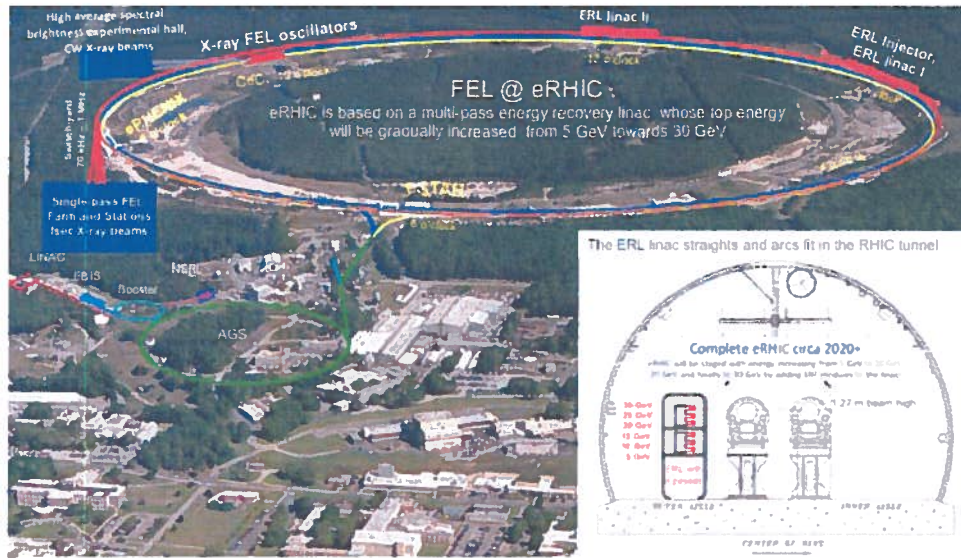


Fig. 1. Schematic layout of possible FEL-based light source facilities surrounding future eRHIC energy recovery linac [2].

TECHNICAL PROGRESS AND RESULTS:

During first part of the 2010 main focus was on selecting appropriate soft-ware and hardware for massive simulation of beam and FEL dynamics. We also made preliminary simulation of the X-ray FEL osciillator – even though this effort is incomplete and will continue.

In August 2011 we hired a post-doc, Dr. Yichao Jing, who is actively pursues the selection of the bam parameters and bunching scheme for X-ray FEL farm. One of the main challenges of using ERL as an FEL drive is effect of coherent synchrotron radiation in the arcs and in the beam compressor. Specifically, since electron's trajectory is bent in the ERL arcs, it is necessary to

accelerate a longer bunches in ERL compared with those in straight linac, i.e. a buncher with large compression is required to generate kA levels of peak current necessary for X-ray SASE FELs. It can result in significant emittance degradation.

Accurate choice of the beam energy and advanced strategy of compressing the bunches is of critical importance for creating necessary beams. Simple-minded approach would result in serious degradation of the e-beam quality and in the resulting quality and power of the FEL's X-ray beam. For a better FEL performance in hard X-ray regime, a multi-GeV electron beam with high peak current and low natural emittance is required. We choose to operate FEL with e- beam at the energy of 10 GeV to reach to hard X-ray regime with current available undulator technology. During this process, a chicane is needed to compress the bunch to reach a high peak current with order of a few kAs for SASE FEL operation.

The bunch compressor system will be located at 12 o'clock in a bypass and the electron beam will be guided into this channel in its second pass in eRHIC where the beam energy is accelerated to about 7.55 GeV. The cavity located at 2 o'clock will be detuned from on crest operation to induce a correlated energy spread for bunch compress. However, due to the lack of energy spread compensation afterwards (electron beam will be accelerated to 10 GeV and then extracted), the energy spread at this stage needs to be constrained within a small value ($\sim 2E-4$). Thus a large R56 is required to get a large compression. This induces very strong coherent synchrotron radiation (CSR) effect which can easily blow up the beam emittance by a factor 3-to-4 fold.

To address this problem, we developed an analog of emittance preservation technique in a merger developed for space charge dominated beam –so called ZigZag scheme [6]. Our cure for this is to avoid full rotation while maintaining a high peak current (~ 1.1 kA) and implement a proper combination of chicane magnets to minimize CSR effect.

Preliminary results are very encouraging and the results of this study demonstrating CSR-affect suppression are in preparation for publication in a refereed journal. A brief summary of the studies is presented below.

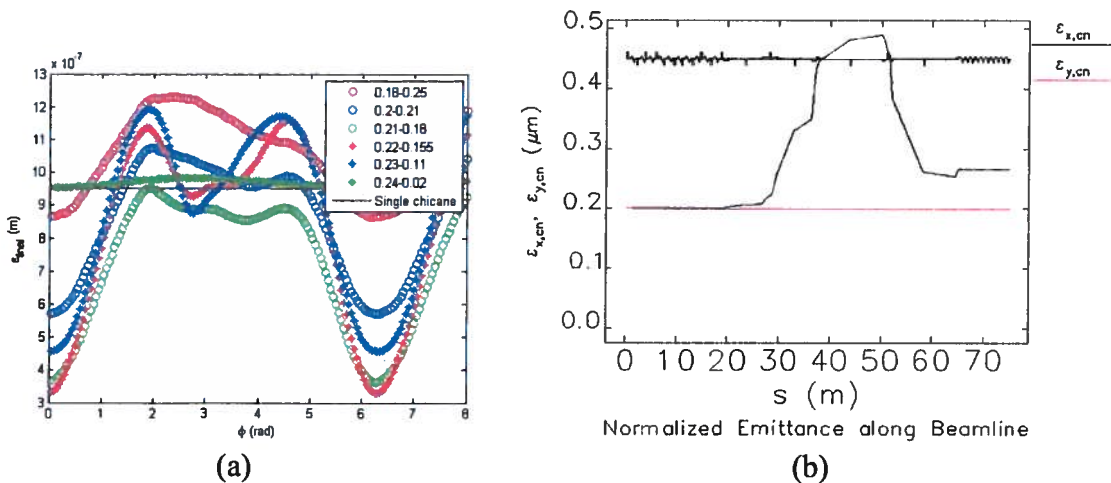


Fig.1. (a) a scan with the dipole strengths (in rad) in first and second chicanes. Horizontal is the phase advance between two chicanes and vertical is the final emittance after bunch compressors (b) the normalized emittance along the bunch compressor system. The CSR effect in second bunch compressor cancels out the CSR in the first chicane thus final emittance is minimized.

We used a Gaussian distribution with the normalized emittance is $0.2 \mu\text{m}$ in both planes and track 200000 particles along the whole system using the code ELEGANT. We assume an initial energy spread is $1e-6$. CSR effect and synchrotron radiation are included in the process and random higher order field errors are also included in dipoles and quadrupoles.

Calculations confirm our expectation that using only one chicane is a really bad choice. The normalized emittance induced by the CSR effect would blow 4-fold. However, using two chicanes with opposite bending directions (zigzag scheme), we can minimize the CSR effect by choosing proper betatron oscillation phase advance between the two chicanes. The relative strengths between two chicanes are also scanned and an optimal working point is observed with emittance growth of 33%, which is an order of magnitude better than single chicane layout (see Fig.2). It means that the CSR effects in second bunch compressor cancel out the CSR effects in the first chicane, and the final emittance is minimized.

We use the particle distribution after the chicane as input into GENESIS and simulate the FEL process. As is shown in Fig. 3, we observe an excellent power growth in a 1 \AA FEL with a gain length of 3.1 m.

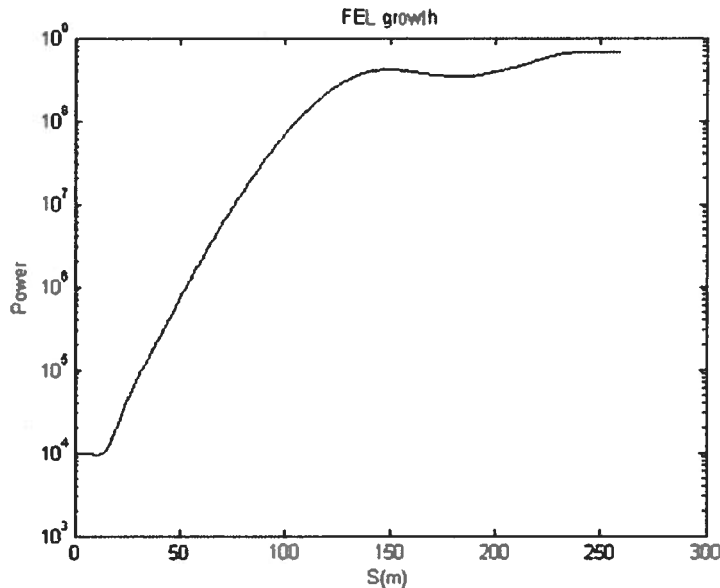


Fig. 3. shows the FEL power growth along the undulator after bunch compressor. The calculated 3D gain length is 3.1 m.

The FEL performance so far seems to be reasonable and we plan to extend simulations into entire set of FEL array spanning from soft- to hard- X-rays

During FY11 we published three conference papers relevant to this research [7-9].

REFERENCES

Proceedings of FEL 2004, <http://accelconf.web.cern.ch/AccelConf/f04/>

[2] S. Aronson, Director's report to BSA, March 26, 2010, Material on FEL eRHIC report prepared by I. Ben-Zvi, C. Kao, V. Litvinenko and J. Murphy

[3] V.N. Litvinenko, Proceedings of FEL conference, August 2002, APS, Argonne, IL, Eds. K.J. Kim, S.V. Milton, E. Gluskin, p. II-1

[4] V.N. Litvinenko, Optics-Free FEL Oscillator, FEL prize talk, FEL 2005 conference, August 2005, Stanford, CA

[5] V.N. Litvinenko, X-ray Optics-Free FEL Oscillator, Future Light Sources 2010 ICFA Beam Dynamics Workshop, SLAC, Menlo Park, CA, March 4, 2010, https://slacportal.slac.stanford.edu/sites/ad_public/events/FLS2010/Lists/WorkingGroup8/Attachments/32/OFFELO_FLS_2010.pdf

[6] Merger Designs for ERLs, Vladimir N. Litvinenko, Ryoichi Hajima, Dmitry Kayran, Nuclear Instruments and Methods in Physics Research A 557 (2006) 165–175, DOI: 10.1016/j.nima.2005.10.065, <http://www.sciencedirect.com/science/article/B6TJM-4HK5NY4-M/2/01fff4af20702a7cb864e75b38a8ed5b>

[7] V. Litvinenko, Y. Hao, D. Kayran, D. Trbojevic, *Optics-free X-ray FEL Oscillator*, Proceedings of 2011 Particle Accelerator Conference, New York, NY, USA, March 25-April 1, 2011, pp. 802-804, <http://accelconf.web.cern.ch/AccelConf/PAC2011/papers/tuods5.pdf>

[8] V. Litvinenko, I. Ben-Zvi, Y. Hao, C.C. Kao, D. Kayran, J.B. Murphy, V. Ptitsyn, T. Roser, D. Trbojevic, N. Tsoupas, *FEL Potential of eRHIC*, Proceedings of 2011 Particle Accelerator Conference, New York, NY, USA, March 25-April 1, 2011, pp. 2151-2153, <http://accelconf.web.cern.ch/AccelConf/PAC2011/papers/thp007.pdf>

[9] V. Yakimenko, M. Fedurin, V.N. Litvinenko A.V. Fedotov, D. Kayran, P. Muggli, *CSR Shielding Experiment*, Proceedings of 2011 Particle Accelerator Conference, New York, NY, USA, March 25-April 1, 2011, pp. 1977-1679, <http://accelconf.web.cern.ch/AccelConf/PAC2011/papers/wep107.pdf>

<http://www.c-ad.bnl.gov/pac2011/proceedings/papers/wep107.pdf>

Overcoming Electromagnetic Interference in Simultaneous PET and MRI for Biological and Clinical Imaging

LDRD Project 11-050

Paul Vaska, David Schlyer and Craig Woody

PURPOSE:

Recently the concept of acquiring PET images simultaneously with MRI has generated considerable excitement in biomedical science. The new possibilities engendered by this fusion of two distinct but complementary imaging modalities are numerous in medicine, relating to the accurate image alignment between the functional image and its anatomical reference frame, and to the potential for interrogation of multiple functional measures simultaneously using functional modes of MRI such as fMRI, spectroscopy, or diffusion tensor imaging. Further, this approach is being applied to the broader context of biological imaging, in particular to understand basic biochemical mechanisms in plants in an effort to develop improved biofuels and to predict the impact of climate change on critical plant species. Our group has been one of the pioneers in the area of multimodality PET-MRI imaging, having developed modular PET detectors and prototype imaging systems that can tolerate the punishing MRI environment which consists of strong static and dynamic magnetic fields and high power radio-frequency transmission. However, the integration of the two systems has been challenging, in particular due to the interference between the modalities each of which rely on high fidelity radio-frequency electromagnetic signals. In our prototype systems, significant interference has been observed in both PET and MRI data despite initial attempts at isolating them with electromagnetic shielding. In this proposal, we plan to investigate the generation and propagation of the electromagnetic interference (EMI) in a rigorous and methodical manner, and to develop and test technological approaches to mitigate the problem to the greatest extent possible. This will build a foundation for multiple ongoing and planned projects in simultaneous PET and MRI imaging.

APPROACH:

We aim to analyze the potentially deleterious signals in the relevant PET and MRI subsystems, and then develop ways to shield or otherwise mitigate the effects. This includes analysis of the sources of electromagnetic waves, the transmission paths, and the circuits that are sensitive to them. Building upon this analysis, we will design and test various shielding configurations.

TECHNICAL PROGRESS AND RESULTS:

Fundamental analysis:

Due to the short distance between the RF coil and the PET system relative to the RF wavelength, we are considered to be in the near field which unfortunately is much harder to analyze than the far field. Based on a study of the literature, it turns out that absorption loss does not depend on the characteristic impedance of the wave (ratio of E and H), but only on the frequency and material properties (permeability and conductivity). Both E and H components of the field are attenuated with the same skin depth factor. At the RF frequency of the coil, we should be able to shield both magnetic and electric fields with minimal shield thickness. Reflection on the other hand, does depend on the wave impedance (E vs H), but in our case we want to minimize reflection rather than maximize it, because absorption should be sufficient and reflected waves might interfere with the MRI.

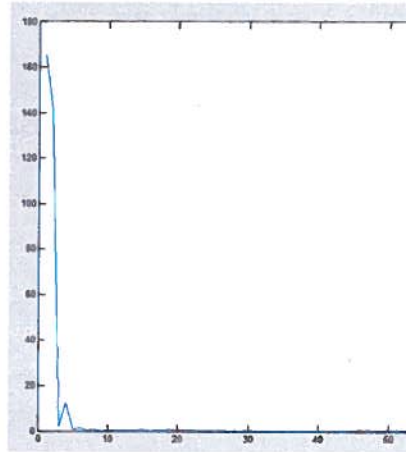
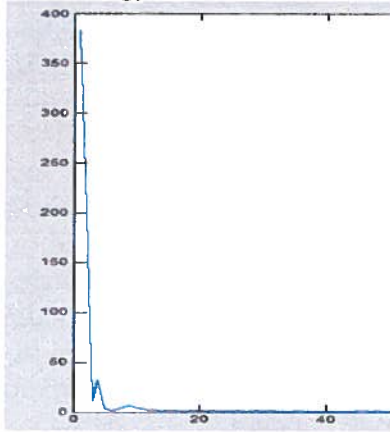
However, at lower frequencies (from the gradients and maybe the wave packets constituting the pulse sequence) shielding of the mainly magnetic component found in the near field becomes difficult (electric shielding is fine because of a large reflected component). At 1 kHz and 0.02 in thick Al, you get only about 25 dB in one geometry example.

So at high frequencies, absorption will be sufficient, reflection will be minimized (by choosing a material whose characteristic impedance is closest to 377 ohms), and apertures become the biggest concern. For low frequencies, we have to work very hard to improve the shielding or else live with the interference. It is important to figure out how much of each problem we are having, perhaps by looking at the frequencies we see on the analog output of the chip.

PET clock frequency decomposition into harmonics:

50 MHz Clock (left below)

The energy for 400 MHz harmonics is only about 0.04% of the whole clock energy.



106 MHz (right below)

The energy for harmonics near 400MHz is very limited (about 0.0002% of the whole energy). Since the interference only appears after plugging in the optical fiber used for data transmission, it appears that the 50 MHz is the problem and the harmonic energy near 400MHz is the main concern.

Segmented, dual-layer, offset shield:

We built and tested this shield which reduced PET artifacts significantly but not completely. Gating is still required which reduces PET detection efficiency.

More detailed results can be found in the publications noted on the Data Collection Form, including imaging results and tests with different shield configurations.

PLANS:

We plan to have a closer look at the effects of apertures in the shield, including screw holes and cable ports. We want to use an RF pickup coil to directly measure the RF that penetrates our PET enclosure. Analyzing the frequency structure can identify the sources more effectively. Ultimately, based on the results of the basic studies above, we need to design, build, and test an optimized RF enclosure for our next-generation PET-MRI prototype imager.

Estrogen Biosynthesis as a Novel Imaging Target with Multiple Applications

LDRD Project 11-051

Anat Biegon

PURPOSE:

The goal of the work pursued was to explore the availability and role of aromatase in different brain regions and peripheral organs in healthy subjects and use this new knowledge for the exploration of the use of aromatase in normal brain function as well as a diagnostic or treatment target in a wide spectrum of diseases.

APPROACH:

Steroid biosynthesis is a multistep process starting with the transport of cholesterol from the cytoplasm into mitochondria and ending with the aromatization of androgens to estrogens. The first, rate limiting step is mediated by peripheral benzodiazepine receptors (PBR) and the last step is uniquely catalyzed by aromatase (Cyp19a gene product). Estrogen is a pluripotent hormone involved in a large number of physiological processes, including among others the maintenance of reproductive function, bone density, sexual behavior and cognitive function. Estrogens also play a crucial role in several types of cancer and in obesity. Increased density of PBR is associated with tumor progression and inflammation caused by bacteria, viruses and autoimmune disease.

The relationship between regional brain aromatas, personality traits and normal brain function (e.g verbal memory) is studied in collaboration with Dr. Alia LKlein form the neuropsychology group. Studies on the involvement of brain aromatase in obesity are performed in collaboration with Dr. Wang. Breast cancer studies are planned in collaboration with breast surgeons and radiologists from Stony Brook University Medical School and University of Pennsylvania. Studies in Alzheimer's disease involve collaborators from SBUMED dept. Psychiatry, neuropsychology service and VA hospital.

TECHNICAL PROGRESS AND RESULTS:

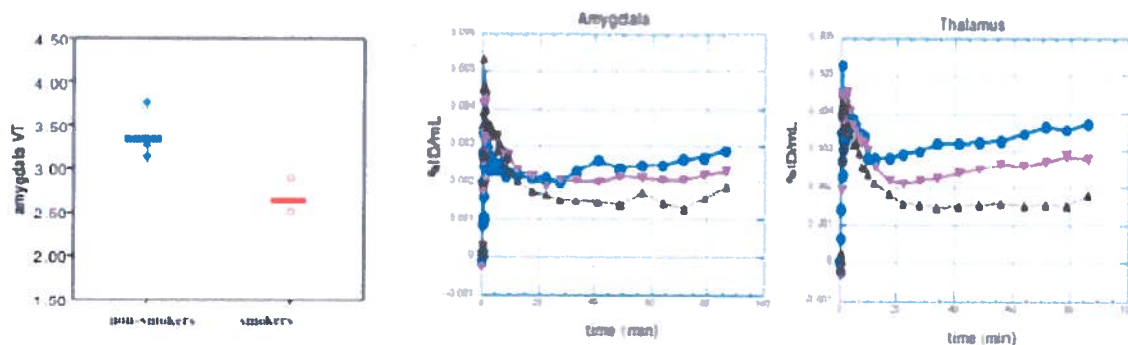
Thirty healthy subjects were enrolled and scanned. Kinetic analysis was completed for brain regions with high uptake (thalamus, amygdala) and is ongoing for other brain regions and peripheral organs. Validation, distribution, pharmacokinetics and modeling of [11C]vorozole in healthy human brain was accomplished and published. Briefly, the regional distribution of [11C]vorozole in the human was found to be highly regional and unique. The highest concentrations of tracer were found in thalamic nuclei, followed by amygdala and inferior olive. As expected, tracer uptake was reduced following administration of a pharmacological dose of letrozole. Kinetic modeling of the blood and brain activity curves showed that a 2 tissue compartment model was superior to a single compartment model and equally suitable to the model-independent Logan graphic analysis).

Brain aromatase involvement in personality and cognition: we found a significant, positive correlation between aromatase levels in amygdala and trait constraint, which was especially significant in women. Brain levels of aromatase were also correlated with verbal memory in a region- and sex dependent fashion.

Brain aromatase involvement in obesity: Overweight and obese persons were found to have significantly lower levels of aromatase in several brain regions, with the largest effects found in amygdala and hypothalamus.

Brain aromatase and cigarette smoking: Of four smokers recruited (2 men and 2 women) two had measurable amounts of nicotine and cotinine in the blood on the day of the study. These subjects had lower aromatase availability in the thalamus and amygdala compared to controls matched for age, sex and BMI (Fig. 1).

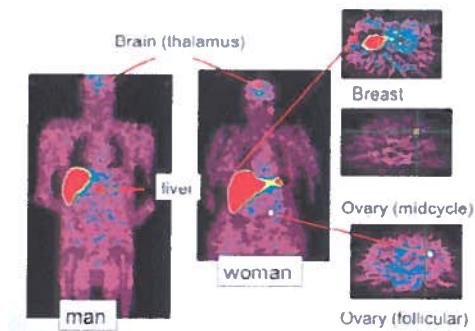
Fig. 1. Effect of cigarette smoking on [11C]vorozole time activity curves and total distribution volume (VT)



Left Panel: Mean amygdala VT of four male non-smoking subjects (on left, circles) matched for age and BMI with 2 male smokers (on right, triangles, $p=0.052$, Student's t test, 2 tailed). Right panels: Time activity curves in amygdala and thalamus of one pair of matched subjects. Circles=non-smoking man, inverted triangles-smoking subject, both at baseline conditions. The upright triangles represent the time activity curves following the ingestion of a pharmacological dose of letrozole (blocking experiment). The TAC shown is from the smoker, since the non-smoking and smoking subjects' TACs after letrozole were superimposable.

Tracer concentrations in most peripheral organs (heart, kidney, lungs) were low and short lived, with several notable exceptions including the liver in all subjects and the ovary in young women imaged at midcycle (Fig. 2).

Fig. 2. Distribution of [11C]vorozole in the human body



Significance and plans for next funding period: The results summarized here indicate that [11C]vorozole is indeed a novel useful tool for measuring aromatase availability in the living human brain. The data gathered from healthy subjects help reveal the role of estrogen synthesis capacity in normal physiology and provide a baseline for future studies of various brain neuropathologies and cancer. Protocols and grant proposals in specific areas (obesity, neurodegeneration, smoking) are being developed and submitted during this and the 2nd funding year.

Magnetic Nanoparticles as Tracers in Biological Systems

LDRD Project 11-052

David J. Schlyer

PURPOSE:

This project will use magnetic nanoparticles as tracers in living systems to attempt to improve the type of information that can be obtained via MR-PET studies and to study the interactions of magnetic nanoparticles with respect to physiological changes. The first goal will be to develop radioactive nanoparticles and to create specific markers for in vivo use in both PET and MR. These particles may be targeted through the use of external magnetic fields which would be a major therapeutic advance. There are many applications of these nanoparticle constructs including targeted nanoparticles for drug delivery, nanoparticle inclusion in cells for microbe tracking in soils, biodistribution of nanoparticles deposited on leaves for plant toxicity and MRS of living systems combined with PET quantitation of uptake to monitor the physiological response to nanoparticles.

APPROACH:

We have developed the synthesis of iron-52 labeled superparamagnetic iron oxide nanoparticles (SPIOs) as a basis for imaging them simultaneously with PET and MRI. The SPIO probe is a MRI contrast agent in a form of single iron oxide nanoparticle with a core containing a positron-emitting radionuclide. This dual probe concept combines the strengths of both PET and MRI into a powerful new tool for quantitative molecular imaging. With the dual probe approach, the strength of one modality can compensate for the weakness of the other. With appropriate functional groups attached, this type of dual modality probe is the basis for the diagnostic constructs we are studying.

The specific aim of this project is to use these constructs to study a variety of biological systems including plants and animals. We have successfully labeled the iron oxide nanoparticles with iron-52 and obtained a PET image in a phantom. The same formulation was used to produce a contrast enhanced image in the 4T MRI. The nanoparticles produced with this procedure had better contrast properties than the commercial preparation of Feridex.

The imaging will be done using two different PET scanners depending on the type of study being done. The first is the commercial MicroPET scanner and the second is the simultaneous PET/MRI scanner mentioned previously and developed here at BNL. The preliminary experiments will use microPET imaging and [⁵²Fe]SPIOs to systematically investigate the effect of particle size on the kinetics of nanoparticles following intravenous dosing into mice. In these dynamic scanning protocols, the injection of radiotracer occurs simultaneously with the start of the microPET acquisition. This allows us to directly visualize the time course of SPIO distribution and accumulation during the first 3 hours following injection. The mouse will be removed from the scanner after three hours and allowed to recover from anesthesia. The following day at 24 hours after injection, another static scan will be carried out to determine the distribution at that time. The procedure will be repeated and a second static scan carried out on the third day 48 hours after injection of the labeled SPIO.

These studies were carried out with the assistance of Dmitri Medvedev from the CAD and David Smith of the Medical Department who conducted the experiments carried out in the 9.4T magnet

TECHNICAL PROGRESS AND RESULTS:

We have successfully labeled the iron oxide nanoparticles with iron-52 and obtained a PET image in a phantom. The same formulation was used to produce a contrast enhanced image in the 4T MRI. The nanoparticles produced with this procedure had better contrast properties than the commercial preparation of Feridex. These labeled nanoparticles have been used to image the biodistribution in a rat with PET and MRI and this is shown in Figure 1.

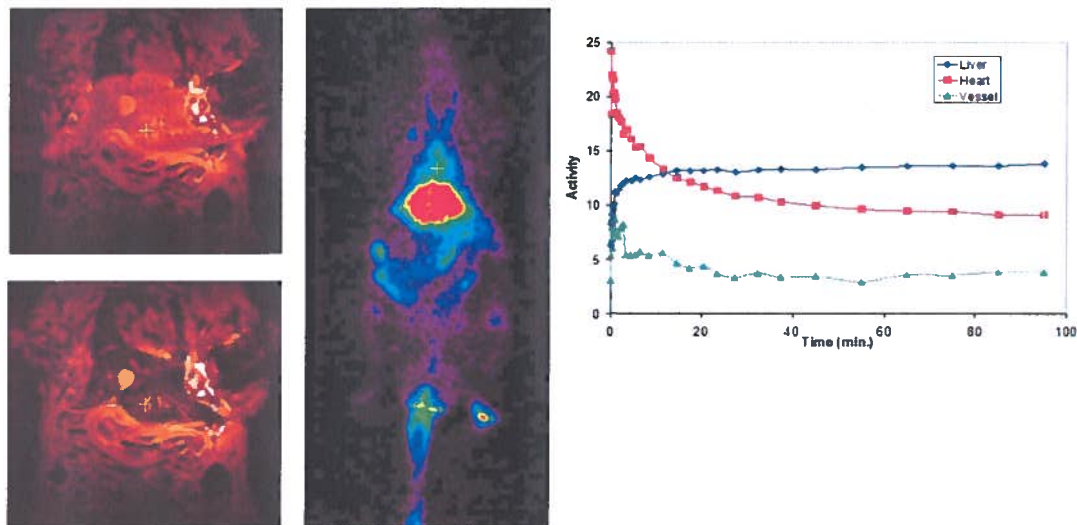


Fig. 1. MR (left) and PET (center) images of labeled iron oxide nanoparticles in rodent liver with the time activity curve from the PET image (right)

We have carried out experiments using the iron-52 labeled nanoparticles in the MicroPET scanner in a rat over a period of 72 hours to determine the fate of the nanoparticles over longer periods of time. The results from this experiment showed that the nanoparticles were retained in the liver over this time period with very little loss. This implies that the nanoparticles are not eliminated quickly from the liver and the half-life in the organ is days rather than hours.

We have also done dynamic studies of the iron oxide nanoparticles in the mouse in the 9.4T MRI. In these studies, we use simultaneous PET and MRI imaging to determine the location and fate of the iron oxide nanoparticles. The images from these studies are shown in Figure 2.

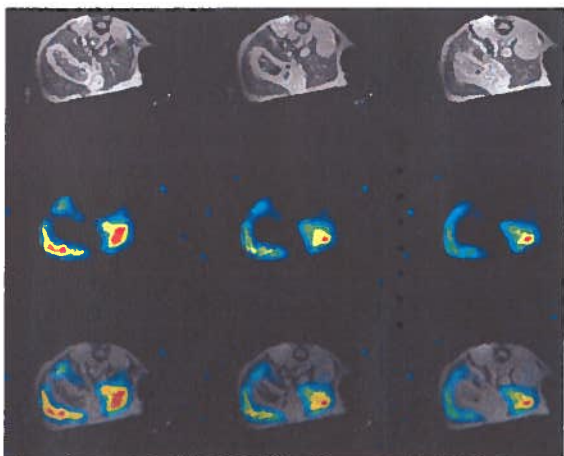


Fig. 2. Uptake of iron oxide nanoparticles in mouse liver. Upper frame is the MRI images, center is the PET images taken simultaneously and the bottom frame shows the combined image.

High Throughput Screening in Biological Systems using Radiometric Approaches

LDRD Project 11-053

Richard A. Ferrieri

PURPOSE:

Our aim is to identify and develop potential technologies using short-lived radioisotopes in combination with non-invasive imaging and radiometric bioassays that not only support the general systems biology approach to conducting research in plant sciences but also are amenable to development into high-throughput screening tools for assessing gene function in systems relevant to the DOE mission to harness biomass feedstock for alternative renewable energy. Our emphasis in the last years has been to develop rapid *in vivo* imaging approaches for screening basic root functions in intact plants. These new tools offer potential for program growth aligned with the DOE Bioenergy Centers providing a needed National resource in screening new lines of genetically engineered feedstock and for assessing sustainability of future feedstock when grown under marginal conditions.

APPROACH:

PET imaging provides a unique look at the dynamic processes involved from the fixation of atmospheric CO₂ to its conversion to sugars and their transport belowground to roots where they are used in growth and storage. We have identified several basic plant functions including root allocation, transport speed and root exudation, and have been working this past year to define the relationship of these basic functions to root sink strength for carbohydrates and root growth rates. Root radiography also provides opportunities to capture snapshots in time of root allocation giving higher spatial resolution than PET and information on growth characteristics as a function of root system architecture including root branching.

TECHNICAL PROGRESS AND RESULTS:

Plant root physiology is an often neglected part of basic plant function owing to the lack of investigational tools that enable one to measure root responses to environmental cues. Over the last year we have developed a root phenotype screen involving measuring shoot-root allocation, root transport speed and root exudation of ¹¹C-photosynthate using a combination of PET imaging, root radiography and nuclear counting in conjunction with administration of ¹¹CO₂ to leaves of intact plants. In preliminary studies, we compared our basic root function measurements between 93-11, a cold climate rice variety and Caiapo, a tropical rice variety for plants grown under low light (50 μ mol m⁻² s⁻¹) and high light (300 μ mol m⁻² s⁻¹) conditions for a 12-hr photoperiod. The results showed that all radiometric root functions that we can measure increased significantly for the tropical Caiapo variety with higher light growth conditions, but not for the cold climate 93-11 variety.

From studies conducted by our group spanning rice and maize grasses, we realize that general perceptions about plant roots and how they respond to environmental cues may be inaccurate due to the lack of direct experimental measurements of their physiology. For example, it seems intuitive that root sink strength for aboveground carbohydrates would be driven by the density of the root biomass. However, in preliminary studies using the Caiapo rice variety, we

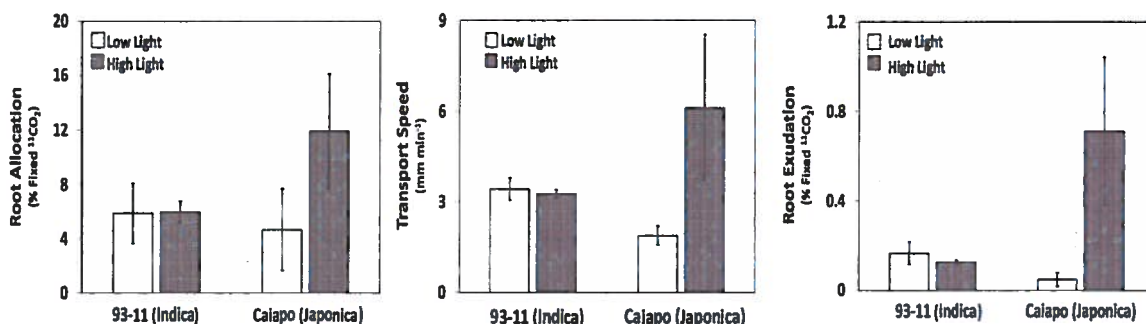


Fig. 1. Basic root physiological measurements that can be measured using $^{11}\text{CO}_2$ administration to leaves.

demonstrated that plants grown on high iron (10ppm Fe) versus low iron (1ppm Fe) under identical conditions ($300 \text{ umol m}^{-2} \text{ s}^{-1}$, 12 hr photoperiod) exhibited an inverse correlation between root biomass and root sink strength for ^{11}C -photosynthate.

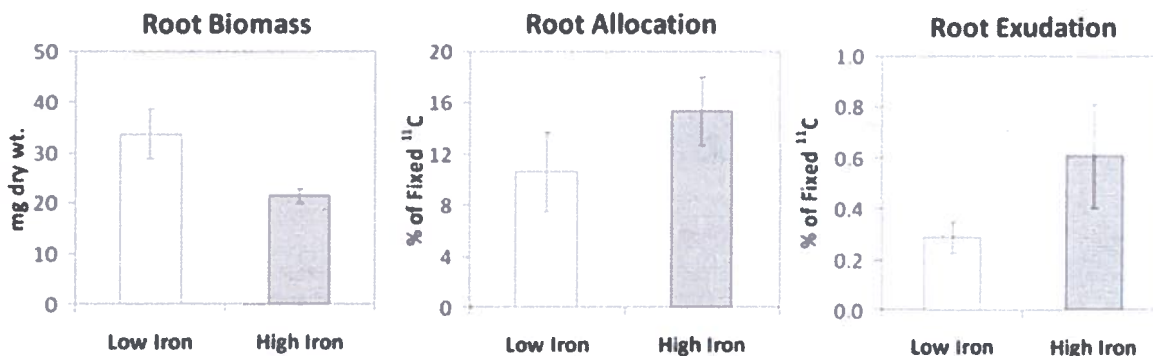


Fig. 2. Negative correlation demonstrated between root density and basic root physiological measurements.

We also realize now that what these early studies lacked was a direct correlation between our radiometric physiological root assays and root growth rates to give biological relevance to our measurements. Experimentally, this is possible to measure non-invasively using PET imaging by retesting same plants over several days of growth. While PET root imaging does not afford opportunity to measure disposition of radiotracer with high spatial resolution, it does enable us to measure the movement of radiotracer through individual roots and determine changes in root length and in sink strength through transport and allocation of ^{11}C -photosynthate. A key advantage of using a PET radioisotope like carbon-11 over other carbon isotopes is that its 20.4 minute radioactive half-life affords a unique opportunity to retest the same plant over time. The figure below highlights our present capabilities at BNL to image multiple plant root systems simultaneously using the microPET camera.

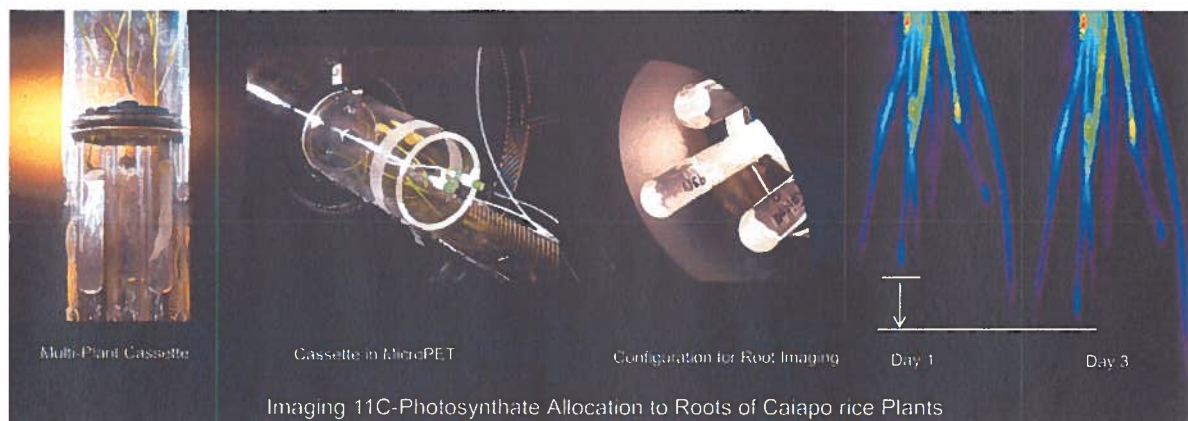


Fig. 3. Multi-plant imaging cassette. The ability to re-image roots over the course of days and growth will afford opportunity to relate basic root physiological measurements to root growth rates and root sink strength.

The figure also portrays the basic concept of being able to image the same root over time and growth. For grasses, we expect a sufficient root growth rate (up to 0.5 mm hr^{-1} in some instances) so that over a period of a few days, roots will have grown well beyond to limiting spatial resolution of the imaging camera enabling us to measure of a growth rate non-invasively.

Root radiography affords an additional opportunity to capture a high resolution snapshots in time of the radiotracer distribution between the primary and branch root structures (ie. lateral roots) giving feedback on how root system architecture impacts growth rate and sink strength.

A goal of this project is to establish a direct relationship between our radiometric root functions (including resource allocation both to primary and fine root structures, transport speed and root exudation) and root growth. We believe that root growth will be positively correlated with increases in these basic root functions. Furthermore, we believe that overall root density will not be a major driver defining root sink strength, but rather the root substructures (ie. lateral root branching) and their growth rates will be the defining factor. Further detailed studies are needed that scale across other grasses in order to generalize the relationship between root function and root growth rates.



Fig. 4. Root radiography gives opportunity to measure sink strength of root substructures (ie. lateral roots). This set of images shows the effect of root auxin treatment on lateral root growth promotion.

Outcomes from this research will better enable us to define root sink strength in the context of growth rates and relate these functions to our radiometric imaging assays measuring root allocation, transport and root exudation. This work has already yielded new partnerships with EMSL at PNNL, JGI, U. Missouri, U. Minnesota and Washington U. in a new initiative to

explore the belowground commodities exchange between plant roots and their surrounding rhizosphere. BNL's unique capabilities to image root function will play a key role in screening early mutant lines for future studies.

Improving Safety with a Brain-Computer Interface

LDRD Project 11-054

R. Goldstein

PURPOSE:

The main goal of the current project is to develop and evaluate an automatic brain computer interface (BCI) to use “brain power” to control external devices (e.g., computer mouse/program), behavior (e.g., movement) and internal states (e.g., thoughts and emotions/motivations).

We expect that this computationally-heavy system will 1) identify stable neural correlates of specific brain functions (e.g., the motivation to move, even before an individual can label or identify these functions/motivations); 2) use these neural correlates to control an external device (e.g., a computerized task); and 3) provide automatic feedback to modify/control such neural processes and subsequent individuals’ experiences (i.e., by changing the computerized task to elicit a different experience/neural signature of experience).

APPROACH:

To achieve these goals, four aims were described:

- (1) Extraction of EEG priors based on automatic information processing;
- (2) Real-time detection and processing of event-related brain activity and device control;
- (3) System validation and application;
- (4) Human subject testing.

TECHNICAL PROGRESS AND RESULTS:

To extract EEG features/priors that are sensitive and specific to automatic information processing we first focused on emotional processing in cocaine addicted individuals and healthy control subjects. We designed a neurocognitive task where we measured EEG and subsequently ascertained event-related potentials (ERP) while subjects viewed drug-related, pleasant, unpleasant and neutral pictures. Results, just published (**Dunning et al., European Journal of Neuroscience 2011**), showed that an ERP component that tracks motivated attention in human subjects [the late positive potential (LPP)], distinguished between pleasant and unpleasant from neutral pictures in healthy control subjects; in addicted individuals, the cocaine pictures elicited increased LPP component in ways similar to affectively pleasant and unpleasant pictures. Another important results of this study was that, in drug addicted individuals, such attention bias to cocaine pictures, and any emotional processing, decreased with time (as measured 1000 – 2000 msec after picture onset), indicative of impairments in sustaining emotional reactivity in this population. These results allow us to use the LPP to track emotional arousal and its impairments in cocaine addiction.

A follow-up study, now under revision (**Moeller et al., Am J Psychiatry**) showed that this ERP component, the LPP, is predictive of drug-related choice in addicted individuals. The importance of this study to the current goals is that such behavioral prediction was most robust in the individuals who were not aware of their own choice, that is, whose insight into behavior was compromised. It suggests that we can use the LPP for our current goals (especially to identify stable neural correlates of specific brain functions - even before an individual can label or identify these functions /associated motivations).

Our immediate goal for the next quarter is to finalize analyses of the EEG data using specialized time-frequency analysis to quantify changes in functionally relevant EEG oscillations, which may distinguish between different types of emotions (note the LPP did not distinguish between pleasant and unpleasant pictures in the control subjects in the studies above). We already started analyzing this data using time-domain and time-frequency analysis tools implemented in Statistical Parametric Mapping. Establishing such high-level emotion differentiation will have marked the achievement of goal 1 – expected to happen during the next quarter.

In parallel, we also continue working on goal 2. Specifically, we are in the process of designing some hardware modifications for our EEG setup to allow for real-time data acquisition, data processing and feedback generation. We have now implemented BCI2000 platform that is able to acquire EEG data, analyze it while providing feedback - all in real-time. We have tested this platform with two test subjects and have acquired promising results. The next quarter will be dedicated to testing the hardware modifications using the classical P300-Speller task.

Next milestones to be achieved are:

- Pilot testing of a miniaturized EEG/ERP BCI system.
 - 60 addicted individuals will undergo training: 20 under BCI, 20 under Peniston protocol and 20 under placebo training.
 - Results will be shared with EIM and OTT for further deliberations.

- Prototype development.
 - A pocket size real-time data processing unit (that performs all the functions from data acquisition to feedback generation).
 - Conveniently wearable/removable EEG electrodes connected wirelessly to the processing unit (e.g., through Bluetooth, similar to contemporary wireless heart rate monitors).
 - Testing/validation of the prototype in consultation with EIM and OTT.

Astrophysics and Cosmology Initiative

LDRD Project 11-055

Anže Slosar

PURPOSE:

The purpose of the project is to establish the techniques required and to actually perform the measurement of dark energy properties through the detection of the baryonic acoustic oscillations in the correlation function of fluctuations in the Lyman-alpha forests of distant quasars. The success of this program will help establish the new Astrophysics and Cosmology group at BNL in the relevant scientific community.

APPROACH:

The Lyman-alpha forest is a series of absorption features in the spectra of distant quasars, blueward of the Lyman-alpha emission line. These features arise as the light from the quasar is absorbed by the intervening neutral hydrogen. This gives one-dimensional information about the fluctuation in the neutral hydrogen density along the line of sight to the quasar. When spectra of many quasars are combined, it allows one to build a three-dimensional image of the fluctuation in the neutral hydrogen density and thus infer the corresponding fluctuation in the matter density. This makes the Lyman-alpha forest a unique probe of the medium redshift ($z \sim 2-3$) universe with very different systematic errors compared to most other techniques. It allows constraints on dark energy, dark matter, neutrino properties and inflation. The BOSS experiment is currently taking data and will take spectra of approximately 150,000 quasars over the five-year span of the project. It is anticipated that BOSS will detect the baryonic acoustic oscillation (BAO) feature in the correlation function of the Lyman-alpha forest in the next two years. This will be the first experiment to do so at redshift above $z = 1$. We propose to build a comprehensive framework to analyze the Lyman forest spectra in this dataset with strong emphasis on understanding the systematic errors arising from astrophysical and instrumental effects, as well as to develop novel and robust analysis techniques. This will result in a plethora of new constraints on cosmological parameter, allow a good scientific return on DOE's investment in the BOSS experiment and pave the way for the future experiments. This work is done within the BOSS Lyman-alpha working group which I chair. My closest collaborators on the project are Patrick McDonald (50% employed by BNL), Vid Iršič (PhD student at University of Ljubljana, Slovenia), Stephen Bailey (LBL) and Andreu Font (Zurich)

TECHNICAL PROGRESS AND RESULTS:

We have begun analyzing the data and published a paper with a detection of the fluctuations in the Lyman-alpha forest on cosmological distances. This was the first detection of the fluctuations at distances relevant for the BAO measurement and was a proof of concept for the technique. We have detected both the correlation and the redshift-space distortions. Our main results are summarized in the figure below, reproduced from our paper:

We are currently working on a second-generation data reduction package. This generation will bring significant improvements, both in the control of systematics as well as a more optimal detection of fluctuation. The resulting paper will be submitted before the Data Release 9 (planned by July 12). We hope to be able to detect the BAO feature in that work and hence constrain the properties of Dark Energy in the high-redshift Universe.

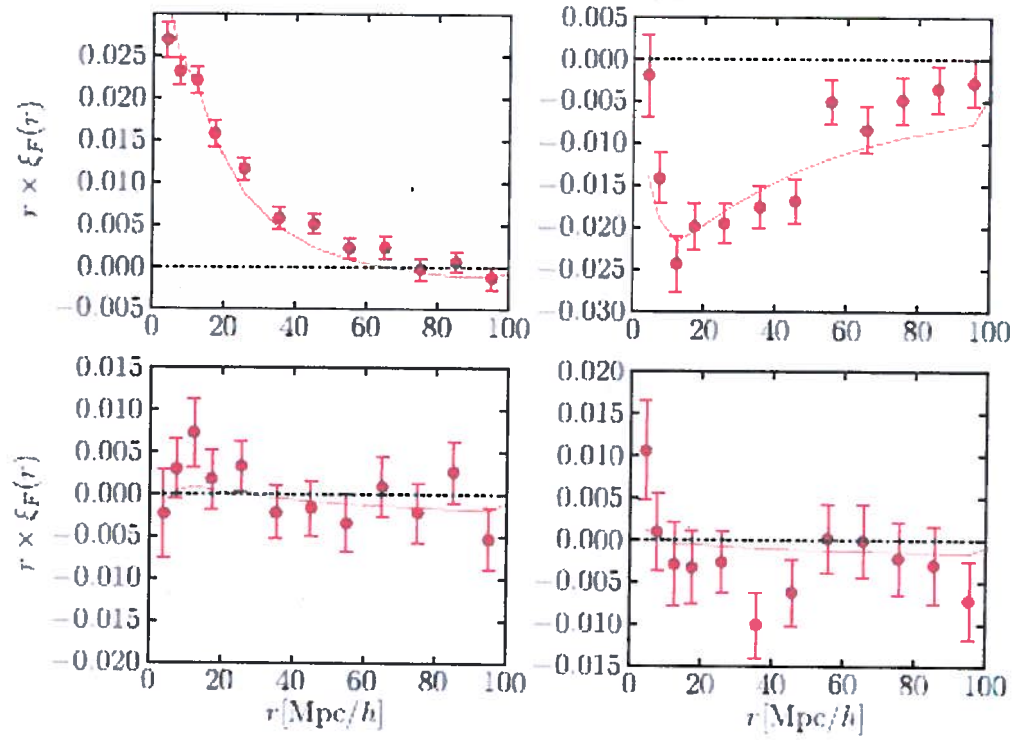


Figure 18. Results of Figure 16 converted to multipoles. The four panels correspond to the redshift-averaged monopole, quadrupole (top row), hexadecapole and $\ell = 6$ moment (bottom row). Lines are best-fit theory.